AD_____
(Leave blank)

Award Number: W81XWH-07-1-0172

TITLE: Beta 2-Microglobulin: A Novel Therapeutic Target for the Treatment of Human Prostate Cancer Bone Metastasis

PRINCIPAL INVESTIGATOR: Leland W. K. Chung, Ph.D.

CONTRACTING ORGANIZATION: Emory University
Atlanta, GA 30322

REPORT DATE: March 2009

TYPE OF REPORT: Annual

PREPARED FOR: U.S. Army Medical Research and Materiel Command
Fort Detrick, Maryland 21702-5012

DISTRIBUTION STATEMENT: (Check one)

X Approved for public release; distribution unlimited

☐ Distribution limited to U.S. Government agencies only; report contains proprietary information

REPORT DOCUMENTATION PAGE

Form Approved
OMB No. 0704-0188

1. REPORT DATE *(DD-MM-YYYY)*	**2. REPORT TYPE**	**3. DATES COVERED** *(From - To)*
14-03-2009	**Annual**	02/15/2008-02/14/2009

4. TITLE AND SUBTITLE

Beta 2-Microglobulin: A Novel Therapeutic Target for the Treatment of Human Prostate Cancer Bone Metastasis

5a. CONTRACT NUMBER
W81XWH-07-1-0172

5b. GRANT NUMBER

5c. PROGRAM ELEMENT NUMBER

6. AUTHOR(S)

Leland W. K. Chung, PhD

Email: lwchung@emory.edu

5d. PROJECT NUMBER

5e. TASK NUMBER

5f. WORK UNIT NUMBER

7. PERFORMING ORGANIZATION NAME(S) AND ADDRESS(ES)

Emory University
Department of Urology
1365B Clifton Rd, Suite B5100
Atlanta, GA 30322

8. PERFORMING ORGANIZATION REPORT NUMBER

9. SPONSORING / MONITORING AGENCY NAME(S) AND ADDRESS(ES)

USA Med Research and Materiel Command
1077 Patchel St.,
Fort Detrick, MD 21702

10. SPONSOR/MONITOR'S ACRONYM(S)

11. SPONSOR/MONITOR'S REPORT NUMBER(S)

12. DISTRIBUTION / AVAILABILITY STATEMENT

Distribution is unlimited

13. SUPPLEMENTARY NOTES

14. ABSTRACT - None provided.

15. SUBJECT TERMS – None provided.

16. SECURITY CLASSIFICATION OF:			**17. LIMITATION OF ABSTRACT**	**18. NUMBER OF PAGES**	**19a. NAME OF RESPONSIBLE PERSON**
a. REPORT	**b. ABSTRACT**	**c. THIS PAGE**		48	Leland W. K. Chung, PhD
					19b. TELEPHONE NUMBER *(include area code)* 404-778-3672

TABLE OF CONTENTS

Page

Introduction:

This proposal focuses on defining the role of beta 2-microglobulin (β2-M) as a growth factor and signaling molecule contributing to prostate cancer bone metastasis. In this proposal, we proposed two Aims.

Specific Aim 1 is to investigate the possible signaling pathway regulated by β2-M in human prostate cancer cells with specific emphasis on the role of bradykinin (BK) receptor as the possible mediator of β2-M signaling. We will define signaling transduction pathway mediated by β2-M in promoting osteomimicry and prostate cancer cell growth and bone metastasis.

Specific Aim 2 is to determine the effectiveness of BKM-1740, a BK receptor antagonist chemically conjugated with bisphosphonate known to accumulate in bone, in the inhibition of prostate cancer growth in mouse bone. By targeting BK receptor on the cell surface of prostate cancer cells using a synthetic BK inhibitor, BKM-1740, we expect this will increase prostate cancer cell death in bone.

During this funding period, we have accomplished the following tasks:

Body:

Task 1: To evaluate the role of β2-M-mediated cell signaling in human prostate cancer cells.

A. *To determine the comparative expression by RT-PCR of the potential β2-M binding proteins, including BK B1 and B2 receptors, Gaq, MHC Class I protein, prostate specific PSGR, and endotehlin 1A receptor in prostate cancer cell lines. Confirm the expression of these proteins by immunohistochemistry and Western blot in prostate cancer cell lines with different degree of malignant potential.*

   We have evaluated β2-M, MHC Class I, and prostate specific PSGR expression in human prostate cancer cell lines. Results of this study showed that a close correlation between β2-M and MHC Class I expression in human prostate cancer cell lines. There appears to be an inverse relationship between the ability of prostate cancer cells to metastasize to bone (e.g., $ARCaP_M$ and LNCaP). $ARCaP_M$ is more aggressive and contains more of the MHC Class I and β2-M, whereas LNCaP is less aggressive and seems to contain less of the MHC Class I and β2-M. The relationship between the aggressiveness of the prostate cancer cells and their MHC ClassI and β2-M expression is proportional. We have also examined the possible involvement of prostate-specific PSGR, a G-protein couple receptor in prostate cancer cells. We found there was no relationship of the expression of PSGR and the responsiveness of prostate cancer cells to β2-M.

B. *To survey β2-M downstream target expression and to confirm their expression by RT-PCR and Western blot.*

We have completed most of the cell signaling pathways involved in β2-M-mediated intracellular signaling in prostate cancer cells. In this study, we have shown that β2-M activates at least three signaling pathways: 1) β2-M-induced androgen receptor downstream signaling (see recently accepted manuscript by Huang et al., *Clinical Cancer Research*, 2008, In press); 2) Activation of survival pathway mediated by vascular endothelial growth factor; and 3) Activation of epithelial to mesenchymal transition that resulted in overexpression of receptor activator of NFκB ligand (RANKL) that increase bone turnover and subsequent bone colonization (see Zhau et al., *Clinical and Experimental Metastasis*, 2008, In press).

C. *To correlate the expression of β2-M responsive genes in a variety of human prostate cancer cell lines with the steady-state levels of β2-M and its binding proteins as described above (see 1a).*

We have initiated studies to examine the role of β2-M in prostate cancer cells by using the knockdown and pull down studies. In the knockdown studies, we have shown that β2-M knockdown is a highly effective way to decrease prostate cancer growth and the ability to metastasize to bone (Huang et al., *Cancer Research*, 2006). We began to examine if β2-M knockdown also could have a significant effect on the epithelial to mesenchymal transition in $ARCAP_M$ cells. Results of this study show that β2-M knockdown could reverse EMT by promoting $ARCAP_M$ cells to express $ARCAP_E$ morphology and gene expression. Currently, we are in the process of selecting ARCAP β2-M knockdown clones and the ability of these cells to grow and metastasize in mouse models. Since β2-M function in cells is intimately related to its binding partner, we also initiated studies to examine the type of proteins β2-M may be co-precipitated during the pull down assays. We found that MHC Class 1 and HFE (hereditary hemochromatosis gene), a MHC Class 1-like protein can be pulled down together with β2-M. Further investigations are proposed to examine the potential role of MHC Class I and HFE in prostate cancer growth, metastasis, and EMT.

D. *To purify and characterize the recombinant His-tagged β2-M protein from bacteria.*

We have completed a part of this study in which β2-M protein has been cloned from bacteria and has shown activity in our assay. Because of the success of cloning β2-M protein from bacteria, we feel that the His-tagged β2-M protein may not be necessary at this time.

E. *To develop the immunoprecipitation procedures and recover the co-immunoprecipitated products from different cellular compartments, membrane, cytosol and nucleus, for further positive identification of the recovered proteins from prostate cancer cells that may bind to recombinant β2-M. To evaluate if any of the protein isolated may belong to the class of proteins identified as possible candidate cited above (see 1a).*

We have developed an effective co-immunoprecipitation protocol in which β2-M interactive proteins can be isolated by the use of anti-β2-M antibody in the presence of β2-M protein complex with its potential binding proteins in the cell extracts. As illustrated above (see item D), we have shown that anti- β2-M antibody can bring down MHC Class 1 protein and a closely related MHC Class 1-like protein, HFE. Functional analysis is under way to determine a potential function of MHC Class 1, and HFE, a MHC Class 1-like molecule in human prostate cancer cells.

F. To identify protein that may bind to recombinant β2-M using Emory Proteomics and Microchemical Facility Core.

We have to overcome some barriers in performing this particular aim because of the relocation of Dr. Jan Pohl from Emory University to the Center for Disease Control at Atlanta. However, we will pursue this aim in collaboration with Dr. David Agus' laboratory at the University of Southern California after relocation to Cedars-Sinai Medical Center – UCLA beginning August 2009.

G. To evaluate the responsiveness of cells to β2-M by modifying the levels of expression of the genes that have been indentified as β2-M binding proteins either on the cell membrane, in the cytosol, and/or associated with cell nucleus.

We have successfully knockdown HFE in ARCaP-M cells and have observed a reversion of morphology and gene expression of these cells to resemble ARCaP-E. Corresponding with this knockdown, we have observed increased intracellular iron and subsequently increased reactive oxygen species. These results are consistent with our hypothesis that HFE may be a novel β2-M receptor.

H. To link the effects of β2-M on gene expression to the ability of β2-M in the promotion of prostate cancer cell growth in vitro and tumor growth in mice through the induction of cell cycle or apoptosis regulated genes.

We have committed our time to the investigation of β2-M effect on prostate cancer growth and survival to androgen receptor regulated mechanism. In addition, we have raised antibodies that are specific to recognizing β2-M protein as a potential therapeutic agent in the management of prostate cancer growth in mice bearing prostate tumors in tibia. With the availability of tissue specimens from these studies, we will begin to assess the roles of β2-M protein as a major signal and growth factor molecule that could affect the cell cycle progression and the blockade of β2-M signaling using anti-β2-M antibody can induce apoptosis in prostate cancer but not affect the growth of normal prostate epithelial cells.

Task 2: To assess the targeting potential of blocking BK and its receptor signaling on the growth of prostate tumors in mouse skeleton.

A. *To correlate the growth inhibition and gene expression profiles of human prostate cancer cells treated with BKM-1740, a bisphosphonate conjugate of a BK receptor antagonist.*

   This task has been successfully completed, a paper related to this proposed study has now been accepted for publication (Seo et al., Clinical Cancer Research, 2008, In press).

B. *To evaluate the effectiveness of BKM-1740 in mice bearing prostate tumors at various anatomical sites, including subcutaneous, orthotopic and intraosseous to determine if the effects of this compound on tumor growth may be affected by tumor surrounding microenvironment.*

   This task has also been successfully completed as stated above. (See Seo et al., Clinical Cancer Research, 2008).

C. *To evaluate the histopathology and gene expression profiles of the tumor specimens harvested from mice treated with BKM-1740.*

   This task has been accomplished in part and data were also submitted for publication by Seo et al., Clinical Cancer Research, 2008.

D. *Based on the information obtained on β2-M binding proteins and its interactive proteins from Task 1, we will explore the methods to increase BKM-1740-induced therapeutic responsiveness of the prostate tumors.*

   This task has been completed in part. Additional work will be performed in the coming years to determine if BKM-1740 may have therapeutic effect on prostate tumor growth in mice through the induction of apoptosis in endothelial cells. In addition, we will also explore the possibility of using anti-β2-M antibody as a therapeutic agent co-targeting human prostate cancer bone tumor growth in combination with BKM-1740.

E. *To write up scientific papers for report and publication.*

   This task will be performed on a continued basis as more scientific information becomes available to us.

Key Research Accomplishments:

• Define β2-M downstream signaling pathways that could lead to the understanding of prostate cancer local growth and distant metastasis.

• Define the blockade of BK receptor using BK bisphosphonate conjugates for the treatment of prostate cancer bone metastasis.

• Define the activity of blocking β2-M signaling that can lead to increased prostate cancer death and slow down prostate cancer cell cycle progression.

Reportable Outcomes:

1. Huang WC, Havel JJ, Zhau HE, Qian WP, Lue HW, Chu CY, Nomura T, and **Chung LWK**. (2008) β2-Microglobulin signaling blockade inhibited androgen receptor axis and caused apoptosis in human prostate cancer cells. *Clin Cancer Res*, 14(17):5341-7.
2. Seo SI, Gera L, Zhau HE, Qian W-P, Iqbal S, Johnson NA, Zhang S, Zayzafoon M, Stewart J, **Chung LW**, and Wu D. BKM1740, an acyl-tyrosine bisphosphonate amide derivative, inhibits the bone metastatic growth of human prostate cancer cells through the inhibition of survivin expression. *Clinical Cancer Res*. 14(19):6198-206.
3. Zhau HE, Odero-Marah V, Lue HW, Nomura T, Wang R, Chu G, Huang WC, and **Chung LWK**. (2008). Epithelial to Mesenchymal Transition (EMT) in Human Prostate Cancer: Lessons Learned from ARCaP Model. *Clinical and Experimental Metastasis*. 25 (6):601-10, 2008.
4. Odero-Marah V, Wang R, Chu G, Xu J, Shi C, Marshall FF, Zhau HE, and **Chung LWK**. (2008). Receptor activator of NFkB ligand (RANKL) expression is associated with epithelial to mesenchymal transition in human prostate cancer cells. *Cell Research*. 18(8):858-70, 2008.

Conclusions:

We have made steady progress on this project.

References:

None

Appendix:

1. Huang WC, Havel JJ, Zhau HE, Qian WP, Lue HW, Chu CY, Nomura T, and **Chung LWK**. (2008) β2-Microglobulin signaling blockade inhibited androgen receptor axis and caused apoptosis in human prostate cancer cells. *Clin Cancer Res*, 14(17):5341-7.

2. Seo SI, Gera L, Zhau HE, Qian W-P, Iqbal S, Johnson NA, Zhang S, Zayzafoon M, Stewart J, **Chung LW**, and Wu D. BKM1740, an acyl-tyrosine bisphosphonate amide derivative, inhibits the bone metastatic growth of human prostate cancer cells through the inhibition of survivin expression. *Clinical Cancer Res*. 14(19):6198-206.
3. Zhau HE, Odero-Marah V, Lue HW, Nomura T, Wang R, Chu G, Huang WC, and **Chung LWK**. (2008). Epithelial to Mesenchymal Transition (EMT) in Human Prostate Cancer: Lessons Learned from ARCaP Model. *Clinical and Experimental Metastasis*. 25 (6):601-10, 2008.
4. Odero-Marah V, Wang R, Chu G, Xu J, Shi C, Marshall FF, Zhau HE, and **Chung LWK**. (2008). Receptor activator of NFkB ligand (RANKL) expression is associated with epithelial to mesenchymal transition in human prostate cancer cells. *Cell Research*. 18(8):858-70, 2008.

β2-Microglobulin Signaling Blockade Inhibited Androgen Receptor Axis and Caused Apoptosis in Human Prostate Cancer Cells

Wen-Chin Huang,[1] Jonathan J. Havel,[2] Haiyen E. Zhau,[1] Wei Ping Qian,[1] Hui-Wen Lue,[3] Chia-Yi Chu,[3] Takeo Nomura,[4] and Leland W.K. Chung[1]

Abstract

Purpose: β2-Microglobulin (β2M) has been shown to promote osteomimicry and the proliferation of human prostate cancer cells. The objective of this study is to determine the mechanism by which targeting β2M using anti-β2M antibody inhibited growth and induced apoptosis in prostate cancer cells.

Experimental Design: Polyclonal and monoclonal β2M antibodies were used to interrupt β2M signaling in human prostate cancer cell lines and the growth of prostate tumors in mice. The effects of the β2M antibody on a survival factor, androgen receptor (AR), and its target gene, *prostate-specific antigen* (*PSA*) expression, were investigated in cultured cells and in tumor xenografts.

Results: The β2M antibody inhibited growth and promoted apoptosis in both AR-positive and PSA-positive, and AR-negative and PSA-negative, prostate cancer cells via the down-regulation of the AR in AR-positive prostate cancer cells and directly caused apoptosis in AR-negative prostate cancer cells *in vitro* and in tumor xenografts. The β2M antibody had no effect on AR expression or the growth of normal prostate cells.

Conclusions: β2M downstream signaling regulates AR and PSA expression directly in AR-positive prostate cancer cells. In both AR-positive and AR-negative prostate cancer cells, interrupting β2M signaling with the β2M antibody inhibited cancer cell growth and induced its apoptosis. The β2M antibody is a novel and promising therapeutic agent for the treatment of human prostate cancers.

β2-Microglobulin (β2M) is produced by all nucleated cells as a 119-amino-acid residue protein and, after processing, is secreted in a 99-amino-acid form (11,800 Da; refs. 1, 2). The most common known function of β2M, a light-chain antigen-presenting molecule, is to serve as a coreceptor for the presentation of the MHC class I in nucleated cells for cytotoxic T-cell recognition (3). However, cancer cells frequently down-regulate the expression of MHC class I to evade recognition by the immune system (4–7), presumably allowing the secretion of free β2M into circulation or in the tumor microenvironment. Our laboratory first identified β2M, an active component secreted by prostate cancer, and prostate and bone stromal cells, as a major growth factor and signaling molecule (8). β2M conferred osteomimicry, the ability of cancer cells to mimic gene expression by bone cells, in prostate cancer cells through the activation of a cyclic AMP (cAMP)–dependent protein kinase A (PKA) and cAMP-responsive element binding (CREB) protein signaling pathway (9). The use of a sequence-specific small interfering RNA (siRNA) targeting β2M and its signaling resulted in extensive prostate cancer cell death *in vitro* and greatly promoted prostate tumor regression in immunocompromised mice (8). We also showed that interrupting β2M signaling similarly blocked human renal cell carcinoma growth (10). β2M has recently been shown to be a useful biomarker for advanced human prostate cancer (11). β2M seems to be a downstream androgen target gene, more specific than prostate-specific antigen (PSA), under the control of the androgen receptor (AR), in a human LNCaP prostate cancer cell line (11).

Anti–β2M antibody is a potent interrupter of β2M-mediated signaling (8, 12). The β2M antibody was shown to be a highly cytotoxic reagent against the growth of solid tumors like renal cell carcinoma (13) as well as liquid tumors, such as leukemia, lymphoma, and multiple myeloma (12). We showed here that the β2M antibody inhibited the expression of a survival factor, AR, and its target gene, *PSA*, in AR-positive and PSA-positive human prostate cancer cell lines, including androgen-dependent LNCaP and androgen-independent C4-2B cells (14),

Authors' Affiliations: [1]Molecular Urology and Therapeutics Program, Department of Urology and Winship Cancer Institute and [2]Graduate Program in Molecular and Systems Pharmacology, Emory University School of Medicine; [3]Department of Biology, Georgia State University, Atlanta, Georgia; and [4]Department of Oncological Science (Urology), Oita University Faculty of Medicine, Oita, Japan

Received 3/26/08; revised 4/28/08; accepted 5/2/08.

Grant support: NIH grant P01 CA98912 (L.W.K. Chung) and U54 CA119338 and Department of Defense grants PC040260 (L.W.K. Chung), W81XWH-07-1-0172, and W81XWH-08-1-0321 and PC073356 (W-C. Huang).

The costs of publication of this article were defrayed in part by the payment of page charges. This article must therefore be hereby marked *advertisement* in accordance with 18 U.S.C. Section 1734 solely to indicate this fact.

Note: Supplementary data for this article are available at Clinical Cancer Research Online (http://clincancerres.aacrjournals.org/).

Requests for reprints: Wen-Chin Huang or Leland W.K. Chung, Molecular Urology and Therapeutics Program, Department of Urology and Winship Cancer Institute, Emory University School of Medicine, Room B5101, 1365-B Clifton Road, Atlanta, GA 30322. Phone: 404-778-3672; Fax: 404-778-3965; E-mail: whuang3@emory.edu or lwchung@emory.edu.

doi:10.1158/1078-0432.CCR-08-0793

and in androgen-independent C4-2 tumor xenograft models. The β2M antibody also suppressed growth and induced apoptosis in both AR-positive and PSA-positive, and AR-negative and PSA-negative human prostate cancer cells and in xenograft tumors in mice. Moreover, our studies showed that the β2M antibody induced prostate cancer cell death through an activation of a caspase-9–mediated apoptotic cascade pathway without affecting normal or nontumorigenic prostatic epithelial and stromal cells. These results support the idea that targeting β2M signaling via the external application of the β2M antibody can profoundly alter intracellular cell signaling networks, including, but not limited to, the AR downstream signaling axis. Effective β2M antibody–mediated targeting of the growth of both AR-positive and PSA-positive, and AR-negative and PSA-negative human prostate cancer cells may prove to be an attractive and safe therapeutic approach for the treatment of human prostate cancer and its lethal progression.

Materials and Methods

Cell lines, cell culture, and β2M antibody. The human prostate cancer cell line LNCaP (androgen dependent), the LNCaP lineage–derived bone metastatic subline C4-2B (androgen independent; ref. 14), DU-145 (brain metastatic, androgen independent), PC3 (bone metastatic, androgen independent), and ARCaP (ascites-fluid–derived, androgen repressive; refs. 15, 16) were cultured in T-medium (Invitrogen) supplemented with 5% fetal bovine serum, 100 IU/mL penicillin, and 100 μg/mL streptomycin. A human normal/nontumorigenic prostatic epithelial cell line, RWPE-1 (American Type Culture Collection), was cultured in keratinocyte serum-free medium supplemented with 5 ng/mL human recombinant epidermal growth factor and 0.05 mg/mL bovine pituitary extract (Invitrogen). These prostate cancer and normal cell lines were maintained in 5% CO_2 at 37°C. The anti-β2M antibody, a polyclonal antibody, was obtained from Santa Cruz Biotechnology, Inc. (sc-15366), for *in vitro* cell culture studies and *in vivo* animal experiments. We also tested the β2M monoclonal antibody (Santa Cruz Biotechnology; sc-13565) and found it to have similar inhibitory effects on the growth of human prostate cancer cells *in vitro* (data not shown).

Reverse transcription-PCR. LNCaP and C4-2B cells were plated on six-well dishes at 3×10^5 cells per well and grown to 70% confluence in T-medium with 5% fetal bovine serum. The cells were gently washed with PBS and incubated in T-medium plus 5% dextran-coated, charcoal-treated fetal bovine serum for overnight incubation. The cells were then treated with 0, 1, 5, or 10 μg/mL of β2M antibody; the β2M antibody was preincubated for 30 min with the same amounts of purified human β2M protein (Sigma) or 10 μg/mL of isotype control IgG for 24 h. The total RNA was isolated from these treated cells using a RNeasy Mini Kit (Qiagen) and subjected to reverse transcription according to the manufacturer's instructions (Invitrogen). The primer sequences used for PCR analysis were AR [5′-ATGGCTGTCATTCAGTACTCCTGGA-3′ (forward) and 5′-AGATGGGCTTGACTTTCCCAGAAAG-3′ (reverse)], PSA [5′-ATGTGGGTCCCGGTTGTCTTCCTCACCCTGTC-3′ (forward) and 5′-TCAGGGGTTGGCCACGATGGTGTCCTTGATC-3′ (reverse)], and glyceraldehyde-3-phosphate dehydrogenase [5′-ACCACAGTCCATGCCATCA-3′ (forward) and 5′-TCCACCACCCTGTTGCTGT-3′ (reverse)], respectively. The thermal profiles for AR, PSA, and glyceraldehyde-3-phosphate dehydrogenase cDNA amplification are 25 cycles, starting with denaturation for 1 min at 94°C, followed by 1 min of annealing at 61°C (for AR), 55°C (for PSA), and 60°C (for glyceraldehyde-3-phosphate dehydrogenase), and 1 min of extension at 72°C. The reverse transcription-PCR products were analyzed by agarose gel electrophoresis.

Western blot analysis and ELISA. Cell lysates were prepared from β2M monoclonal antibody–treated or IgG-treated prostate cells using a lysis buffer [50 mmol/L Tris (pH 8), 150 mmol/L NaCl, 0.02% NaN_3, 0.1% SDS, 1% NP40, and 0.5% sodium deoxycholate] containing 1 mmol/L phenylmethylsulfonyl fluoride and a protease inhibitor cocktail (Roche Applied Science). The protein concentration was determined by the Bradford assay using the Coomassie Plus Protein Reagent (Pierce). Western blot was done with the Novex system (Invitrogen) as described previously (8, 10). The primary antibodies anti-AR (1:500 dilution) and PSA (1:1,000 dilution; Santa Cruz Biotechnology); anti–caspase-9, caspase-3, and poly(ADP)ribose polymerase (PARP; 1:1,000 dilution; Cell Signaling Technology); and the secondary antibodies that were conjugated with horseradish peroxidase (1:5,000 dilution; GE Healthcare) were used. The detection of protein bands was done with the use of enhanced chemiluminescence Western Blotting Detection Reagents (GE Healthcare). The soluble PSA levels were determined by microparticle ELISA with the Abbott IMx machine (Abbott Laboratories).

Cell proliferation assay. LNCaP (6,000 cells per well), C4-2B (6,000 cells per well), DU-145 (3,000 cells per well), PC3 (3,000 cells per well), ARCaP (5,000 cells per well), and RWPE-1 (6,000 cells per well) cells were plated on 96-well plates and treated with the β2M antibody or control IgG for a 3-d incubation. The cell numbers were measured every 24 h by mitochondrial 3-(4,5-dimethylthiazol-2-yl)-5-(3-carboxymethoxyphenyl)-2-(4-sulfophenyl)-2*H*-tetrazolium, inner salt (MTS), assay with the use of the CellTiter 96 AQueous One Solution Cell Proliferation Assay (Promega) according to the manufacturer's instructions.

Sub-G_1 DNA content measurement. LNCaP and C4-2B prostate cancer cells were plated on six-well plates at 3×10^5 per well in T-medium containing 5% dextran-coated, charcoal-treated fetal bovine serum and exposed to 10 μg/mL of β2M monoclonal antibody or control IgG for 48-h incubation. The treated cells were collected by trypsinization and fixed in 70% ice-cold ethanol, incubated with RNase A (100 μg/mL; Sigma) for 30 min, and stained with propidium iodide (25 μg/mL; Chemicon) for 30 min. The cell cycle was determined by a FACScan flow cytometer and CellQuest software (Becton Dickinson Labware) for analysis of sub-G_1 DNA content.

In vivo *animal experiments.* All the animal experiments were approved and done in accordance with institutional guidelines. The mice were maintained at the Animal Research Facility in Emory University. To test the antitumor efficacy and AR expression regulated by the β2M antibody *in vivo*, 4-wk-old male athymic *nu/nu* mice (National Cancer Institute) were inoculated s.c. with C4-2 or PC3 prostate cancer cells with 2×10^6 cells per mouse. After 3 wk (PC3 tumor) or 4 wk (C4-2 tumor) of inoculation, 10 μg of β2M monoclonal antibody mixed with Surgifoam (Ethicon Inc.) to keep and slow release the β2M antibody around the tumors were given by intratumoral implantation, one shot per mouse. The control group mice received equal doses of isotype IgG or placebo (saline) implanted the same way as the β2M antibody. After 1 wk of treatment, tumor tissues were harvested from the euthanized mice and fixed in 10% formalin, dehydrated in ethanol, embedded in paraffin, and sectioned in slides. The blank tissue slides were subjected to immunohistochemical staining with anti-AR antibody (Santa Cruz Biotechnology) and M30 CytoDeath marker (DiaPharma Group, Inc.), and detected by the Dako Autostainer Plus system (Dako Corp.). For quantification of AR and M30 CytoDeath staining, 100 cells at five randomly selected areas were counted and the positive-staining cells were recorded.

Statistical analysis. Statistical analyses were done as described previously (9). Student's *t* test and two-tailed distribution were applied in the analysis of statistical significance.

Results

β2M antibody decreased AR and PSA expression in human prostate cancer cells. We previously showed that β2M is a novel signaling and growth-regulating molecule capable of

promoting cell proliferation and survival in human prostate and renal cancer cells (8, 10). Interrupting β2M and its downstream signaling by β2M siRNA induced cell death in both human prostate and renal carcinoma models (8, 13). Because the downstream targets for β2M signaling interruption are not completely clear in human prostate cancer cells, we conducted a cDNA microarray study (17) comparing β2M siRNA stably transfected AR-positive and PSA-positive C4-2B prostate cancer cells with their scramble stably transfected control clones. The results of these studies showed a 4-fold and 16-fold decreased expression of AR and PSA mRNA, respectively, in C4-2B cells, and these data were confirmed by reverse transcription-PCR and Western blot.[5] To test the hypothesis that blocking β2M-mediated signaling pathways may affect AR gene expression and transactivation, which are involved in prostate cancer cell growth, survival, and progression, we tested the effect of a new reagent, β2M polyclonal antibody, on AR and PSA expression in AR-positive and PSA-positive LNCaP (androgen dependent) and C4-2B (androgen independent) cells. Consistent with cDNA microarray data, interrupting β2M by the β2M antibody decreased endogenous AR and PSA mRNA expression as determined by reverse transcription-PCR (Fig. 1A). The inhibitory effect of the β2M antibody (0-10 μg/mL) was concentration dependent, and the addition of purified β2M protein rescued the decreased AR and PSA mRNA expression that had been inhibited by the β2M antibody in LNCaP and C4-2B cells. Isotype-matched control IgG (10 μg/mL) did not suppress AR and PSA mRNA expression. In parallel, the β2M antibody (0-10 μg/mL) also inhibited AR and PSA protein levels in a concentration-dependent manner as analyzed by Western blot (Fig. 1B), and this inhibition can also be rescued by the addition of purified β2M protein to the cultured LNCaP and C4-2B cells. The control IgG did not change AR and PSA protein expression. Consistent with the blockade of AR expression, we found that secreted soluble PSA levels, assayed by ELISA, were also decreased by the β2M antibody, but not the control IgG, in LNCaP and C4-2B cells (Fig. 1C). These results indicate that the β2M antibody diminished AR and PSA mRNA and protein expression in both androgen-dependent and androgen-independent human prostate cancer cells.

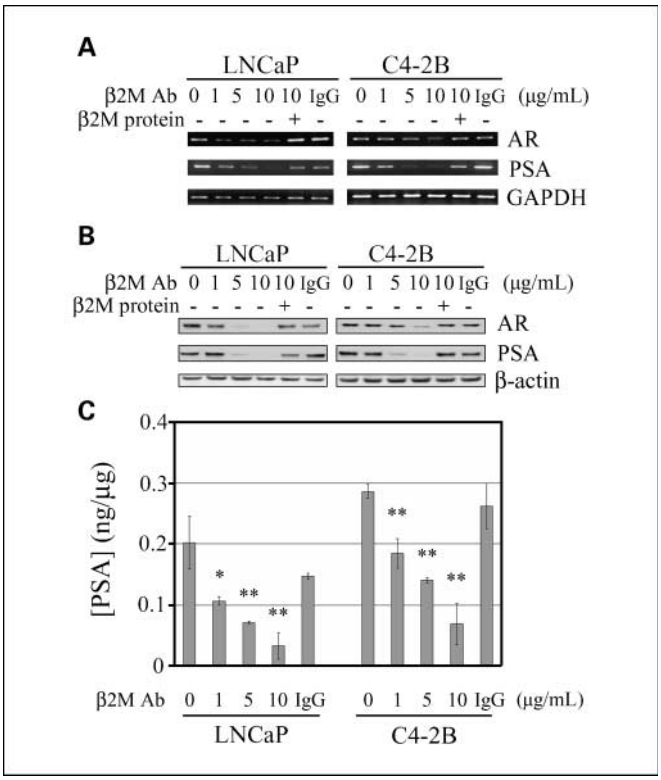

Fig. 1. β2M antibody inhibited AR and PSA mRNA and protein expression in human prostate cancer cells. *A,* β2M antibody (*β2M Ab*) decreased AR and PSA mRNA expression in a dose-dependent manner (0-10 μg/mL, 24-h treatment) in both LNCaP (androgen dependent) and C4-2B (androgen independent) prostate cancer cell lines detected by reverse transcription-PCR. The inhibitory effect was restored by the preincubation of the β2M antibody with purified β2M protein. Isotype control IgG (10 μg/mL) did not affect AR and PSA mRNA expression. The expression of glyceraldehyde-3-phosphate dehydrogenase (*GAPDH*) was used as a loading control. *B,* β2M antibody inhibited AR and PSA protein expression in a dose-dependent pattern (0-10 μg/mL, 24-h treatment) in LNCaP and C4-2B cells assayed by Western blot. The inhibitory effect was abrogated by the preincubation of β2M antibody with β2M protein. Control IgG (10 μg/mL) did not change AR and PSA protein expression. β-Actin was used as an internal loading control. *C,* secreted soluble PSA levels were also decreased by the β2M antibody (0-10 μg/mL), but not the control IgG, in a concentration-dependent inhibition in LNCaP and C4-2B cells determined by ELISA. The concentrations of PSA (ng) were normalized by total proteins (μg). *, $P < 0.05$; **; $P < 0.005$, significant differences from the β2M-antibody – untreated group. Columns, mean; bars, SD.

β2M antibody inhibited cell proliferation in human prostate cancer cell lines. Because β2M stimulated prostate and renal cancer cell growth through the promotion of cAMP/PKA/CREB signaling pathway and the activation of cyclins and cell cycle progression (8, 10), we investigated the possibility that interrupting the β2M-mediated signaling axis may be cytotoxic to prostate cancer cells. When the LNCaP and C4-2B cells were exposed to the β2M antibody (0-20 μg/mL) for a 2-day incubation, the growth of these two prostate cancer cell lines was inhibited in a concentration-dependent manner, with an IC_{50} of 10.3 and 7.4 μg/mL, respectively (Fig. 2A). The purified β2M protein was shown to rescue the β2M antibody–induced inhibition of prostate cancer cell proliferation, whereas the control IgG did not affect the growth of the LNCaP and C4-2B cells (Fig. 2A). Because of the AR heterogeneity in human prostate cancer cells (18), we compared the effects of the β2M antibody on the cell proliferation of AR-positive (LNCaP, C4-2B, and ARCaP) and AR-negative (PC3 and DU-145) human prostate cancer cell lines. Figure 2B shows that the β2M antibody (10 μg/mL) inhibited the proliferation of these prostate cancer cells at day 3 by 57% (LNCaP), 82% (C4-2B), 91% (DU-145), 93% (PC3), and 94% (ARCaP). These data suggest that the β2M antibody significantly inhibited cell proliferation in a broad range of human prostate cancer cell lines.

β2M antibody induced apoptotic death and inhibited AR expression of prostate cancer cells* in vitro *and in mouse xenograft models. To determine the molecular mechanism by which the β2M antibody inhibited the growth of prostate cancer cells, we first examined apoptotic death in LNCaP and C4-2B cells, including sub-G_1 DNA content analysis and activation of caspase (19) and PARP expression. The results of flow cytometric analysis revealed that the β2M antibody greatly increased sub-G_1 DNA contents in LNCaP (% sub-G_1 = 82.49) and C4-2B (% sub-G_1 = 79.45) cells compared with the control IgG-treated LNCaP (% sub-G_1 = 0.86) and C4-2B (% sub-G_1 = 0.54) cells (Fig. 3A). Western blot analysis of

[5] Unpublished data.

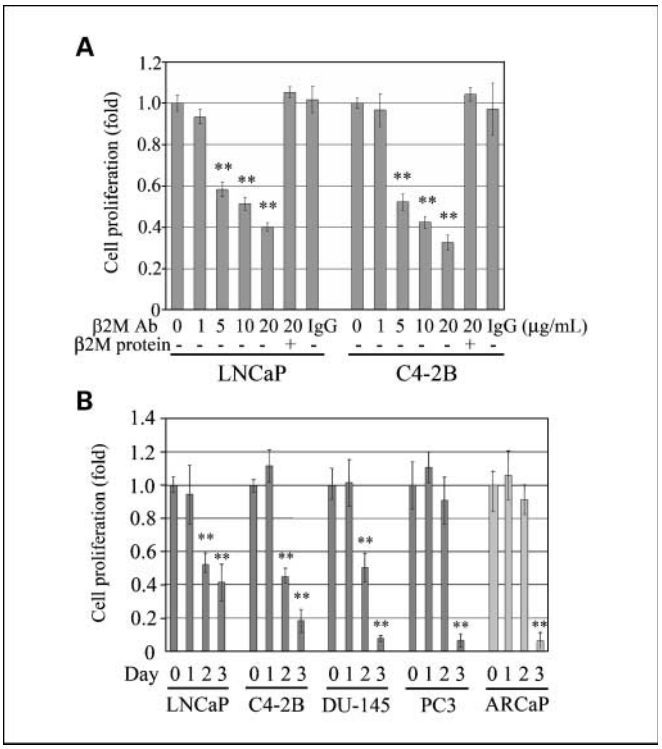

Fig. 2. β2M antibody inhibited the growth of prostate cancer cell lines. *A,* β2M antibody significantly affected the cell proliferation of LNCaP and C4-2B prostate cancer cells, with a dose-dependent inhibition (0-20 μg/mL) after 2-d incubation determined by mitochondrial MTS assay (Promega). Purified β2M protein rescued the inhibitory effect on cell growth regulated by the β2M antibody. IgG (20 μg/mL) did not decrease the growth of LNCaP and C4-2B cells. The relative fold was assigned as 1.0 in the absence of β2M antibody treatment. **, $P < 0.005$, significant differences from the β2M-antibody – untreated group. Columns, mean of five replicate experiments; bars, SD. *B,* β2M antibody (10 μg/mL) inhibited the cell proliferation of a broad range of human prostate cancer cell lines, LNCaP, C4-2B, DU-145, PC3, and ARCaP, during 3-d treatment. The cell numbers were measured daily with a mitochondrial MTS method. The relative fold was assigned as 1.0 at day 0 for each prostate cancer cell line. **, $P < 0.005$, significant differences from day 0 for each cell line. Columns, mean of four or five replicate experiments; bars, SD.

caspases showed that cleaved caspase-9, caspase-3, and PARP, a downstream factor of caspases, were increased by exposing the LNCaP and C4-2B cells to the β2M antibody, but not the control IgG, for a 48-h incubation (Fig. 3B). The induction of cleaved caspases and PARP was attenuated by the preincubation of the β2M antibody with purified β2M protein. In addition, cell death induced by the β2M antibody was also confirmed at the level of light microscopy in LNCaP and C4-2B cells (Fig. 3C).

Next, we examined the effects of the β2M antibody on cell death and/or the status of AR in preexisting C4-2 (AR positive) and PC3 (AR negative) prostate tumors grown in mice as subcutaneous xenografts, with the antibody delivered as Surgifoam implants, and isotype-matched IgG and saline delivered similarly as controls. After 1-week treatment, tumor tissues were harvested from the euthanized mice and subjected to immunohistochemical staining of the AR and a commercially available cell death marker, M30 CytoDeath. Figure 4A and B shows that the β2M antibody dramatically inhibited AR expression in C4-2 tumors and induced cell death in both C4-2 and PC3 tumors in mice compared with the IgG-treated and saline-treated controls. The cell numbers of positive AR staining in the β2M-antibody–treated C4-2 tumor xenografts were greatly decreased from 81 ± 6 per 100 cells (IgG controls) and 76 ± 4 per 100 cells (saline controls) to 10 ± 3 per 100 cells. Markedly increased prostate cancer death from the β2M antibody was observed in both C4-2 (the positive M30 CytoDeath staining cells were 36 ± 8 cells per 100 cells) and PC3 (55 ± 15 cells per 100 cells) tumor specimens compared with the IgG-treated (C4-2, 9 ± 2 cells per 100 cells; PC3, 16 ± 3 cells per 100 cells) and saline-treated (C4-2, 10 ± 3 cells per 100 cells; PC3, 13 ± 2 cells per 100 cells) control groups.

We further investigated whether the β2M antibody may be a safe reagent to selectively kill cancer but not normal or nontumorigenic immortalized cell lines. A human nontumorigenic prostatic epithelial cell line, RWPE-1, was exposed to the β2M antibody and the control IgG. In contrast to human prostate cancer cells, the β2M antibody did not inhibit RWPE-1 cell growth (Fig. 5A), did not decrease its endogenous AR expression (Fig. 5B), and did not activate apoptotic marker expression as assayed by Western blot (Fig. 5B). While the β2M antibody showed low cytotoxicity in RWPE-1 cells, it also did not affect the growth of P69, a SV40-immortalized human normal prostatic epithelial cell line (20), and human normal prostatic stromal cells (data not shown).

In summary, our results collectively indicate that the β2M antibody effectively induced human prostate cancer, but not normal prostate, cell apoptosis in culture. The β2M antibody induced cell death in prostate tumor xenografts in mice regardless of their AR status. The β2M antibody was also shown to down-regulate AR and PSA expression in AR-positive and PSA-positive human prostate cancer cells grown in culture and as subcutaneous xenografts in mice.

Discussion

Prostate cancer progression from an androgen-dependent to an androgen-independent state symbolizes its hormone-refractory status and occurs in patients clinically. Because there is currently no effective therapy for the management of hormone-refractory prostate cancer, we undertook the investigation of the molecular mechanisms and effects of a recently identified novel molecular target, β2M, using β2M antibody as a single agent in experimental models of human prostate cancer. Our results showed that the β2M antibody exerted growth inhibitory and apoptotic action in AR-positive and PSA-positive human prostate cancer cells. The β2M antibody was also shown to induce similar apoptotic death in AR-negative and PSA-negative, and androgen-unresponsive human prostate cancer cells. Because aberrant androgen signaling mediated by the AR, a ligand-activated transcription factor and a survival factor, plays a key role in regulating prostate cancer growth and survival even in cells that are considered as androgen refractory (21, 22), we investigated the effects of the β2M antibody on the AR-signaling axis based on a cDNA microarray study, in which targeting β2M was shown to markedly down-regulate AR and PSA in AR-positive human prostate cancer cells C4-2B. Our results confirmed that the β2M antibody blocked AR signaling and PSA production in a series of AR-positive and PSA-positive, and lineage-related LNCaP (androgen dependent), C4-2 (androgen independent), and C4-2B (androgen independent) cells in a β2M-dependent manner (i.e., β2M protein could rescue the inhibitory effects of the β2M antibody).

We previously reported that a small protein, β2M, which was considered as a "housekeeping" gene product (23), was a key growth and signaling molecule regulating osteomimicry and promoting growth and survival in prostate cancer cells (8, 9). Targeting β2M and its signaling by β2M siRNA greatly induced prostate cancer cell death both in cultured cells and in mice with preestablished human prostate tumors (8). In the present study, we used the β2M antibody to block β2M-related signaling pathways, hoping to induce apoptosis in prostate tumors and rationalize the exploration of the β2M antibody as a novel agent for clinical trial in men with hormone-refractory cancer. We showed that the β2M antibody as a single agent significantly inhibited AR and PSA mRNA and protein expression in both LNCaP and C4-2B cells and induced apoptotic cell death in prostate tumor cells *in vitro* and in mouse xenografts (C4-2 and PC3 tumors) *in vivo* regardless of their AR status. The selective ability of the β2M antibody to block prostate tumor growth without affecting normal or nontumorigenic cells, including human normal prostatic epithelial and stromal cells, and normal hematopoietic cells *in vitro* or other normal tissues *in vivo* (12), suggests that the β2M antibody is a cancer-specific targeting agent that can be applied in the treatment of human prostate cancers. This conclusion is supported by previous studies in which immune intact mice with β2M knockdown survived and developed mild degrees of iron overload and arthritis without compromising their life expectancy (24–26). In addition, during a 10-week observation period, we have not noted any toxicity in mice treated intratumorally with the β2M antibody as evaluated by their body weights and physical appearance (data not shown). This observation is concurred by the early report of Yang et al. (12) although additional work is warranted to test the potential cytotoxicity of this antibody in immune intact hosts. We envision, nevertheless, that the β2M antibody can be applied in a cyclic manner to patients with prostate cancer, allowing

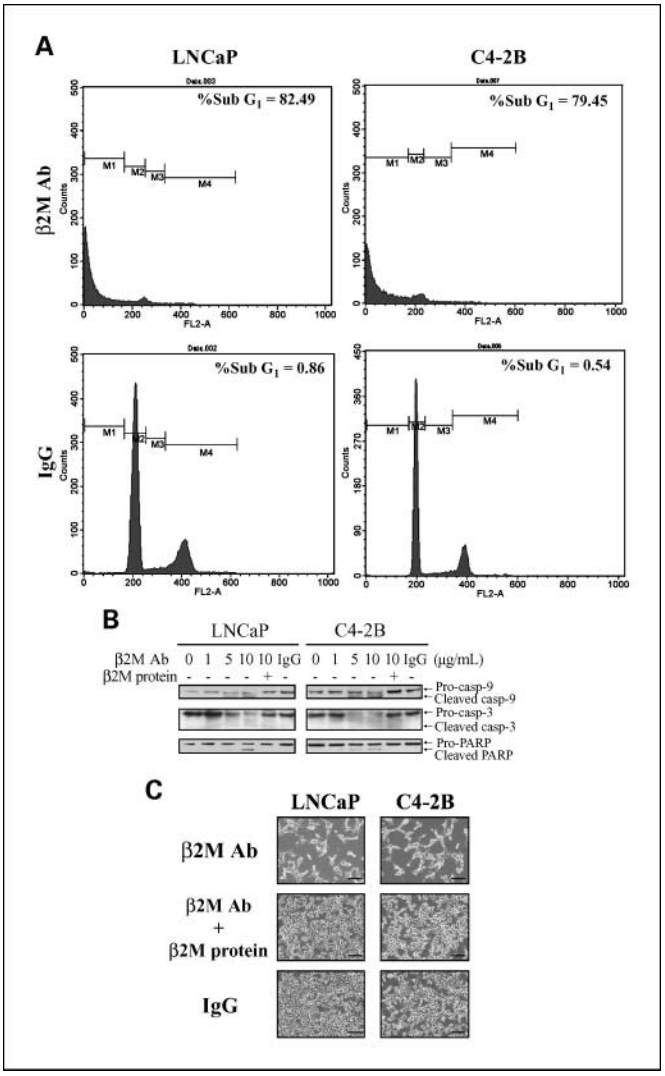

Fig. 3. β2M antibody induced the cell death of prostate cancer cells through an apoptotic cascade pathway. *A,* LNCaP and C4-2B cells were exposed to either the β2M antibody or isotype control IgG (10 μg/mL) for 48-h incubation and subjected to cell cycle analysis determined by flow cytometry. Both LNCaP and C4-2B cells treated with the β2M antibody showed a marked increase in the sub-G_1 DNA contents compared with IgG-treated cells. *B,* β2M antibody (0-10 μg/mL, 48-h treatment) activated the expression of cleaved caspase-9, caspase-3, and PARP proteins in a dose-dependent pattern in LNCaP and C4-2B cells as assayed by Western blot. β2M protein rescued the apoptotic effect of the β2M antibody. Control IgG (10 μg/mL) did not activate cleaved caspase and PARP expression. *C,* LNCaP and C4-2B cells were treated with the β2M antibody; the β2M antibody was preincubated with β2M protein or control IgG (10 μg/mL) for 48 h and examined by light microscopy. Bar, 250 μm.

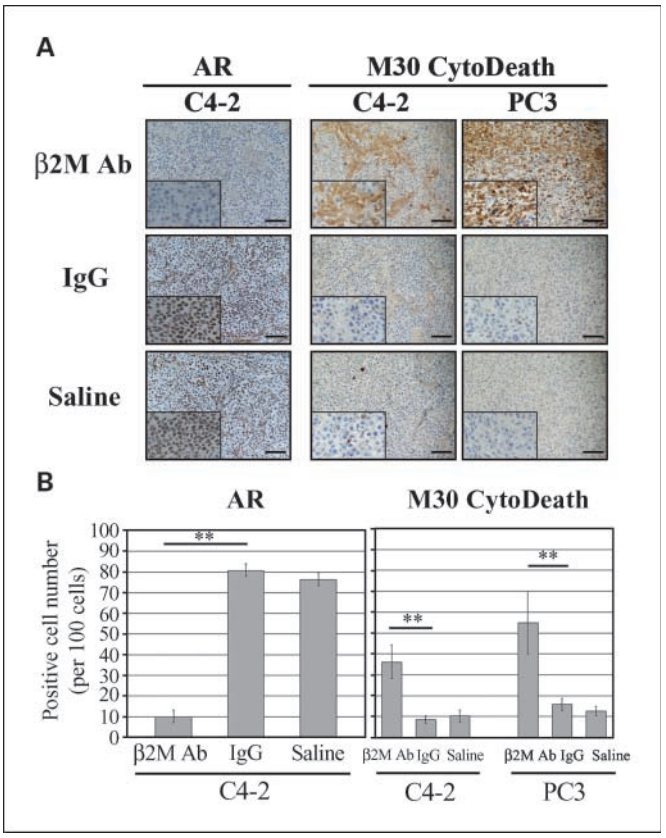

Fig. 4. β2M antibody decreased AR expression and induced the cell death of subcutaneous C4-2 and PC3 prostate tumor growth in athymic *nu/nu* mice. *A,* immunohistochemical analysis showed dramatic down-regulation of AR expression in β2M antibody – treated subcutaneous C4-2 tumor mouse xenografts ($n = 4$) but not in the control IgG-treated ($n = 4$) or saline-treated ($n = 4$) C4-2 tumor-bearing mice. The β2M antibody also markedly induced apoptotic death in both subcutaneous C4-2 ($n = 4$) and PC3 ($n = 4$) prostate tumors in xenograft mice assayed by M30 CytoDeath marker staining. Bar, 100 μm. *B,* quantification of the positive AR and M30 CytoDeath marker staining cells in C4-2 and PC3 tumor specimens from the immunohistochemical analysis (*A*). One hundred cells at five randomly selected areas were counted. **, $P < 0.005$, significant differences from the control IgG group. Columns, mean; bars, SD.

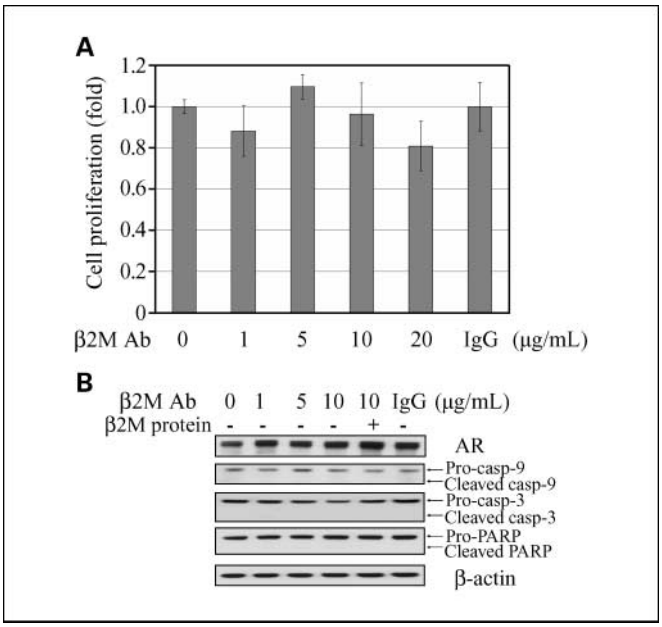

Fig. 5. β2M antibody did not affect cell proliferation and endogenous AR expression; it also did not induce apoptotic death in human normal/nontumorigenic prostatic epithelial cells. *A,* β2M antibody (0-20 μg/mL, 3-d incubation) did not significantly affect cell proliferation of human normal prostatic epithelial cells, RWPE-1, as determined by mitochondrial MTS assay. Control IgG (20 μg/mL) also did not affect the growth of RWPE-1 cells. The relative fold was assigned as 1.0 in the absence of β2M antibody treatment. Columns, mean of five replicate experiments; bars, SD. *B,* β2M antibody (0-10 μg/mL, 24-h treatment) did not inhibit AR nor activate cleaved caspase-9, caspase-3, and PARP protein expression in RWPE-1 cells assayed by Western blot. Control IgG (10 μg/mL) also did not affect AR, cleaved caspase, or PARP protein expression.

the immune system to return to normal function during the off-cycle of the β2M antibody application.

Other than the blockade of the β2M antibody on AR survival factor expression, the detailed molecular mechanisms by which the β2M antibody induced prostate cancer apoptosis are unclear. We previously showed that β2M promoted the expression of cell cycle markers, cyclin D1 and cyclin A, and cell growth in prostate cancer cells through the activation of a cAMP/PKA/CREB signaling pathway (8). We also showed that β2M stimulated renal cancer cell proliferation via the induction of phosphatidylinositol 3-kinase (PI3K)/Akt, mitogen-activated protein kinase (MAPK), and cAMP/PKA/CREB pathways (10). This pleiotropic cell signaling network activated by β2M is likely to be the target for the β2M antibody. It has been amply documented that the activation of AR, PI3K/Akt, and MAPK pathways are important features contributing to uncontrolled prostate cancer cell growth and survival (22, 27, 28). Indeed, we observed that the β2M antibody blocked not only the AR (Fig. 1A and B) but also the cell signaling network mediated by PI3K/Akt and MAPK pathways in LNCaP and C4-2B cells (Supplementary Fig. S1). These results are consistent with previous presentations that blocking β2M-mediated signaling pathways can interrupt the PI3K/Akt and MAPK signaling pathways and induce c-Jun-NH_2-kinase phosphorylation, resulting in the activation of a caspase-9–dependent apoptotic cascade in human renal cell carcinoma (13) and hematologic cancer cells (12). The constitutive activation of a PI3K/Akt signaling pathway has been shown in prostate cancer cell lines by the inactivation of the PTEN tumor suppressor (29). Because the PI3K/Akt signaling pathway has been reported to mediate AR mRNA and protein expression through AR promoter regulation (30), we anticipated that the β2M antibody inhibition of the PI3K/Akt and MAPK signaling pathways would cause growth retardation, apoptosis, and down-regulation of AR expression and activity in AR-positive and PSA-positive LNCaP/C4-2/C4-2B cells. Likewise, because of the blockade of these critical signaling pathways, we also expected diminished growth and induced apoptosis in AR-negative prostate cancer cells *in vitro* and *in vivo*. These results could have significant clinical implications. For example, the β2M antibody could be superior to other antiandrogenic therapies with actions that rely on intrinsic AR expression by prostate cancer cells. The β2M antibody could be used either as a single reagent or in combination with other therapeutic modalities for the treatment of both hormone-dependent and hormone-refractory prostate cancers because these have been shown to exhibit marked heterogeneity of AR expression (31). This approach is promising, considering recent success in the development of therapeutic antibodies (32), such as trastuzumab, a HER2/erbB2 antibody for breast cancers; bevacizumab, a vascular endothelial growth factor antibody; and cetuximab, an epidermal growth factor receptor antibody for metastatic colon cancers.

In summary, our investigation revealed for the first time that (*a*) the β2M antibody inhibited the expression of the AR and PSA in both androgen-dependent and androgen-independent AR-positive and PSA-positive human prostate cancer cells; (*b*) the β2M antibody has a broad spectrum of growth-inhibitory effects in both AR-positive and AR-negative prostate cancer cells; and (*c*) although the β2M antibody has been shown to be a potent pleiotropic signaling and growth inhibitor and to induce programmed cell death through a caspase-9–dependent pathway in prostate cancer cells, this antibody exhibited low cytotoxicity in human normal prostatic epithelial and stromal cells, which make it an attractive and safe therapeutic agent for future clinical application to treat prostate cancer and its progression.

Disclosure of Potential Conflicts of Interest

No potential conflicts of interest were disclosed.

Acknowledgments

We thank Gary Mawyer for editing the manuscript, our colleagues for helpful discussions, and Dr. Peter S. Nelson and colleagues (Fred Hutchinson Cancer Research Center, Seattle, WA) for performing the cDNA microarray in this study.

References

1. Gussow D, Rein R, Ginjaar I, et al. The human β 2-microglobulin gene. Primary structure and definition of the transcriptional unit. J Immunol 1987;139:3132–8.
2. Cunningham BA, Wang JL, Berggard I, Peterson PA. The complete amino acid sequence of β2-microglobulin. Biochemistry 1973;12:4811–22.
3. Pedersen LO, Hansen AS, Olsen AC, Gerwien J, Nissen MH, Buus S. The interaction between β2-microglobulin (β2m) and purified class-I major histocompatibility (MHC) antigen. Scand J Immunol 1994;39:64–72.
4. Abdul M, Hoosein N. Changes in β-2 microglobulin expression in prostate cancer. Urol Oncol 2000;5:168–72.

5. Vitale M, Rezzani R, Rodella L, et al. HLA class I antigen and transporter associated with antigen processing (TAP1 and TAP2) down-regulation in high-grade primary breast carcinoma lesions. Cancer Res 1998; 58:737–42.

6. Korkolopoulou P, Kaklamanis L, Pezzella F, Harris AL, Gatter KC. Loss of antigen-presenting molecules (MHC class I and TAP-1) in lung cancer. Br J Cancer 1996;73:148–53.

7. Vegh Z, Wang P, Vanky F, Klein E. Selectively down-regulated expression of major histocompatibility complex class I alleles in human solid tumors. Cancer Res 1993;53:2416–20.

8. Huang WC, Wu D, Xie Z, et al. β2-Microglobulin is a signaling and growth-promoting factor for human prostate cancer bone metastasis. Cancer Res 2006; 66:9108–16.

9. Huang WC, Xie Z, Konaka H, Sodek J, Zhau HE, Chung LW. Human osteocalcin and bone sialoprotein mediating osteomimicry of prostate cancer cells: role of cAMP-dependent protein kinase A signaling pathway. Cancer Res 2005;65:2303–13.

10. Nomura T, Huang WC, Zhau HE, et al. β2-Microglobulin promotes the growth of human renal cell carcinoma through the activation of the protein kinase A, cyclic AMP-responsive element-binding protein, and vascular endothelial growth factor axis. Clin Cancer Res 2006;12:7294–305.

11. Gross M, Top I, Laux I, et al. {β}-2-Microglobulin is an androgen-regulated secreted protein elevated in serum of patients with advanced prostate cancer. Clin Cancer Res 2007;13:1979–86.

12. Yang J, Qian J, Wezeman M, et al. Targeting β2-microglobulin for induction of tumor apoptosis in human hematological malignancies. Cancer Cell 2006;10:295–307.

13. Nomura T, Huang WC, Seo S, Zhau HE, Mimata H, Chung LW. Targeting β2-microglobulin mediated signaling as a novel therapeutic approach for human renal cell carcinoma. J Urol 2007;178:292–300.

14. Thalmann GN, Sikes RA, Wu TT, et al. LNCaP progression model of human prostate cancer: androgen-independence and osseous metastasis. Prostate 2000;44:91–103.

15. Xu J, Wang R, Xie ZH, et al. Prostate cancer metastasis: role of the host microenvironment in promoting epithelial to mesenchymal transition and increased bone and adrenal gland metastasis. Prostate 2006; 66:1664–73.

16. Zhau HY, Chang SM, Chen BQ, et al. Androgen-repressed phenotype in human prostate cancer. Proc Natl Acad Sci U S A 1996;93:15152–7.

17. Nelson PS, Clegg N, Arnold H, et al. The program of androgen-responsive genes in neoplastic prostate epithelium. Proc Natl Acad Sci U S A 2002;99: 11890–5.

18. Ruizeveld de Winter JA, Janssen PJ, Sleddens HM, et al. Androgen receptor status in localized and locally progressive hormone refractory human prostate cancer. Am J Pathol 1994;144:735–46.

19. Thornberry NA, Lazebnik Y. Caspases: enemies within. Science 1998;281:1312–6.

20. Bae VL, Jackson-Cook CK, Brothman AR, Maygarden SJ, Ware JL. Tumorigenicity of SV40 Tantigen immortalized human prostate epithelial cells: association with decreased epidermal growth factor receptor (EGFR) expression. Int J Cancer 1994;58:721–9.

21. Dehm SM, Tindall DJ. Regulation of androgen receptor signaling in prostate cancer. Expert Rev Anticancer Ther 2005;5:63–74.

22. Heinlein CA, Chang C. Androgen receptor in prostate cancer. Endocr Rev 2004;25:276–308.

23. Schmittgen TD, Zakrajsek BA. Effect of experimental treatment on housekeeping gene expression: validation by real-time, quantitative RT-PCR. J Biochem Biophys Methods 2000;46:69–81.

24. Muckenthaler MU, Rodrigues P, Macedo MG, et al. Molecular analysis of iron overload in β2-microglobulin-deficient mice. Blood Cells Mol Dis 2004;33: 125–31.

25. Kingsbury DJ, Mear JP, Witte DP, Taurog JD, Roopenian DC, Colbert RA. Development of spontaneous arthritis in β2-microglobulin-deficient mice without expression of HLA-B27: association with deficiency of endogenous major histocompatibility complex class I expression. Arthritis Rheum 2000;43:2290–6.

26. Koller BH, Marrack P, Kappler JW, Smithies O. Normal development of mice deficient in β2M, MHC class I proteins, and CD8+ T cells. Science 1990;248: 1227–30.

27. Uzgare AR, Isaacs JT. Enhanced redundancy in Akt and mitogen-activated protein kinase-induced survival of malignant versus normal prostate epithelial cells. Cancer Res 2004;64:6190–9.

28. Murillo H, Huang H, Schmidt LJ, Smith DI, Tindall DJ. Role of PI3K signaling in survival and progression of LNCaP prostate cancer cells to the androgen refractory state. Endocrinology 2001;142: 4795–805.

29. Vlietstra RJ, van Alewijk DC, Hermans KG, van Steenbrugge GJ, Trapman J. Frequent inactivation of PTEN in prostate cancer cell lines and xenografts. Cancer Res 1998;58:2720–3.

30. Yang L, Xie S, Jamaluddin MS, et al. Induction of androgen receptor expression by phosphatidylinositol 3-kinase/Akt downstream substrate, FOXO3a, and their roles in apoptosis of LNCaP prostate cancer cells. J Biol Chem 2005;280:33558–65.

31. Magi-Galluzzi C, Xu X, Hlatky L, et al. Heterogeneity of androgen receptor content in advanced prostate cancer. Mod Pathol 1997;10:839–45.

32. Lin MZ, Teitell MA, Schiller GJ. The evolution of antibodies into versatile tumor-targeting agents. Clin Cancer Res 2005;11:129–38.

BKM1740, an Acyl-Tyrosine Bisphosphonate Amide Derivative, Inhibits the Bone Metastatic Growth of Human Prostate Cancer Cells by Inducing Apoptosis

Seong Il Seo,[2] Lajos Gera,[3] Haiyen E. Zhau,[1] Wei Ping Qian,[1] Shareen Iqbal,[1] Nicole A. Johnson,[1] Shumin Zhang,[1] Majd Zayzafoon,[4] John Stewart,[3] Ruoxiang Wang,[1] Leland W.K. Chung,[1] and Daqing Wu[1]

Abstract

Purpose: Survivin overexpression has been associated with an unfavorable outcome in human PCa; however, its role in metastasis remains elusive. We aim to (*a*) evaluate the clinical implications of survivin expression in PCa bone metastasis; (*b*) determine *in vivo* efficacy of BKM1740, a small-molecule compound, against PCa skeletal growth and survival; and (*c*) investigate molecular mechanism by which BKM1740 augments apoptosis in bone metastatic PCa cells.

Experimental Design: Survivin expression was analyzed in PCa specimens and experimental models. Bone metastatic C4-2 and ARCaP$_M$ cell lines were used to evaluate the *in vitro* effects of BKM1740 and molecular mechanism for the induction of apoptosis. C4-2 cells were grown intratibially in athymic nude mice to evaluate the *in vivo* efficacy of BKM1740. Tumor growth in mouse bone was assessed by serum prostate-specific antigen and radiography and confirmed by immunohistochemical analyses.

Results: Survivin expression is positively associated with clinical PCa bone metastasis. BKM1740 induced apoptosis in PCa cells by repressing survivin. Mice with established C4-2 tumors in tibia showed a marked decrease in serum prostate-specific antigen and much improved bone architecture radiographically after treatment with BKM1740. Immunohistochemical assays of mouse tumor samples confirmed that the *in vivo* effects were mediated by inhibition of survivin and induction of apoptosis.

Conclusions: Survivin expression is associated with PCa bone metastasis. BKM1740 treatment specifically inhibited survivin and induced apoptosis *in vitro* and was efficacious in retarding PCa skeletal growth in a mouse model. BKM1740 is a promising small-molecule compound that could be used to treat PCa bone metastasis.

Authors' Affiliations: [1]Molecular Urology and Therapeutics Program, Department of Urology and Winship Cancer Institute, Emory University School of Medicine, Atlanta, Georgia; [2]Department of Urology, Samsung Medical Center, Sungkyunkwan University School of Medicine, Seoul, Republic of Korea; [3]Department of Biochemistry and Molecular Genetics, University of Colorado Health Sciences Center, Denver, Colorado; and [4]Department of Pathology, University of Alabama at Birmingham, Birmingham, Alabama

Received 4/21/08; revised 5/20/08; accepted 5/21/08.

Grant support: NIH grants 1P01 CA098912, 1R01 CA108468, and 5P20GM072069 (L.W.K. Chung) and Department of Defense grants PC040260 (L.W.K. Chung) and PC060566 (D.Wu).

The costs of publication of this article were defrayed in part by the payment of page charges. This article must therefore be hereby marked *advertisement* in accordance with 18 U.S.C. Section 1734 solely to indicate this fact.

Note: Supplementary data for this article are available at Clinical Cancer Research Online (http://clincancerres.aacrjournals.org/).

S.I. Seo and L. Gera contributed equally to this work.

Requests for reprints: Daqing Wu or Leland W.K. Chung, Molecular Urology and Therapeutics Program, Department of Urology and Winship Cancer Institute, Emory University School of Medicine, 1365-B Clifton Road, Suite 5100, Atlanta, GA 30322. Phone: 404-778-4845; Fax: 404-778-3965; E-mail: dwu2@emory.edu or lwchung@emory.edu.

doi:10.1158/1078-0432.CCR-08-1023

Bone metastasis and skeletal complications are the major contributing factors to human prostate cancer (PCa) morbidity and mortality (1). The gain of function of antiapoptotic factors and/or loss of function of proapoptotic proteins may allow PCa cells to evade apoptosis during dissemination and growth in bone tissue (2). As a member of the inhibitor of apoptosis family, survivin intersects multiple survival signals and is highly differentially expressed in cancer (3). In PCa, survivin overexpression has frequently been associated with an unfavorable outcome. Survivin expression is significantly elevated in tumors with a high Gleason score and lymph node metastasis (4, 5). Survivin also mediates resistance to antiandrogen therapy, chemotherapy, and irradiation (6–8). However, despite the well-defined function of survivin in antagonizing death signals during tumorigenesis, little is known about its role in tumor invasion and metastasis (9).

Currently, several strategies are being pursued to target survivin expression or interrupt its antiapoptotic function. Some have been in clinical trials for a variety of human cancers (see ref. 10 for review). Some small-molecule antagonists exert their antitumor function by indirectly targeting pathways implicated in survivin regulation (such as STA-21 inhibition

Translational Relevance

Bone metastasis is the leading cause of prostate cancer (PCa) death. Current therapy does not improve patient survival. It is critical to identify novel targets for developing efficacious treatments. This study showed that overexpression of survivin, a critical antiapoptotic protein, is associated with clinical PCa progression and bone metastasis. We developed BKM1740, a small-molecule acyltyrosine bisphosphonate amide derivative, and found that BKM1740 efficaciously retards PCa skeletal growth in athymic nude mice. Mechanistic study confirmed that the *in vivo* effects were mediated by specific inhibition of survivin and induction of apoptosis. This study validated the clinical implications of survivin expression in PCa bone metastasis and may have a significant effect on the development of efficacious and safe therapeutic regimens for metastatic PCa and other types of cancers.

of the signal transducer and activator of transcription 3 pathway or flavopiridol inhibition of cyclin-dependent kinase 1 activity) or by perturbing protein-protein interaction between survivin and its partners (such as shepherdin, a peptidyl antagonist that may disrupt the interaction between heat shock protein 90 and survivin). Some agents have been developed to directly suppress survivin expression, including an antisense molecule (LY218130B) and transcriptional repressors (YM155 and EM-1421). In established human PCa PC-3 xenografts, YM155, a small imidazolium-based compound, was shown to specifically suppress survivin transcription (11). Two phase I trials for YM155 have been completed in 41 patients with PCa, non–Hodgkin lymphoma, or colorectal cancer. The treatment was well tolerated and exhibited encouraging antitumor efficacy (12). Nonetheless, the portfolio of truly survivin-directed antagonists or suppressors available for clinical testing, particularly in metastatic cancer, is small (10).

Bradykinin-related compounds are emerging as promising antitumor agents (13–15). In experimental models for human PCa and lung cancer, a bradykinin antagonist peptide dimer, B-9870 (CU201), and its nonpeptide mimetic, BKM-570, suppress tumor growth and act synergistically with standard chemotherapy drugs such as cisplatin and Taxotere (16–18). Mechanistic study indicated that the bradykinin-related compounds induce caspase-dependent apoptosis in cancer cells while inhibiting angiogenesis and reducing tissue permeability mediated by matrix metalloproteinases (MMP) in tumors (15). Therefore, these compounds may be pluripotent anticancer agents. To explore novel drugs that may specifically target bone metastatic PCa cells, we developed a BKM-570 analogue conjugated with an aminobisphosphonate group. This compound, termed BKM1740, was found to be efficacious in retarding skeletal growth of human PCa cells through direct inhibition of survivin in a xenograft model.

Materials and Methods

Cell lines and culture conditions. Human PCa cell lines LNCaP, C4-2 (19), $ARCaP_E$, and $ARCaP_M$ (20) were regularly maintained in T-medium (Invitrogen) supplemented with 5% fetal bovine serum (Sigma), 100 IU/L penicillin G, and 100 μg/L streptomycin at 37°C under 5% CO_2.

Chemicals. BKM1740 was developed and synthesized by Gera in the Stewart laboratory according to previously described methods (18, 21, 22). For the *in vitro* and *in vivo* studies, the BKM1740 was dissolved in DMSO (Sigma) at 10 mg/mL stock solution and its purity was determined to be a minimum of 99% by high-performance liquid chromatography.

Cell proliferation assay. Cell proliferation was measured using the CellTiter 96 AQueous Non-Radioactive Cell Proliferation Assay [3-(4,5-dimethylthiazol-2-yl)-5-(3-carboxymethoxyphenyl)-2-(4-sulfophenyl)-2*H*-tetrazolium salt (MTS) assay; Promega]. Briefly, cells suspended in T-medium plus 5% fetal bovine serum were added to 96-well plates at 5,000 per well in sextuplicate. After 24 h of culture, BKM1740 or DMSO was added in various concentrations, and cells were cultured for the indicated time. Combined MTS/phenazine methosulfate solution (20 μL/well) was added to the cells and the absorbance at 490 nm was recorded after 1 h of incubation at 37°C using a microplate reader (Bio-Rad Laboratories). Cell viability was expressed as relative survival with controls recorded as 100%.

Reporter assay. Cells were seeded at a density of 1.5×10^5 per well in 12-well plates 24 h before transfection. pSurvivin-luc1430 (23) and pRL-TK (as internal control; Promega) were introduced using Lipofectamine 2000 (Invitrogen). A Dual-Luciferase Reporter Assay kit (Promega) was used to determine the firefly luciferase activity and *Renilla* luciferase activity. Data were presented as relative luciferase activity (firefly luciferase activity normalized to *Renilla* luciferase activity).

Western blot analysis. Total cell lysates were prepared using radioimmunoprecipitation assay buffer (Santa Cruz Biotechnology). Protein concentrations in the supernatants were measured with the bicinchoninic acid protein assay kit (Pierce Biotechnology). Total protein (50 μg) was loaded to each lane, resolved on a 4% to 12% NuPAGE Bis-Tris–buffered (pH 7.0) polyacrylamide gel (Invitrogen), and transferred onto a nitrocellulose membrane (Bio-Rad Laboratories). The membrane was incubated with anti-survivin (Novus Biologicals), anti-caspase-3, anti-cleaved caspase-3, anti-caspase-8, anti-cleaved caspase-8, anti-caspase-9, anti-poly(ADP-ribose) polymerase (Cell Signaling), and anti-myeloid cell leukemia-1 (Mcl-1) and MMP-9 (Santa Cruz Biotechnology), with anti-β-actin (Sigma) or anti-EF1α (BD Transduction Laboratories) as loading controls. The reactive bands were visualized by an enhanced chemiluminescence assay kit (Amersham Pharmacia Biotech). Quantification of band intensity was measured by densitometry and analyzed with ImageJ (NIH). Relative protein expression was expressed as fold change compared with control (β-actin or EF1α).

Reverse transcription-PCR. Total RNA was prepared using a Qiagen RNeasy kit. One microgram was used as a template in a reaction using the SuperScript III One-Step reverse transcription-PCR (RT-PCR) kit (Invitrogen). The primer pairs specific for human survivin are 5′-ccaccgcatctctacattca-3′ (forward) and 5′-gcactttcttcgcagtttc-3′ (reverse); for human Mcl-1, 5′-gaggaggaggaggacgagtt-3′ (forward) and 5′-gtcccgttttgtccttacga-3′ (reverse). The primers for vascular endothelial growth factor (VEGF) and glyceraldehyde-3-phosphate dehydrogenase were described previously (24). The thermal profile is 23 cycles for human survivin, Mcl-1, and VEGF amplification or 20 cycles for glyceraldehyde-3-phosphate dehydrogenase, with 94°C, 15 s; 55°C, 30 s; and 68°C, 60 s. Quantification of band intensity was measured by densitometry and analyzed with ImageJ. Relative mRNA abundance was expressed as fold change compared with control (glyceraldehyde-3-phosphate dehydrogenase).

Condition medium preparation. Subconfluent C4-2 cells were serum starved overnight and further treated with BKM1740 or DMSO in fresh serum-free T-medium for 48 h before condition media were collected (24).

ELISA. Vascular endothelial cell growth factor (VEGF) concentration was analyzed using a Quantikine ELISA kit (R&D Systems).

Apoptosis analysis. Cells treated with DMSO or BKM1740 were trypsinized and washed with PBS and resuspended in Annexin-binding buffer (BD PharMingen). Cells were then stained with both Annexin V-phycoerythrin and 7-amino-actinomycin for 15 min at room temperature. The stained samples for apoptosis assay were measured using a fluorescence-activated cell sorting (FACS) caliber bench-top flow cytometer (Becton Dickinson). The data were analyzed using FlowJo software (Tree Star, Inc.). The experiments were repeated at least thrice independently.

Assessment of **in vivo** *effects of BKM1740 on human prostate tumor xenografts in mouse bone.* All animal procedures were done in compliance with Emory University Institutional Animal Care and Use Committee and NIH guidelines. A total of 1.0×10^6 C4-2 cells were inoculated in mouse bilateral tibia using a previously established procedure (25, 26). Blood specimens (70 μL) were obtained from the retro-orbital sinus vein every 2 wk for serum prostate-specific antigen (PSA) determination. Serum PSA was determined by microparticle ELISA using an Abbott IMx instrument (Abbott Laboratories). A total of 20 athymic male nude mice (BALB/c *nu/nu*; National Cancer Institute, Bethesda, MD) were divided into two groups: a vehicle control group ($n = 11$) and a BKM1740 treatment group ($n = 9$). The treatments were initiated at 4 wk after tumor cell inoculation with confirmed tumors in bone by X-ray and positive serum PSA (25, 27). BKM1740 was dissolved in 100% DMSO as a stock solution of 10 mg/mL. Mice were given BKM1740 every 2 d at 5 mg/kg via the i.p. route for an 8-wk period. Control mice received vehicle injections for the same duration. Mice were weighed every week and tumor growth in bilateral tibia was followed by serum PSA and X-ray every 2 wk. Mice were sacrificed 8 wk after the initiation of treatment. The bilateral tibia were removed, fixed in 10% neutralized formalin for 48 h, and decalcified in EDTA (pH 7.2) for 15 d. Tibia specimens were dehydrated and paraffin embedded for immunohistochemical analyses. To assess the systemic toxicity of BKM1740, athymic nude mice ($n = 4$) were administered at a high dose of 20 mg/kg via the i.p. route, twice per week, for 4 wk.

Immunohistochemical analysis. Survivin expression was analyzed in five human normal/benign prostatic glands, five each of well-differentiated and poorly differentiated primary PCa, and four bone metastatic PCa tissue specimens. Cell proliferation (Ki67), cell death (M30), and survivin in bone tumor specimens obtained from control and BKM1740-treated mice (two in each group) were conducted. Antibodies used were goat polyclonal antibody against Ki67 (1:500; Santa Cruz Biotechnology), mouse monoclonal antibody against M30 CytoDeath (1:500; DiaPharma Group, Inc.), and rabbit polyclonal antibody against survivin (1:200; Novus Biologicals). Tissues were deparaffinized, rehydrated, and subjected to 5-mn pressure-cooking antigen retrieval, 10-min double endogenous enzyme block, and 30-min primary antibody incubation, and subjected to 30-min DakoCytomation EnVision+ horseradish peroxidase reagent (for M30 and survivin) or 15 min each of biotinylated link and streptavidin-peroxidase label reagents (for Ki67) incubation. Signals were detected by adding substrate hydrogen peroxide using diaminobenzidine as chromogen and counterstained by hematoxylin. All reagents were obtained from Dako Corp. Matching sera and IgG were used as negative controls. Relative expression of Ki67, M30, and survivin was shown as the number of positively stained cells in 200 cells ± SE at three randomly selected areas at ×100 magnification.

Data analysis. All data represent three or more experiments. Treatment effects were evaluated using a two-sided Student's t test. Errors are SE values of averaged results, and values of $P < 0.05$ were taken as a significant difference between means.

Results

Elevation of survivin is correlated to bone metastasis status in human PCa tumors. To investigate the clinicopathologic significance of survivin expression in human PCa progression, we analyzed the immunohistochemical protein expression of

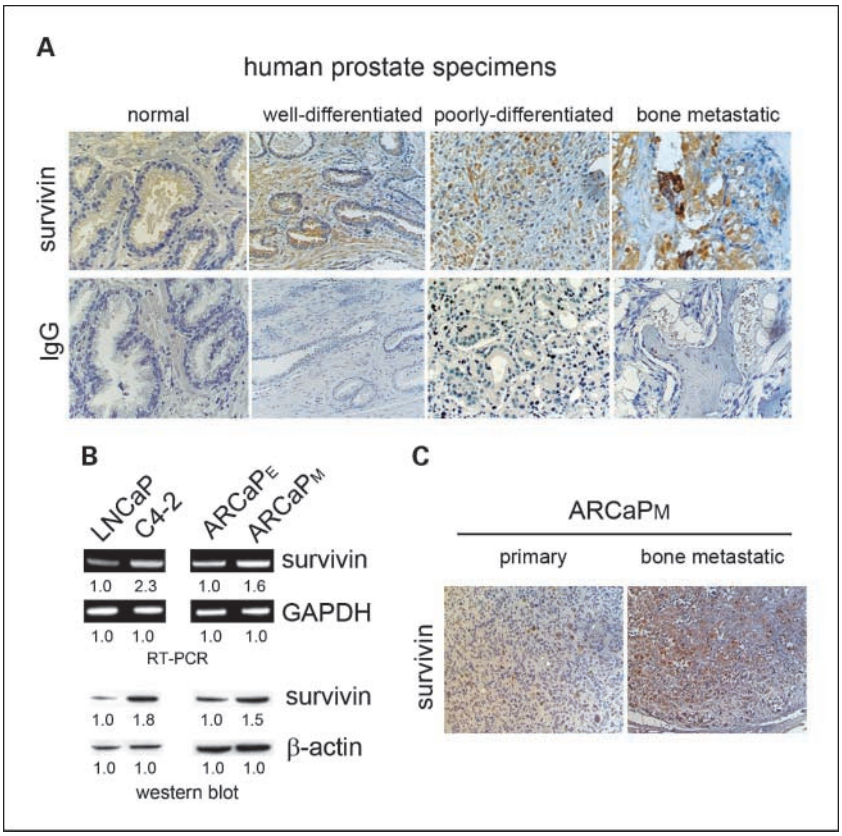

Fig. 1. Survivin expression is associated with bone metastasis in human PCa specimens and the ARCaP experimental model. *A,* survivin expression increased during PCa progression from normal to primary cancer to bone metastasis. *B,* RT-PCR and Western blot analyses of survivin expression in human PCa cell models. Survivin increased in bone metastatic C4-2 and $ARCaP_M$ cells compared with their parental LNCaP and $ARCaP_E$ cells. Relative expression was expressed as fold change compared with controls. GAPDH, glyceraldehyde-3-phosphate dehydrogenase. *C,* survivin expression in bone metastatic $ARCaP_M$ tumor was higher than in primary tumor.

survivin in primary and bone metastatic PCa tissue. We defined well-differentiated PCa as Gleason score ≤6 and poorly differentiated PCa as Gleason score ≥8. Survivin expression was undetectable to marginal in all normal/benign glands (n = 5) and increased from well-differentiated cancer (n = 5) to poorly differentiated cancers (n = 5). Importantly, survivin was highly expressed in all bone metastatic PCa tumor specimens (n = 4; Fig. 1A). These data suggest that survivin expression is positively associated with PCa progression, particularly bone metastasis.

We have established several lines of human PCa cells that represent a continuum of PCa progression closely mimicking the clinical pathophysiology of bone metastasis (see ref. 28 for review). Two lineage-related sets of PCa cells were used in this study: the LNCaP-C4-2 model (19, 29) and the $ARCaP_E$-$ARCaP_M$ model (20, 24, 30). RT-PCR and Western blotting analyses indicated that survivin expression was elevated in highly bone metastatic C4-2 and $ARCaP_M$ PCa cell lines compared with the less invasive parental cell lines LNCaP and $ARCaP_E$ (Fig. 1B). $ARCaP_M$ cells were inoculated into athymic mice s.c., which resulted in metastases to bone tissues within a short latency period (20, 31). Survivin expression was examined by immunohistochemical staining of the $ARCaP_M$ tumor specimens from either the primary site (s.c. injection) or metastatic bone. Consistently, survivin protein level was significantly increased in bone metastatic tumor compared with the primary tumor (Fig. 1C). These data obtained from *in vivo* PCa models validate a positive correlation between survivin expression and the bone metastatic propensity observed in clinical specimens.

BKM1740 induces apoptosis in metastatic PCa cells. BKM1740 is an acyl-tyrosine bisphosphonate amide derivative, which was developed from the key chemical structure of BKM-570, F5c-OC2Y [*N*-(2,3,4,5,6-pentaflurocinnamoyl)-*O*-(2,6-dichlorobenzyl)-tyrosine; refs. 18, 22]. BKM1740 is expected to have potent antitumor activity exhibited by the F5c-OC2Y moiety and can be selectively taken up and adsorbed to mineral surfaces in bone because of the introduction of the aminobisphosphonate moiety (32).

We first evaluated the cytotoxic effects of BKM1740 on bone metastatic PCa cells. C4-2 and $ARCaP_M$ cells were exposed to the indicated concentrations of BKM1740 for various durations and cell proliferation was determined by MTS assay. BKM1740 was found to inhibit the *in vitro* growth of C4-2 (Fig. 2B) and $ARCaP_M$ cells (Fig. 2C) in a dose- and time-dependent manner, with 50% inhibition (IC_{50}) observed at 2 and 9 μmol/L, respectively. Interestingly, compared with C4-2 cells, $ARCaP_M$ only responded to BKM1740 treatment significantly within a narrow dose range (between 8 and 10 μmol/L), suggesting that this cell line is more resistant to the cytotoxicity of BKM1740 (Fig. 2C).

To further elucidate the mechanism for the effects of BKM1740 on PCa cell viability, we determined Annexin V expression, an indicator of apoptosis, in C4-2 cells treated with BKM1740 at the indicated concentrations for 24 h (Fig. 3A). Fluorescence-activated cell sorting analysis indicated that BKM1740 treatment significantly induced apoptosis in C4-2 cells in a dose-dependent manner. Greater than 40% cell death can be achieved in 24 h with 5 μmol/L BKM1740 (Fig. 3B). Expression of caspases was determined by Western blot analysis of C4-2 cells treated with 5 μmol/L BKM1740. Activation of caspase-3, caspase-8, and caspase-9, as exhibited by increased cleaved protein bands at 17, 40, and 35 kDa, respectively, was observed after incubation with BKM1740 for 12 h. Cleavage of poly(ADP-ribose) polymerase, an indicator of apoptosis shown as a band at 89 kDa, also increased significantly (Fig. 3C). These data suggest that BKM1740 induces apoptosis in metastatic PCa cells through a caspase-dependent pathway.

BKM1740 specifically inhibits expression of survivin in metastatic PCa cells. Multiple factors are involved in the regulation of cell death by apoptosis (33). To elucidate the specific signaling pathway(s) mediating the cytotoxicity of BKM1740 in PCa cells, we analyzed the expression of several antiapoptotic proteins in C4-2 cells treated with BKM1740 (Fig. 4A and B). RT-PCR assay indicated that BKM1740 significantly inhibited survivin expression at the mRNA level. BKM1740 treatment did not significantly affect the expression of antiapoptotic protein Mcl-1 (34). Expression of VEGF, inhibited by treatment with BKM-570 in a previous study (22), was not affected by BKM1740 at either the mRNA (Fig. 4A) or protein level (Fig. 4B). Western blot analysis confirmed the inhibition of survivin protein expression following BKM1740 treatment in C4-2 and $ARCaP_M$ cells (Fig. 4A and C). Basal expression of MMP-9, an important MMP implicated in PCa metastasis (22, 35), was not detected in C4-2 cells by Western blot analysis (data not shown) and not affected by BKM1740 treatment in $ARCaP_M$ cells (Fig. 2C).

C4-2 cells were transiently transfected with a survivin-luciferase reporter (pSurvivin-luc1430) composed of a 1,430-bp region of human survivin promoter (23). The cells were further treated with BKM1740 at the indicated concentrations for 24 h before the luciferase activity assay was done. The data indicated that BKM1740 inhibited the survivin reporter activity in a dose-dependent manner (Fig. 4D), suggesting that survivin transcription was suppressed by BKM1740 treatment in C4-2 cells, which was consistent to the RT-PCR results (Fig. 4A). Taken together, these data showed that BKM1740 specifically inhibits survivin expression in bone metastatic PCa cells, which may mediate the activation of caspase-dependent apoptotic death caused by this compound.

BKM1740 treatment inhibits* in vivo *C4-2 tumor growth in mouse skeleton. To evaluate the *in vivo* effect of BKM1740 against the growth of bone metastatic PCa tumors, we treated athymic nude mice bearing intratibial C4-2 xenografts with BKM1740 at a dose of 5 mg/kg by the i.p. route, once every 2 days. The treatment started on day 28 (4 weeks) after tumor inoculation and continued for 8 weeks. Tumor growth and responsiveness to BKM1740 treatment were determined by serum PSA and skeletal X-ray. As shown in Fig. 5A, there was a significant reduction in serum PSA levels in the BKM1740-treated groups compared with vehicle control at 8 weeks ($P < 0.05$). Representative radiographs are shown in Fig. 5B. Compared with the vehicle control, C4-2 tumor-bearing bone treated with BKM1740 displayed improved architecture with reduced osteolytic destruction and osteoblastic lesions (Fig. 5B, *left*). These X-ray results were consistent with the inhibitory effects of BKM1740 treatment on serum PSA levels in C4-2 tumor-bearing mice. Mice treated with BKM1740 gained weight comparably with the controls (data not shown). To assess the potential *in vivo* toxicity of BKM1740 treatment, athymic nude mice without C4-2 tumor inoculation were treated with a high dose of BKM1740 (20 mg/kg) for 4 weeks. No systemic toxicity

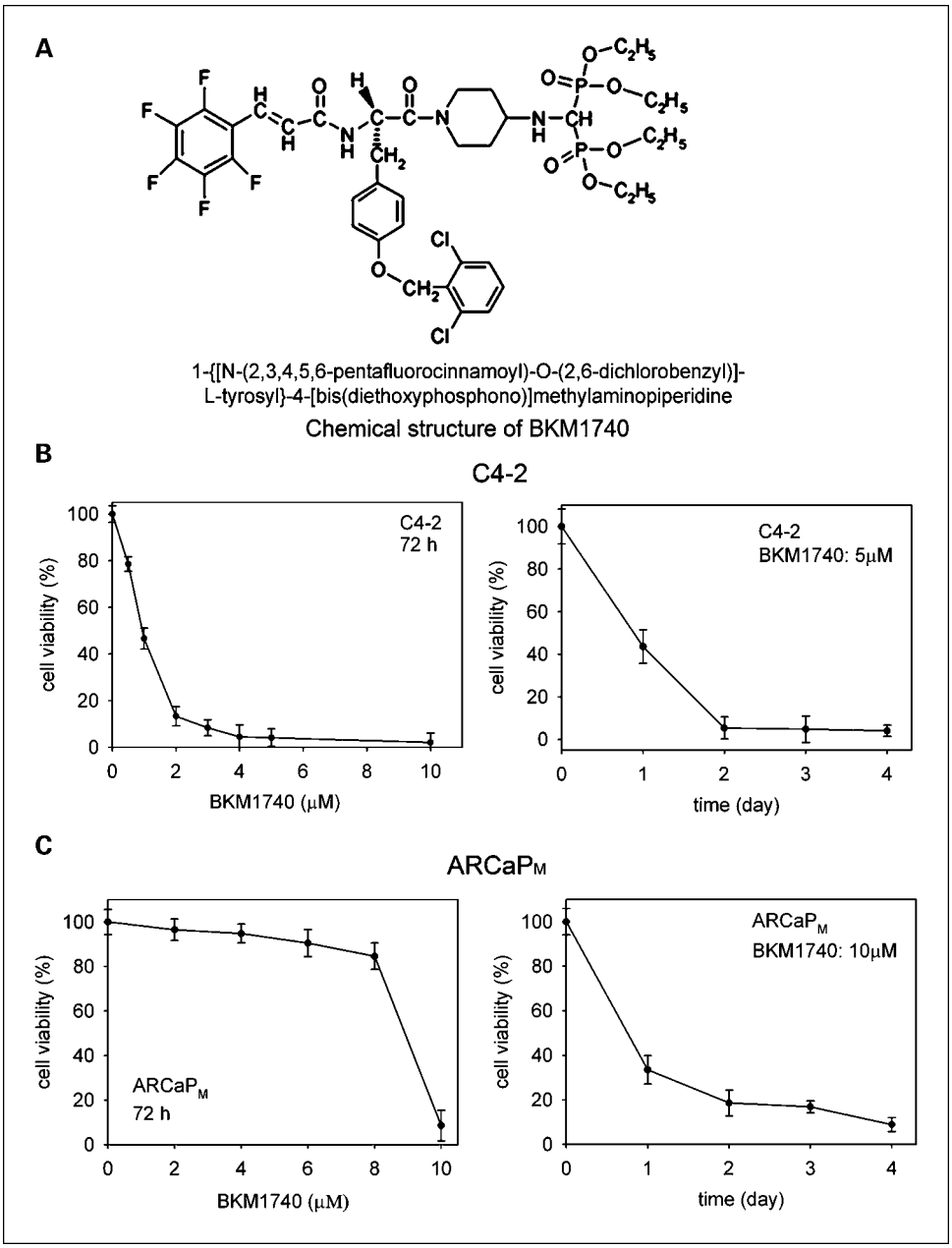

Fig. 2. BKM1740, an acyl-tyrosine bisphosphonate amide derivative, inhibits *in vitro* proliferation of C4-2 and $ARCaP_M$ cells. *A,* chemical structure of BKM1740. *B* and *C,* BKM1740 effects on proliferation of C4-2 (*B*) and $ARCaP_M$ cells (*C*). PCa cells were cultured in the presence of BKM1740 at indicated concentrations for various durations. The effects of BKM1740 treatment on cell numbers were evaluated using MTS assay.

was observed, and the mice gained body weight during the treatment (Supplementary Data). X-ray radiography showed intact bone architecture like that in normal mouse (Fig. 5B, *right*). These results suggested negligible *in vivo* acute toxicity of BKM1740 treatment.

Immunohistochemical analysis of human PCa xenografts subjected to BKM1740 treatment. The effects of BKM1740 treatment on C4-2 tumor growth in tibia were confirmed by immunohistochemical analyses of the harvested tumor specimens at the termination of the experiments. Immunohistochemical staining of mouse tibia indicated that compared with vehicle control, BKM1740 treatment resulted in (*a*) markedly decreased cell proliferation (Ki67) and massive apoptosis (M30) in tumor tissues and (*b*) significant inhibition of survivin expression (Fig. 6A). These differences are statistically significant (Fig. 6B). The data confirmed that the *in vivo* effects of BKM1740 on C4-2 tumor growth were mediated by suppression of survivin expression and induction of apoptosis in PCa tumors.

Discussion

Current regimens treating metastatic PCa by conventional hormone therapy, chemotherapy, or radiation therapy have not resulted in improved patient survival (36). New approaches targeting bone with bisphosphonates to slow down skeletal events, and bone-directed chemotherapy and radiation therapy using strontium-89 or samarium-153, have been approved by the Food and Drug Administration for the clinical treatment of bone metastasis in PCa and breast cancer (37). In addition, "cotargeting" both the tumor and its stromal microenvironment using gene therapy approaches, and drug therapy

targeting osteoblasts, osteoclasts, marrow stromal cells, bone-derived endothelium, cell adhesion to extracellular matrices, or selected growth factor pathways (see refs. 2, 38 for reviews), has shown promise in a large number of bone metastasis models. In this study, we present evidence indicating that BKM1740, a novel bradykinin-related compound conjugated with aminobisphosphonate, induced massive apoptosis and retarded tumor growth in a human PCa bone metastasis model. These data suggest that BKM1740 is an attractive compound for evaluation as a PCa skeletal metastasis drug.

Aberrant signal transduction in both tumors and the bone microenvironment is critical in defining the invasiveness of PCa cells. "Targeted therapy" to interrupt specific signaling pathways implicated in PCa progression is a promising approach supported by recent experimental and clinical studies (39). Multiple signaling molecules have been identified as possible "targets" for rational drug design. Among them, survivin is considered uniquely promising for two reasons: (*a*) survivin intersects multiple signaling networks implicated in the inhibition of apoptosis and therefore blockade of the survivin signal will interrupt tumor progression regardless of the genetic background of the tumor and (*b*) survivin is overexpressed by virtually all solid tumors but undetectable or at very low levels in most terminally differentiated normal tissues; therefore, survivin-based therapy may specifically target tumors with a favorable toxicity profile (3).

Although survivin expression has been correlated to advanced stages of PCa with higher Gleason scores and lymph node metastasis (4, 5), its role in PCa bone metastasis remains elusive. To validate survivin as a rational target for PCa bone metastasis, we first investigated the clinical significance of survivin in human PCa progression. The data showed that survivin expression is positively associated with higher Gleason scores in primary prostatic tumors, indicating that survivin is important in tumorigenesis. Intriguingly, survivin expression is further increased in bone metastatic PCa specimens, which we confirmed in PCa bone metastatic models of LNCaP-C4-2 and ARCaP. Despite the limited numbers of tumor specimens (which were extremely difficult to obtain), these results for the first time suggest a crucial role for survivin in the progression of advanced PCa toward bone metastasis. We hypothesize that overexpression of survivin may confer survival advantages to metastatic PCa cells that allow them to successfully disseminate and colonize. Inhibition of survivin expression may reverse this and induce regression of tumor growth in bone.

Bradykinin-related compounds are being explored as promising anticancer drugs. Several bradykinin antagonists and their mimetic have been found to effectively inhibit tumor growth in

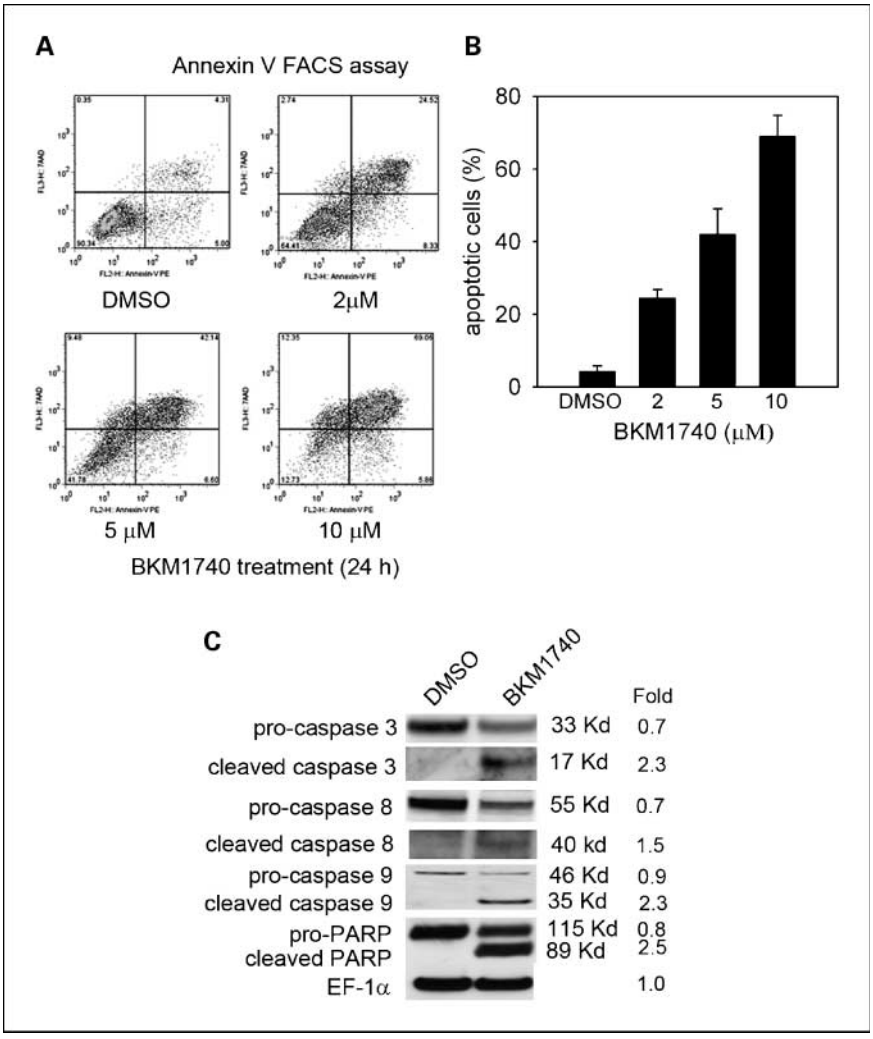

Fig. 3. BKM1740 induces apoptosis in metastatic PCa cells. *A,* C4-2 cells were treated with BKM1740 at the indicated concentrations for 24 h, and Annexin V fluorescence-activated cell sorting (*FACS*) analysis was done. *B,* percentage of apoptotic cells induced by BKM1740 treatment. *C,* Western blot analysis of activation of caspase pathways. C4-2 cells were exposed to 5 μmol/L BKM1740 for 12 h. Activated caspase-3, caspase-8, and caspase-9 and cleavage of poly(ADP-ribose) polymerase (*PARP*) were detected by the increased banding of proteins at 17, 40, 35, and 89 kDa, respectively. Relative expression was expressed as fold change compared with the EF1α controls.

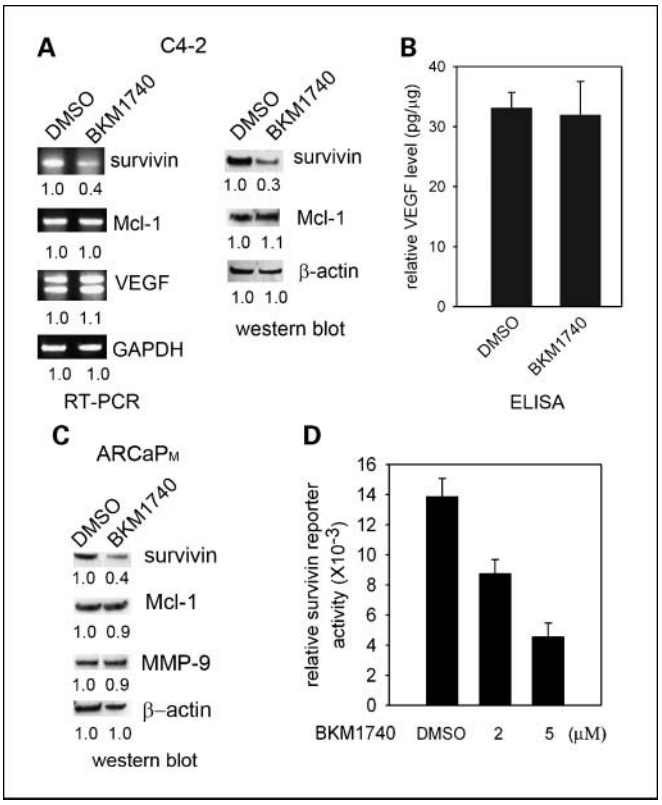

Fig. 4. BKM1740 inhibits survivin expression in metastatic PCa cells. *A,* BKM1740 specifically suppresses survivin expression at both RNA and protein levels in C4-2 cells. Left, C4-2 cells were exposed to 5 μmol/L BKM1740 for 12 h. Total RNA was collected and analyzed by RT-PCR for survivin, Mcl-1, and VEGF, with glyceraldehyde-3-phosphate dehydrogenase as loading control. Right, C4-2 cells were treated with 5 μmol/L BKM1740 for 24 h, and total lysates were analyzed for the expression of survivin and Mcl-1. Relative expression was expressed as fold change compared with the β-actin controls. *B,* ELISA of VEGF levels in conditioned medium of C4-2 cells treated with BKM1740 or vehicle for 48 h. Relative VEGF levels were normalized by dividing VEGF concentrations (pg/mL) by total protein concentrations (mg/mL) in condition medium. *C,* BKM1740 specifically suppresses survivin expression in $ARCaP_M$ cells. $ARCaP_M$ cells were treated with 10 μmol/L BKM1740 for 24 h, and total lysates were analyzed for the expression of survivin, Mcl-1, and MMP-9. Relative expression was expressed as fold change compared with the β-actin controls. *D,* C4-2 cells were cotransfected with pSurvivin-luc1430 and pRL-TK (internal control) for 48 h before exposure to BKM1740 at the indicated concentrations for a further 24-h incubation. Total lysates were analyzed for luciferase activity induced by the survivin promoter and normalized to the *Renilla* luciferase activity.

animal models of PCa and lung cancer (13–16, 18, 40). One of the peptide-based antagonists, CU201, is entering a phase I clinical trial for lung cancer. Mechanistic study showed that CU201 induced cancer cell apoptosis as a "biased" agonist by inhibiting $G\alpha_q$ activation and downstream events and by stimulating $G\alpha_{12,13}$ and downstream cascades (17). Intriguingly, these compounds may act as pluripotent molecules that could simultaneously inhibit cancer cell proliferation by inducing apoptosis, and interrupt angiogenesis by reducing VEGF expression (18). To develop novel anticancer reagents that specifically target PCa bone metastasis, we designed BKM1740 as an analogue that incorporates the key "anticancer" structure (F5c-OC2Y) of BKM-570 and an aminobisphosphonate group to improve specific delivery of the compound into bone, thereby increasing its bioavailability in tumor tissues residing in bone. The mechanism-based evidence presented here shows that (*a*) BKM1740 specifically inhibited survivin expression at both the mRNA and protein levels and induced tumor regression in a mouse model of PCa bone metastasis, suggesting that BKM1740 and its derivatives could be novel small-molecule chemicals that effectively treat PCa bone metastasis, and (*b*) the design scheme for BKM1740 as a "pluripotent" compound could serve as a valuable principle in rational drug development.

Bisphosphonates are nonhydrolyzable pyrophosphate analogues, which have been shown to have inhibitory effects on metastasis-induced osteoclastic bone resorption (32, 41). Introduction of an aminobisphosphonate moiety in BKM1740 was expected to increase its bioavailability in bone metastatic tumor lesions and retain the inhibitory effects on bone resorption initiated by metastatic PCa. However, whether this compound retains the inhibitory activity of the bisphosphonate moiety on the osteolysis process is not clear. Future studies will examine the *in vitro* effects of BKM1740 on osteoclast activity and formation and assess the *in vivo* effects on osteolytic process and bone turnover using the model established in the current study. The results will validate the design strategy for BKM1740 and provide valuable information for developing alternative candidates.

Interestingly, recent studies suggest that bisphosphonates may have direct anticancer activity (42, 43). For example, zoledronic acid was found to be capable of inhibiting *in vitro* proliferation of LNCaP and PC-3 PCa cells (44). Because BKM1740 is conjugated with bisphosphonate, we do not

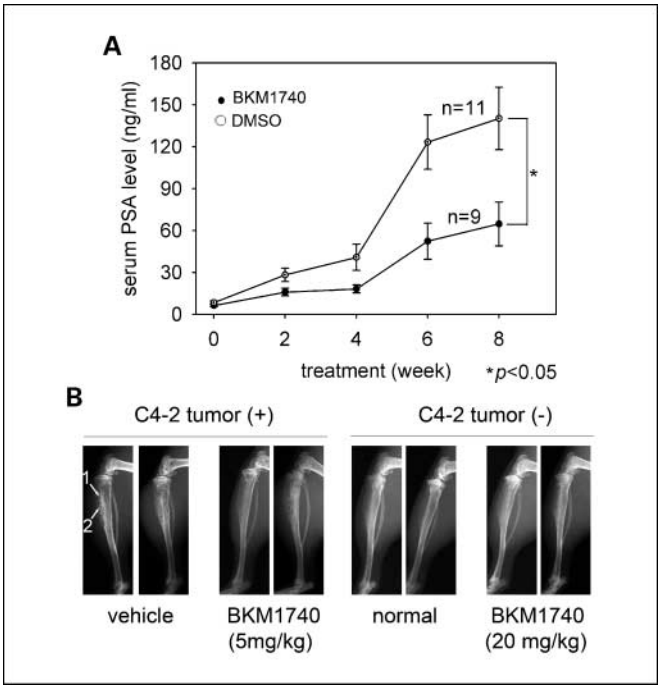

Fig. 5. BKM1740 induces regression of PCa skeletal tumor in C4-2 mouse xenografts. *A,* i.p. injection of BKM1740 reduced serum PSA in mice bearing C4-2 skeletal tumors compared with control group after 8 wk of treatments ($P < 0.05$). ○, vehicle control group; ●, BKM1740-treated group. *B,* representative chromatograms of the bones in each group as detected by X-ray, showing that BKM1740 treatment improves bone X-ray appearances in comparison with control group. Left, tumor-bearing athymic nude mice treated with either vehicle or BKM1740 at a dose of 5 mg/kg, every 2 d, for 8 wk. The osteolytic lesion and osteoblastic lesion in the tumor-bearing bone were indicated by arrows 1 and 2, respectively. Right, normal athymic nude mice or only treated with BKM1740 at a dose of 20 mg/kg, twice per week, for 4 wk.

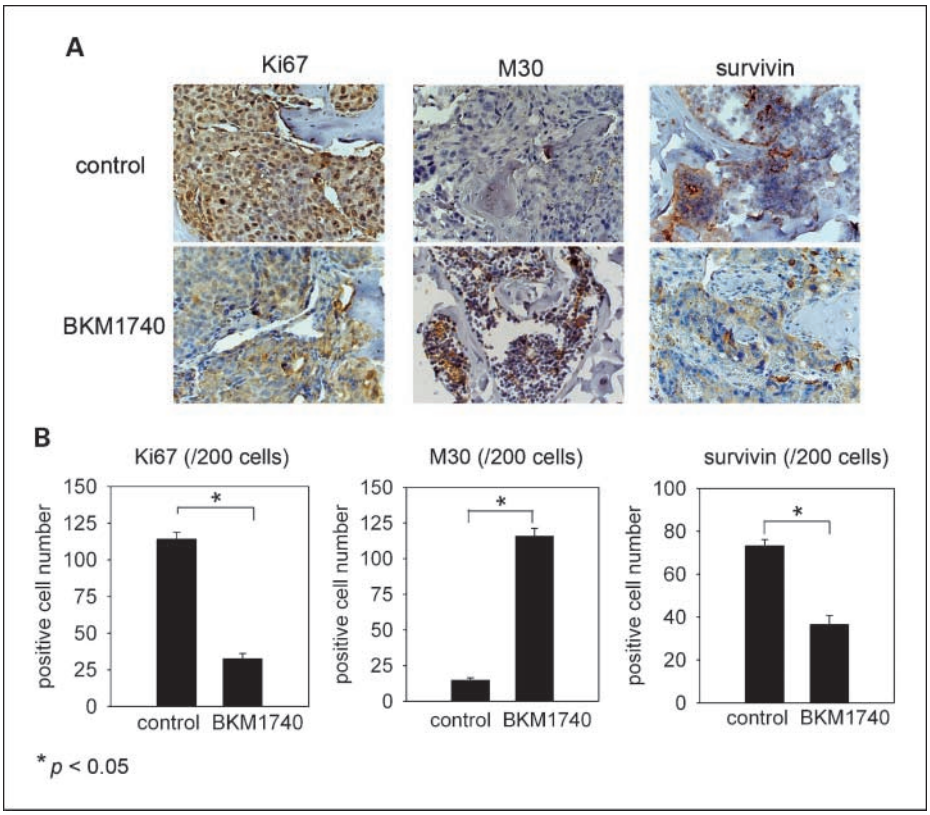

Fig. 6. BKM1740 treatment exhibits growth-inhibitory and proapoptotic activity against C4-2 tumor xenografts in mice. *A,* BKM1740 treatment inhibited cell proliferation (Ki67), induced apoptosis (M30), and suppressed survivin expression *in vivo* by immunohistochemical analysis. *B,* comparative quantification of BKM1740 treatment as opposed to controls on the expression of markers of cell proliferation, apoptosis, and survivin expression ($P < 0.05$).

exclude the possibility that its inhibitory effects on PCa cell survival were partially due to the bisphosphonate moiety. However, the zoledronic acid concentration used in the cited study was much higher (68 μmol/L zoledronic acid in apoptosis analysis; ref. 44) than the BKM1740 concentration used in this report. Further, zoledronic acid only exhibited significant efficacy inhibiting PCa tumor growth in mouse bone, not in s.c. models (44), indicating that zoledronic acid activity on PCa skeletal growth is mainly attributable to indirect effects related to decreased osteolysis. These observations support our notion that the proapoptotic activity of BKM1740 may be primarily mediated by the effects of its F5c-OC2Y moiety on survivin expression.

Multiple growth factors and proteases are involved in PCa growth, survival, and invasion (2, 45, 46). A previous study by Stewart et al. (15) found that CU201 and BKM-570 significantly inhibited angiogenesis by reducing VEGF expression and decreased tissue permeability mediated by MMPs in a PC-3 model. Because BKM1740 is derived from BKM-570, we examined whether it has similar effects on the expression of VEGF and MMPs in C4-2 cells. The data indicated that BKM1740 treatment did not affect VEGF mRNA expression or protein secretion. Unlike in PC-3 cells, basal expression of MMP-9 was undetectable in C4-2 cells and not affected significantly by BKM1740 treatment in $ARCaP_M$ cells. Taken together, these results suggested that BKM1740-induced C4-2 tumor regression in bone may be primarily mediated by specific inhibition of survivin and induction of apoptosis.

Survivin overexpression in human cancers has been associated with resistance to conventional chemotherapy and irradiation therapy (6–8). Furthermore, treatment with certain mitotic inhibitor-based drugs such as Taxol may result in arresting the mitotic process and subsequent accumulation of survivin in the G_2-M phase of cell cycle, which eventually counteracts Taxol-induced apoptosis (47). Inhibition of survivin, particularly by small-molecule suppressants, could sensitize the resistant cells to apoptosis induction, thereby augmenting therapeutic responses (10). Several strategies are being pursued to down-regulate survivin expression and increase the efficacy of chemotherapy in PCa and breast cancer (7, 11). With the shown efficacy of BKM1740 in suppressing survivin and inducing apoptosis in invasive PCa cells, it can be expected that a combination treatment with BKM1740 and chemotherapeutic agents such Taxotere may have therapeutic advantages over a single regimen for the treatment of PCa bone metastasis.

In conclusion, our study shows that BKM1740 is a novel small acyl-tyrosine bisphosphonate amide analogue that specifically suppresses survivin expression and induces massive apoptosis in bone metastatic PCa cells. *In vivo* experiments validated its efficacy in inducing regression of pre-established bone metastatic PCa tumors without acute toxicity. Extensive studies of BKM1740 function and further development of its analogues could provide a novel therapeutic strategy for treating bone metastasis in PCa and other human cancers.

Disclosure of Potential Conflicts of Interest

No potential conflicts of interest were disclosed.

Acknowledgments

We thank Dr. Allen C. Gao (University of California, Davis, CA) for kindly providing the human survivin reporter construct and Gary Mawyer (University of Virginia, Charlottesville, VA) for editorial assistance.

References

1. Jemal A, Siegel R, Ward E, Murray T, Xu J, Thun MJ. Cancer statistics, 2007. CA Cancer J Clin 2007;57: 43–66.

2. Chung LW, Baseman A, Assikis V, Zhau HE. Molecular insights into prostate cancer progression: the missing link of tumor microenvironment. J Urol 2005; 173:10–20.

3. Altieri DC. Molecular circuits of apoptosis regulation and cell division control: the survivin paradigm. J Cell Biochem 2004;92:656–63.

4. Kishi H, Igawa M, Kikuno N, Yoshino T, Urakami S, Shiina H. Expression of the survivin gene in prostate cancer: correlation with clinicopathological characteristics, proliferative activity and apoptosis. J Urol 2004; 171:1855–60.

5. Shariat SF, Lotan Y, Saboorian H, et al. Survivin expression is associated with features of biologically aggressive prostate carcinoma. Cancer 2004;100: 751–7.

6. Nomura T, Yamasaki M, Nomura Y, Mimata H. Expression of the inhibitors of apoptosis proteins in cisplatin-resistant prostate cancer cells. Oncol Rep 2005;14: 993–7.

7. Zhang M, Mukherjee N, Bermudez RS, et al. Adenovirus-mediated inhibition of survivin expression sensitizes human prostate cancer cells to paclitaxel *in vitro* and *in vivo*. Prostate 2005;64:293–302.

8. Zhang M, Latham DE, Delaney MA, Chakravarti A. Survivin mediates resistance to antiandrogen therapy in prostate cancer. Oncogene 2005;24:2474–82.

9. Ouhtit A, Matrougui K, Bengrine A, Koochekpour S, Zerfaoui M, Yousief Z. Survivin is not only a death encounter but also a survival protein for invading tumor cells. Front Biosci 2007;12:1260–70.

10. Altieri DC. Survivin, cancer networks and pathway-directed drug discovery. Nat Rev Cancer 2008;8: 61–70.

11. Nakahara T, Takeuchi M, Kinoyama I, et al. YM155, a novel small-molecule survivin suppressant, induces regression of established human hormone-refractory prostate tumor xenografts. Cancer Res 2007;67: 8014–21.

12. Tolcher AW, Antonia S, Lewis LD, et al. A phase I study of YM155, a novel survivin suppressant, administered by 168 hour continuous infusion to patients with advanced solid tumors [abstract 3014]. Proc Am Soc Clin Oncol Annu Meet 2006; 24:3014.

13. Stewart JM. Bradykinin antagonists as anti-cancer agents. Curr Pharm Des 2003;9:2036–42.

14. Stewart JM. Bradykinin antagonists: discovery and development. Peptides 2004;25:527–32.

15. Stewart JM, Chan DC, Simkeviciene V, et al. Bradykinin antagonists as new drugs for prostate cancer. Int Immunopharmacol 2002;2:1781–6.

16. Chan DC, Gera L, Stewart JM, et al. Bradykinin antagonist dimer, CU201, inhibits the growth of human lung cancer cell lines *in vitro* and *in vivo* and produces synergistic growth inhibition in combination with other antitumor agents. Clin Cancer Res 2002; 8:1280–7.

17. Chan D, Gera L, Stewart J, et al. Bradykinin antagonist dimer, CU201, inhibits the growth of human lung cancer cell lines by a "biased agonist" mechanism. Proc Natl Acad Sci U S A 2002;99:4608–13.

18. Stewart JM, Gera L, Chan DC, et al. Combination cancer chemotherapy with one compound: pluripotent bradykinin antagonists. Peptides 2005;26: 1288–91.

19. Wu HC, Hsieh JT, Gleave ME, Brown NM, Pathak S, Chung LW. Derivation of androgen-independent human LNCaP prostatic cancer cell sublines: role of bone stromal cells. Int J Cancer 1994;57:406–12.

20. Xu J, Wang R, Xie ZH, et al. Prostate cancer metastasis: role of the host microenvironment in promoting epithelial to mesenchymal transition and increased bone and adrenal gland metastasis. Prostate 2006; 66:1664–73.

21. Gera L, Stewart JM, Fortin JP, Morissette G, Marceau F. Structural modification of the highly potent peptide bradykinin B1 receptor antagonist B9958. Int Immunopharmacol 2008;8:289–92.

22. Gera L, Chan DC, York EJ, et al. Combination cancer chemotherapy with a single agent: bradykinin peptide antagonists and their mimetics. Proceedings of the 28th European Peptide Symposium (Flegl M, Fridkin M, Gilon C, Slaninova J, editors), Kenes, Geneva, 2005. p. 846–7.

23. Li F, Altieri DC. Transcriptional analysis of human survivin gene expression. Biochem J 1999;344 Pt 2: 305–11.

24. Wu D, Zhau HE, Huang WC, et al. cAMP-responsive element-binding protein regulates vascular endothelial growth factor expression: implication in human prostate cancer bone metastasis. Oncogene 2007;26: 5070–7.

25. Wu TT, Sikes RA, Cui Q, et al. Establishing human prostate cancer cell xenografts in bone: induction of osteoblastic reaction by prostate-specific antigen-producing tumors in athymic and SCID/bg mice using LNCaP and lineage-derived metastatic sublines. Int J Cancer 1998;77:887–94.

26. Matsubara S, Wada Y, Gardner TA, et al. A conditional replication-competent adenoviral vector, Ad-OC-E1a, to cotarget prostate cancer and bone stroma in an experimental model of androgen-independent prostate cancer bone metastasis. Cancer Res 2001; 61:6012–9.

27. Shigemura K, Arbiser JL, Sun SY, et al. Honokiol, a natural plant product, inhibits the bone metastatic growth of human prostate cancer cells. Cancer 2007; 109:1279–89.

28. Zhau HE, Li CL, Chung LW. Establishment of human prostate carcinoma skeletal metastasis models. Cancer 2000;88:2995–3001.

29. Thalmann GN, Anezinis PE, Chang SM, et al. Androgen-independent cancer progression and bone metastasis in the LNCaP model of human prostate cancer. Cancer Res 1994;54:2577–81.

30. Zhau HY, Chang SM, Chen BQ, et al. Androgen-repressed phenotype in human prostate cancer. Proc Natl Acad Sci U S A 1996;93:15152–7.

31. Xu J, Odero-Marah V, Wang R, Chung LWK, Zhau HE. Epithelial-mesenchymal transition and bone-specific microenvironment contribute to the rapid skeletal metastasis in human prostate cancer. J Urol 2005;173:125.

32. Saad F, Gleason DM, Murray R, et al. A randomized, placebo-controlled trial of zoledronic acid in patients with hormone-refractory metastatic prostate carcinoma. J Natl Cancer Inst 2002;94: 1458–68.

33. Hengartner MO. The biochemistry of apoptosis. Nature 2000;407:770–6.

34. Krajewska M, Krajewski S, Epstein JI, et al. Immunohistochemical analysis of bcl-2, bax, bcl-X, and mcl-1 expression in prostate cancers. Am J Pathol 1996;148: 1567–76.

35. Lokeshwar BL. MMP inhibition in prostate cancer. Ann N Y Acad Sci 1999;878:271–89.

36. Oh WK, Kantoff PW. Management of hormone refractory prostate cancer: current standards and future prospects. J Urol 1998;160:1220–9.

37. Bagi CM. Targeting of therapeutic agents to bone to treat metastatic cancer. Adv Drug Deliv Rev 2005;57: 995–1010.

38. Pienta KJ, Smith DC. Advances in prostate cancer chemotherapy: a new era begins. CA Cancer J Clin 2005;55:300–18; quiz 23–5.

39. Clines GA, Guise TA. Molecular mechanisms and treatment of bone metastasis. Expert Rev Mol Med 2008;10:e7.

40. Stewart JM, Gera L, Chan DC, et al. Bradykinin-related compounds as new drugs for cancer and inflammation. Can J Physiol Pharmacol 2002;80: 275–80.

41. Berenson JR, Rajdev L, Broder M. Managing bone complications of solid tumors. Cancer Biol Ther 2006; 5:1086–9.

42. Hirbe AC, Rubin J, Uluckan O, et al. Disruption of CXCR4 enhances osteoclastogenesis and tumor growth in bone. Proc Natl Acad Sci U S A 2007;104: 14062–7.

43. Miwa S, Mizokami A, Keller ET, Taichman R, Zhang J, Namiki M. The bisphosphonate YM529 inhibits osteolytic and osteoblastic changes and CXCR-4-induced invasion in prostate cancer. Cancer Res 2005;65:8818–25.

44. Corey E, Brown LG, Quinn JE, et al. Zoledronic acid exhibits inhibitory effects on osteoblastic and osteolytic metastases of prostate cancer. Clin Cancer Res 2003;9:295–306.

45. Chung LW, Huang WC, Sung SY, et al. Stromal-epithelial interaction in prostate cancer progression. Clin Genitourin Cancer 2006;5:162–70.

46. Chung LW, Kao C, Sikes RA, Zhau HE. Human prostate cancer progression models and therapeutic intervention. Hinyokika Kiyo 1997;43:815–20.

47. Ling X, Bernacki RJ, Brattain MG, Li F. Induction of survivin expression by taxol (paclitaxel) is an early event, which is independent of taxol-mediated G_2/M arrest. J Biol Chem 2004;279:15196–203.

Clin Exp Metastasis (2008) 25:601–610
DOI 10.1007/s10585-008-9183-1

RESEARCH PAPER

Epithelial to mesenchymal transition (EMT) in human prostate cancer: lessons learned from ARCaP model

Haiyen E. Zhau · Valerie Odero-Marah · Hui-Wen Lue · Takeo Nomura · Ruoxiang Wang · Gina Chu · Zhi-Ren Liu · Binhua P. Zhou · Wen-Chin Huang · Leland W. K. Chung

Received: 1 August 2007 / Accepted: 14 May 2008 / Published online: 6 June 2008

Abstract Androgen refractory cancer of the prostate (ARCaP) cells contain androgen receptor (AR) and synthesize and secrete prostate specific antigen (PSA). We isolated epithelia-like $ARCaP_E$ from parental ARCaP cells and induced them to undergo epithelial–mesenchymal transition (EMT) by exposing these cells to soluble factors including TGFβ1 plus EGF, IGF-1, β2-microglobulin (β2-m), or a bone microenvironment. The molecular and behavioral characteristics of the resultant $ARCaP_M$ were characterized extensively in comparison to the parental $ARCaP_E$ cells. In addition to expressing mesenchymal biomarkers, $ARCaP_M$ gained 100% incidence of bone metastasis. $ARCaP_M$ cells express receptor activator of NF-κB ligand (RANKL), which was shown to increase tartrate-resistant acid phosphatase (TRAP)-positive osteoclasts in culture, and when metastatic to bone in vivo. We provide evidence that RANKL expression was promoted by increased cell signaling mediated by the activation of Stat3-Snail-LIV-1. RANKL expressed by $ARCaP_M$ cells is functional both in vitro and in vivo. The lesson we learned from the ARCaP model of EMT is that activation of a specific cell signaling pathway by soluble factors can lead to increased bone turnover, mediated by enhanced RANKL expression by tumor cells, which is implicated in the high incidence of prostate cancer bone colonization. The ARCaP EMT model is highly attractive for developing new therapeutic agents to treat prostate cancer bone metastasis.

Keywords EMT · Cell signaling · RANKL · Osteoclastogenesis · LIV-1 · Bone metastasis · Prostate · Breast · Lung · Kidney · TGFβ1 · EGF

Abbreviations

AR	Androgen receptor
ARCaP	Androgen-refractory human prostate cancer cell model from a patient with prostate cancer bone metastasis
$ARCaP_E$	ARCaP clone with epithelial phenotype
$ARCaP_M$	ARCaP clone with mesenchymal phenotype
β2-m	β2-Microglobulin
BSP	Bone sialoprotein
C4-2	Lineage derivative cells from LNCaP
C4-2B	C4-2 cells metastasized to bone
CK18/19	Cytokeratin 18/19
CM	Conditioned medium
CREB	cAMP-responsive element-binding protein
E-cad	E-cadherin
EGF	Epidermal growth factor
EMT	Epithelial–mesenchymal transition
FBS	Fetal bovine serum
IC	Intracardiac
IGF-1	Insulin-like growth factor 1
IHC	Immunohistochemistry
IL13Rα2	Interleukin13 receptor α2

H. E. Zhau (✉) · V. Odero-Marah · H.-W. Lue · T. Nomura · R. Wang · G. Chu · W.-C. Huang · L. W. K. Chung (✉)
Molecular Urology & Therapeutics Program, Department of Urology, Emory University School of Medicine, 1365B Clifton Road, Suite 5107, Atlanta, GA 30322, USA
e-mail: hzhau@emory.edu

L. W. K. Chung
e-mail: lwchung@emory.edu

H.-W. Lue · G. Chu · Z.-R. Liu
Department of Biology, Georgia State University, Atlanta, GA 30302, USA

B. P. Zhou
Sealy Center for Cancer Cell Biology, The University of Texas Medical Branch, Galveston, TX 77555, USA

LNCaP	Prostate cancer cells metastasized to lymph node
MET	Mesenchymal–epithelial transition
MErT	Mesenchymal–epithelial-reverting transition
MMT	Mesenchymal–mesenchymal transition
N-cad	N-cadherin
NFκB	Nuclear factor kappa B
OC	Osteocalcin
OPG	Osteoprotegerin
OPN	Osteopontin
RANKL	Receptor activator of NFκB ligand
RT-PCR	Reverse transcriptase-polymerase chain reaction
SCID	Severe combined immunodeficiency
siRNA	Small interfering RNA
Stat	Signal transducer and activator of transcription
TGFβ1	Transforming growth factor β1
TRAP	Tartrate-resistant acid phosphatase
VM	Vimentin

Introduction

Two thirds of the cancer-related deaths in the US involve bone metastasis [1, 2]. ARCaP cells, isolated from the ascites fluid of a patient with bone metastasis, express a host of human prostate cancer biomarkers, have high propensity for rapid and predictable bone and soft tissue growth/metastases through orthotopic, intracardic and intraosseous injections [3–5], and undergo EMT on exposure to soluble factors or host bone microenvironment [4, 6]. The ARCaP EMT confers increased cell migratory, invasive and metastatic potential to soft tissue and bone [4, 6]. Here we used this unique model of prostate carcinoma progression to study soluble growth factor-induced EMT and intracellular signaling pathways that lead to RANKL expression, which activates osteoclastogenesis. We suggest that soluble factor-induced RANKL expression in the ARCaP EMT model accounts for subsequent prostate cancer cell bone colonization. We showed the plasticity of cancer cells, which upon induction by these soluble factors, switch to express markers commonly found in osteoblasts (termed "osteomimicry"), such as non-collagenous bone matrix proteins, osteocalcin (OC), osteopontin (OPN) and bone sialoprotein (BSP), and RANKL, collectively allowing cancer cells to survive and thrive in the bone microenvironment [7–9].

Previous studies of other solid tumors support the association of increased EMT with the ability of cancer cells to migrate, invade and metastasize [10–13]. Several studies have characterized EMT during embryonic development and related it to cancer metastasis. These studies pave the way for novel gene discovery and biomarker validation for cancer progression. In this communication, we have determined the roles of LIV-1, a zinc transporter, in the control of EMT, RANKL and Stat3-Snail-LIV-1 signaling during prostate cancer progression. Below we discuss the plasticity of prostate cancer cells, which are capable of undergoing EMT. In addition, it has been shown by others that prostate cancer cells can also revert via mesenchymal–epithelial transition (MET) [14–16], mesenchymal–epithelial-reverting transition (MErT) [16] and mesenchymal–mesenchymal transition (MMT) [17] to control their malignant and invasive potentials.

Materials and methods

Cell culture, reagents and animal studies

$ARCaP_E$ and $ARCaP_M$ cells were maintained in T medium (Invitrogen, Carlsbad, CA) and 5% fetal bovine serum (FBS) at 37°C supplemented with 5% CO_2 in a humidified incubator. ARCaP cells were established from the ascites fluid of a patient with prostate cancer bone metastasis [5]. $ARCaP_E$ and $ARCaP_M$ are sublines of ARCaP that were generated in our laboratory by single cell dilution cloning [4]. To study the effect of growth factor treatment, ARCaP cells were treated with 4 ng/ml TGF β1 and 50 ng/ml EGF either alone or in combination. Data represent triplicate samples from two independent experiments. Recombinant-human TGF-β1, -mouse RANKL, -mouse M-CSF-1 and -human osteoprotegerin (OPG) were from R&D Systems, Inc. (Minneapolis, MN). FBS, recombinant human EGF, G418, anti-flag M2 monoclonal antibody and mouse monoclonal anti-human actin antibody were from Sigma–Aldrich, Inc. (St. Louis, MO). IGF-1 treatment was reported in a separate manuscript [18].

Animal studies were conducted by previously published procedures [19, 20].

Gene and protein expression

Gene expression was analyzed by RT-PCR (see [4]). In brief, cells were plated on 6-well dishes at 3×10^5 cells per well and grown to 70% confluence, gently washed with PBS and used for RNA isolation. Total RNA was isolated from cells using the RNeasy Mini kit (Qiagen, Valencia, CA) and subjected to reverse transcription using the Superscript first-strand cDNA Synthesis kit (Invitrogen, Carlsbad, CA). The primers used for PCR analysis were: E-cadherin-F-5′-TCCATTTCTTGGTCTACGCC-3′ R-5′-CACCTTCAG CCAACCTGTTT-3′; N-cadherin-F-5′-GTGCCATTAGC CAAGGAATTCAGC-3′ R-5′-GCGTTCCTGTTCCACTC ATAGGAGG-3′; Vimentin-F5′-TGGCACGTCTTGACC TTGAA-3′ R-5′-GGTCATCGTGATGCTGAGAA-3′; LIV-

1-F-5′-GCAATGGCGAGGAAGTTATCT-3′ R-5′-CTATTG TCTCTAGAAAGTGAG-3′; Snail-F-5′-CGAAAGGCCTTC AACTGCAAAT-3′; R-5′-ACTGGTACTTCTTGACATC TG-3′; RANKL-F-5′-CAGCACATCAGAGCAGAGAA AG-3′ R-5′-TGTTGGCATACAGGTAATAAAAGC-3′ and Stat3-F 5′-AACTCTTGGGACCTGGTGTG-3′ R-5′-TAG GCGCCTCAGTCGTATCT-3′. The thermal profiles for E-cadherin, N-cadherin, vimentin, and Stat3 were 32 cycles with denaturation at 95°C for 30 s, annealing at 55°C for 30 s and extension at 72°C for 1 min. LIV-1, Snail and RANKL cDNA amplification were 30, 33 and 35 cycles starting with denaturation for 30 s at 94°C, followed by 1 min of annealing at 43°C (for LIV-1), 55°C (for Snail) and 55°C (for RANKL) and 1 min of extension at 72°C. RT-PCR products were analyzed by agarose gel electrophoresis.

Protein expression was determined by immunohistochemical (IHC) and western blot analyses. For IHC, antibodies and their sources are: monoclonal antibodies against cytokeratin 18/19 (CK18/19), vimentin (VM) (Dako Corp., Ltd., Carpinteria, CA); polyclonal antibodies to E-cadherin and N-cadherin (Santa Cruz Biotechnology, Inc., Santa Cruz, CA); RANKL (CHEMICON International, Inc., Temecula, CA). Cells and deparaffinized, rehydrated tissues after pressure-cooking antigen retrieval at 125°C and 20 p.s.i. for 30 s were subjected to 10-min double endogenous enzyme block, 30-min primary antibody reaction and 30-min DakoCytomation EnVision + HRP reagent incubation. Signals were detected by adding substrate hydrogen peroxide using diaminobenzidine as a chromogen, counterstained by hematoxylin. All detection reagents were obtained from Dako Corporation (Carpinteria, CA). Matched IgG, or diluted rabbit serum was used as a negative control. Antibodies for western blot are: Snail (SN9H2, Rat mAb from Cell Signaling Technology, Inc. Beverly, MA), RANKL (sc-9073, Santa Cruz Biotechnology, Inc.), Stat3 and phosphor-Stat3 (Ser 727; Cell Signaling Technology), and LIV-1 (see below). Total cell lysates were prepared using a lysis buffer [50 mM Tris (pH 8), 150 mM NaCl, 0.02% NaN_3, 0.1% SDS, 1% NP40 and 0.5% sodium deoxycholate] containing 1 mM phenylmethylsulfonyl fluoride and protease inhibitor cocktail (Roche Applied Science, Indianapolis, IN). Protein concentration was determined by Bradford assay using Coomassie Plus Protein Reagent (Pierce, Rockford, IL). Western blot was performed using the Novex system (Invitrogen) as described previously [9, 21] Protein bands were detected by Enhanced Chemiluminescence Western Blotting Detection Reagents (Amersham-Pharmacia Biotech, Piscataway, NJ).

Snail transfection and induction of RANKL expression

A constitutively active Snail, the Flag-tagged Snail-6SA [22] kindly provide by Dr. M. C. Hung (MD Anderson Cancer Center, Houston, TX) was used to transfect $ARCaP_E$ cells. An aliquot of 4 μg plasmid DNA was used in 6-well plate with GenePORTER (Genlantis, San Diego, CA) following manufacturer recommended protocol. A total of 24 single transfected clones were selected subsequent to further selection with G418 (400 μg/ml) and limited dilution.

Over-expression of the Flag-Snail-6SA was confirmed by western blot with antibody (sc-807, Santa Cruz Biotechnology) against the Flag epitope. $ARCaP_E$ cells transfected with empty vector served as controls. EMT of the transfected clones was confirmed both morphologically and biochemically and these results will be reported elsewhere.

In vitro osteoclastogenesis assay

Osteoclastogenesis assay was performed as described previously with minor modifications [23]. Briefly, 1×10^3 cancer cells were seeded with 2×10^5 haematopoietic pre-osteoclasts harvested from adult mouse spleen by disaggregating through a wire sieve. The co-cultures were performed in a 48-well plate containing 500 μl of α-MEM media supplemented with 10% FBS, and 1 ng/ml recombinant mouse M-CSF (R&D Systems, Inc., Minneapolis, MN). As a positive control, 100 ng/ml recombinant mouse RANKL (R&D Systems) was added to 2×10^5 pre-osteoclastic cells. A total of 50 ng/ml recombinant human osteoprotegerin (OPG, R&D Systems) was added to certain wells to block RANKL-mediated osteoclastogenesis. The cells were fed twice weekly by replacing half of the cultured media with fresh media containing M-CSF (and RANKL, for the positive control). After 14 days, the cells were analyzed by TRAP staining (Sigma–Aldrich, Inc., St. Louis, MO), and the $TRAP^+$ multinucleated cells in the entire well were counted as mature osteoclasts.

Cell signaling studies and LIV-1 transfection

Human LIV-1 plasmid DNA (2 μg cloned from human breast cancer cells, characterized and sequenced by Dr. Binhua P. Zhou), cloned into pcDNA 3.1/V5-His vector (Invitrogen), was transfected into $ARCaP_E$ cells using Lipofectamine 2000 Reagent (Invitrogen). The effects of LIV-1 on EMT gene expression were assayed 3 days after transfection. $ARCaP_E$ cells transfected with empty vector served as controls. LIV-1 expression in $ARCaP_M$ cells was silenced transiently by LIV-1 siRNA duplex (0.7 μg of 5′–3′-AUAAAGGACAGCCUGC UUAACGGUC and 5′–3′-GACCGUUAAGCAGGCUGUC CUUUAU interference RNA) using Lipofectamine 2000 Reagent (Invitrogen). EMT marker expression in $ARCaP_M$ cells with LIV-1 knockdown was assessed 3 days

post-transfection. LIV-1 mRNA expression was assayed by RT-PCR and western blot as described above.

LIV-1 polyclonal antibody was produced in rabbits immunized with KLH-conjugated peptide, CPDHDSDSS GKDPRNS. A total of five injections were performed, with each injection consisting of 300–500 μg peptide mixed with complete or incomplete adjuvant. After the fourth injection, blood was collected and centrifuged. For western blotting, primary antibody was used at 1:2,000 dilution and anti-rabbit secondary antibody was used at 1:5,000 dilution. Protein bands were detected by western blot as described above.

Results and discussion

A novel human prostate cancer ARCaP EMT model for the study of prostate cancer progression and metastasis: effects of soluble growth factors

Unlike other animal models bearing human prostate cancer cells, the ARCaP model represents a continuum of prostate cancer progression closely mimicking the pathophysiology of *advanced* and *lethal* clinical human prostate cancer bone metastasis. Epithelium-like $ARCaP_E$ cells had a relatively low propensity for bone metastasis (1/8) after intracardiac (IC) injection but gained 100% metastasis to bone and 33% metastasis to adrenal gland upon recovering from mouse bone [4]. While the derivative ARCaP cells from mouse bone still expressed distinct epithelial cell markers, they also switched their morphology and gene expression profile to mesenchymal cells and thus were designated as $ARCaP_M$. Figure 1 depicted that $ARCaP_M$ cells had decreased expression of E-cadherin (E-cad) and cytokeratins 18 and 19 but increased expression of N-cadherin (N-cad) and two novel EMT associated genes; RANKL, a novel mesenchymal marker in $ARCaP_M$ cells, and IL-13 receptor α2 (IL-13R α2), a decoy IL-13 receptor capable of blocking IL-13Rα1 signaling and enhancing tumor growth [24, 25]. In addition to the observed induction of EMT by the bone microenvironment, we also derived mesenchymal-like $ARCaP_M$ cells in vitro from parental $ARCaP_E$ cells, based on cell morphology, gene expression (see below) and behavioral characteristics. We noted that the transition of $ARCaP_E$ cells to $ARCaP_M$ cells can be promoted by a host of growth factors, such as TGFβ1 plus EGF (see below), IGF-1 [18] or β2-microglobulin (β2-m, [8]). Figure 2 shows an example in which TGFβ1 plus EGF induced the transition of $ARCaP_E$ to $ARCaP_M$ cells. We observed that this transition was transient upon growth factor induction since this induction was reversible based on the expression of EMT markers, such as downregulation of E-cad, and upregulation of vimentin and RANKL upon growth factor removal. These results, when compared with permanent induction of EMT by the inoculation of $ARCaP_E$ cells in mouse tibia [4] suggest that other factors in bone and/or prolonged exposure to bone milieu play a critical role. These results raised the possibility that $ARCaP_E$ cells could "reawaken" from their dormancy to undergo permanent transition and become more aggressive $ARCaP_M$ cells.

RANKL, a novel EMT marker in ARCaP model, increased upon induction by soluble growth factors and functionally induced increased bone resorption

The induction of RANKL on the cell surface of prostate cancer cells is of particular interest to us since we observed a threefold increase of tartrate-resistant acid phosphatase (TRAP)-positive staining osteoclasts in mouse bone upon the introduction of $ARCaP_M$ compared to $ARCaP_E$ cells (33 ± 9 vs. 9 ± 1 TRAP-positive multinucleated osteoclasts/well in $ARCaP_M$ and $ARCaP_E$ co-cultured with hematopoetic pre-osteoclasts). Further, we found that RANKL expressed by $ARCaP_M$ or RANKL expression induced by Snail transfection into $ARCaP_E$ cells is functional in vitro, with increased activation of osteoclasts noted when incubated with mouse macrophages and this induction can be blocked by osteoprotegerin (OPG), a RANK decoy receptor (Fig. 3). Snail, a known TGF-β target gene, suppresses E-cadherin expression through the activation of a series of nuclear transcription factors. These results, in aggregate, suggest that the RANKL expression induced in $ARCaP_M$ cells is functional and promotes osteoclastogenesis, bone turnover and release of growth factors deposited in bone, conditions which favor prostate cancer cell survival and bone colonization [26, 27]. Our results from the $ARCaP_E$ transition to $ARCaP_M$, suggest that increased bone turnover in prostate cancer patients could result from both osteoblast-derived as well as prostate cancer cell-derived RANKL. Targeting RANKL–RANK interaction seems to be a rational approach to reduce bone turnover and subsequent prostate cancer growth and colonization in bone. It should be emphasized that the RANKL–RANK interaction can be both paracrine (such as prostate cancer–osteoclast, osteoblast–osteoclast, or intercellular communication among prostate cancer cells) and autocrine in nature (soluble RANKL–RANK interaction within a cancer cell or RANKL–RANK interaction between cancer cells). This interaction could be affected by the levels of OPG, a decoy RANK receptor [28]. Numerous previous studies demonstrated that a paracrine interaction with RANKL derived from osteoblasts, in response to tumor-derived soluble factors such as PTHrP [26, 29, 30], contributes to increased bone turnover through interaction with RANK, a cell surface receptor of osteoclasts. However, our results show that functional RANKL

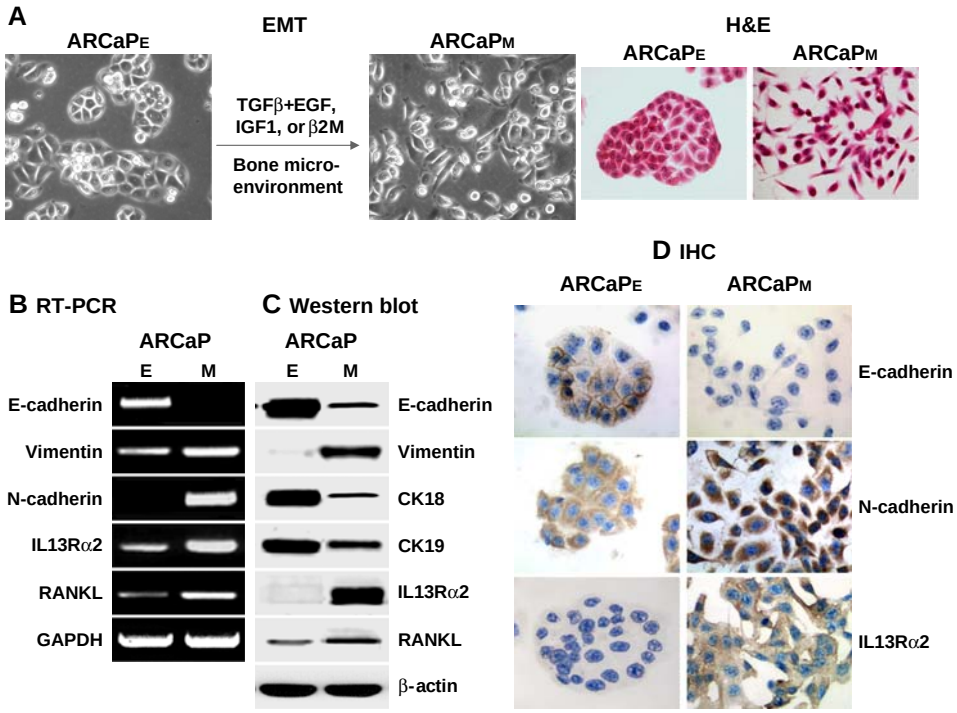

Fig. 1 ARCaP EMT model in which selected growth factors or bone microenvironment drives $ARCaP_E$ cells to undergo mesenchymal-like transition to $ARCaP_M$. Upon this morphologic transition (**a**), $ARCaP_M$ cells expressed both classic EMT markers (decreased expression of E-cadherin and cytokeratins 18/19 and increased expression of vimentin and N-cadherin) and novel markers (increased expression of RANKL and IL13Rα2) as analyzed by RT-PCR (**b**), western blot (**c**) and IHC (**d**)

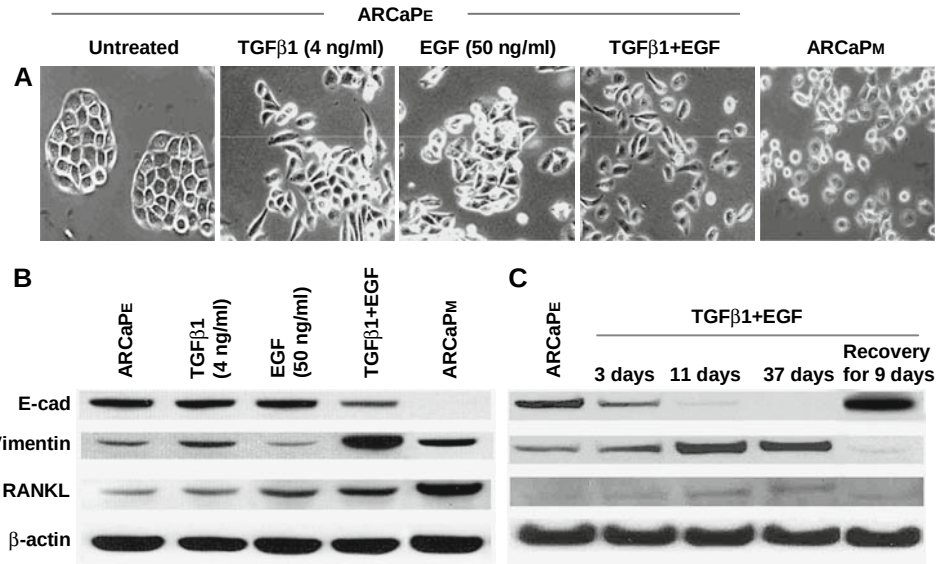

Fig. 2 TGFβ1 and EGF promote ARCaP prostate cancer EMT as evidenced by morphology and gene expression analyses. (**a**) $ARCaP_E$ cells have a typical cobblestone-like epithelial morphology, which could be altered to mesenchymal-like morphology by simultaneous treatment of TGFβ1 and EGF for 3–37 days. (**b**) The treatment inhibited the epithelial E-cad marker, but increased the mesenchymal vimentin and RANKL markers. (**c**) Effect of TGFβ1 and EGF treatment was transient, as termination of the treatment led to re-expression of the E-cad with decreased vimentin expression, 9 days after removal of the growth factors

can also be derived directly from prostate cancer cells along with their osteomimetic properties, and thus contribute to increased bone turnover and cancer cell growth, survival and migration in bone [8]. There remain some discrepancies regarding to the expression of RANKL by prostate cancer cells, since previous reports by others have shown that bone metastatic cancer cell lines lack RANKL expression [31–33], consistent with the view that in osteolytic bone metastasis RANKL is osteoblast-derived and is induced by cancer cell-derived PTHrP [30, 32]. However, we have recently conducted multiplexed quantum dot analysis of RANKL expression in clinical human prostate cancer bone metastatic specimens. In this study, we confirmed, at the single cell level, that RANKL was expressed

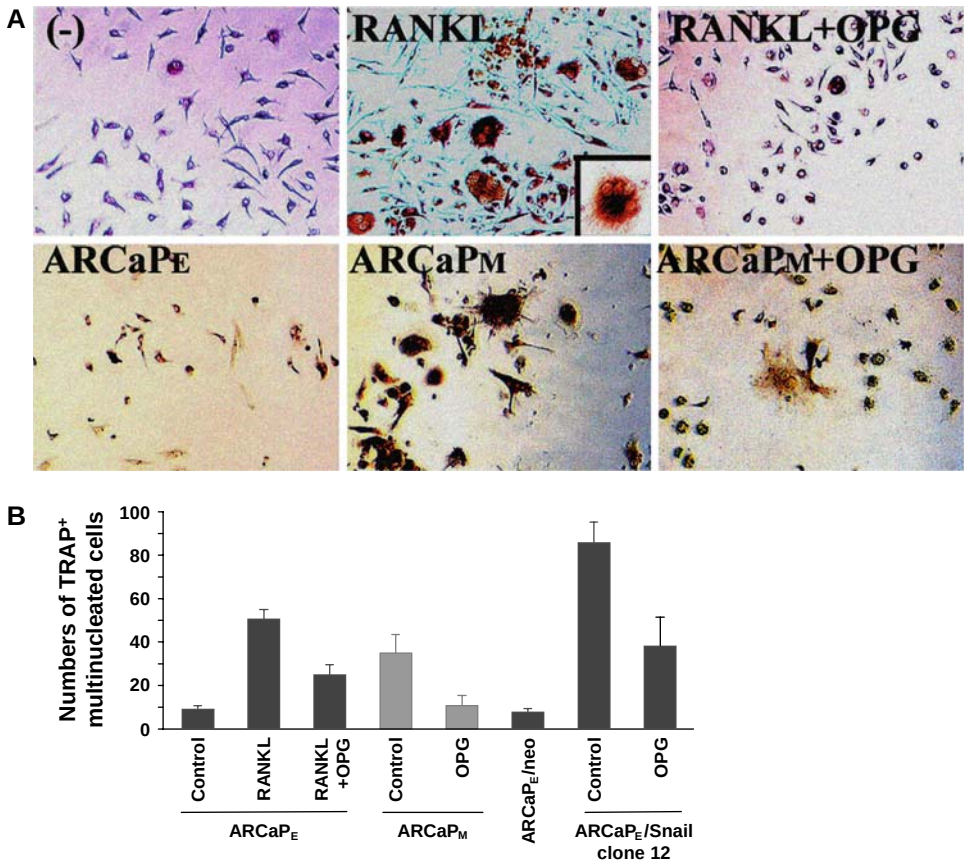

Fig. 3 Increased osteoclastogenesis in vitro after co-culturing mouse haematopoietic pre-osteoclasts with $ARCaP_M$ or $ARCaP_E$-Snail transfectants. (**a**) Top panels: RANKL induced osteoclastogenesis in haematopoietic pre-osteoclastic precursor cells was blocked by OPG. Bottom panels: $ARCaP_M$ cells that overexpress RANKL when co-cultured with mouse haematopoietic pre-osteoclasts induced more TRAP positive staining cells, an indication of inducing osteoclast maturation, as seen under light microscopy, compared to $ARCaP_E$ co-culture. This increased osteoclastogenesis was effectively antagonized by osteoprotegerin (OPG), suggesting that the RANKL overexpressed by $ARCaP_M$ cells is functional (200×). *Inset*, multinucleated osteoclast at 400×. (**b**) Multinucleated TRAP positive cells from $ARCaP_E$, $ARCaP_M$, or $ARCaP_E$-Snail 12 clone co-culture were counted and quantified. Overexpression of Snail induced marked TRAP positive cells indicative of functional RANKL which was blocked by OPG. Data represent triplicates obtained from 2 independent experiments

by human prostate cancer epithelial cells (Ep-CAM+ cells), human prostate epithelial cells that had undergone mesenchymal transition (Ep-CAM+ and vimentin+ cells) and cancer cells expressed only mesenchymal marker (Ep-CAM− but vimentin+ cells), (unpublished results presented and discussed in "The 2008 Frontiers of Cancer Nanotechnology Symposium"). In our study, we found the fixation protocol used in the preservation of prostate cancer specimens is critical for determining the quality and quantity of the RANKL expression. Our results are in agreement with Mori et al. [26], who showed that RANKL–RANK autocrine signaling in human prostate cancer PC-3 and DU-145 cells could drive the migration and survival of these cancer cells and confer their ability to invade and metastasize, the well-known characteristic features of EMT. Because of the potential downstream cell signaling convergence between RANKL–RANK interaction and EMT, we suggest a dual targeting strategy where both the paracrine/autocrine RANKL–RANK interaction and EMT could be interrupted to reduce the overall bone colonization and EMT associated with prostate cancer cell growth, survival and migration. The section below describes our results of the involvement of a developmental gene, LIV-1, in EMT during human prostate cancer progression and bone metastasis.

Involvement of Stat3, Snail and LIV-1 signaling in EMT and RANKL expression by ARCaP cells

To understand how EMT and RANKL may be regulated by soluble factors in cancer cells, we sought to examine the effects of β2-m, a soluble factor that has been shown to contribute to osteomimicry by prostate cancer cells [9, 21], in a number of human cancer models including human breast (MCF-7), lung (H358) and renal (SN12C) cells.

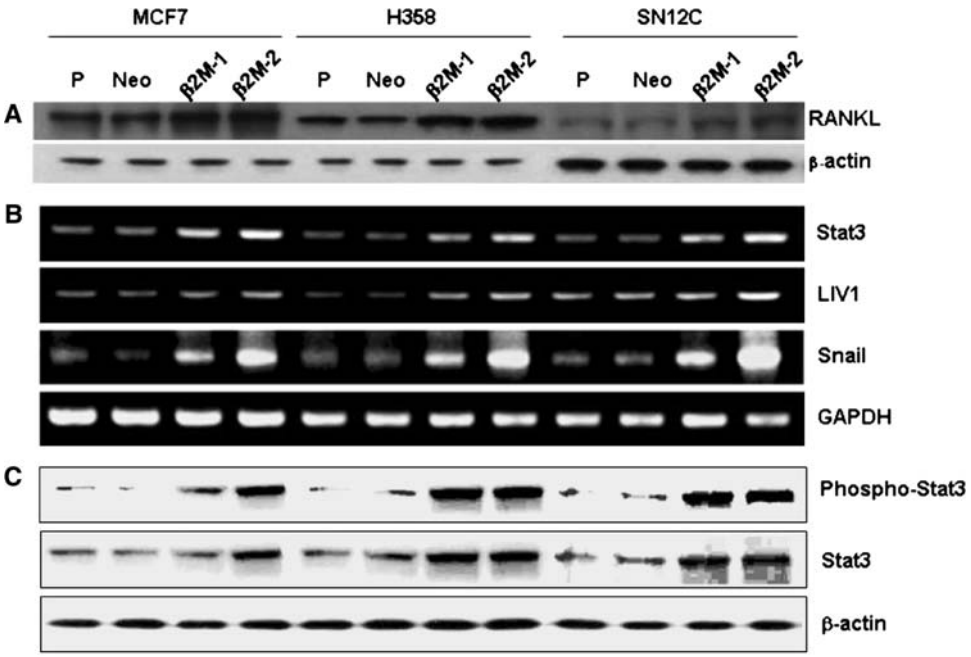

Fig. 4 Stable β2-m expression in human breast (MCF7, **a**), lung (H358, **b**) and renal (SN12C, **c**) cancer cells increased the expression of RANKL protein and the signaling mediated by Stat3 (increased both basal level and pStat3), Snail and LIV1 (a gene drives EMT in Zebrafish). β2-m-1 and β2-m-2 represent, respectively, the intermediate and high β2-m stably expressing clones. Note that the levels of activation of cell signaling correlated with levels of β2-m expression. P: parental cells. Neo: neo-transfected cells. A represents western blots of RANKL and β-actin, B represents the RT-PCR data of stat3, LIV-1 and Snail with GAPDH as a control gene, and C represents the western blots of p-stat3, stat3 with β-actin as the loading control

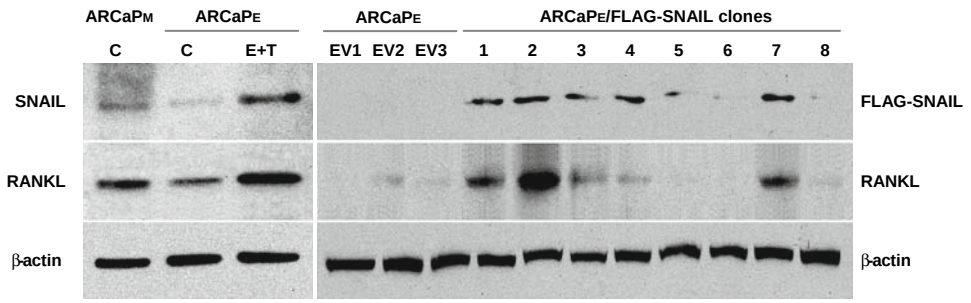

Fig. 5 Combination treatment of $ARCaP_E$.cells with TGFβ1 and EGF induced the protein expression of Snail and RANKL (left panels). Cells were treated with EGF (50 ng/ml) plus TGFβ1 (4 ng/ml) for 3 days (E + T). Note that $ARCaP_M$ cells expressed higher levels of endogenous Snail and RANKL than $ARCaP_E$ (lanes denoted with C). Right panels: over-expression of Snail induced RANKL expression in the $ARCaP_E$ cells. An expression vector containing a constitutively active Snail (Flag-Snail-6SA) was used. EV1-3: vector controls; clones 1–8: stable Snail transfected clones

Figure 4 shows that upon the selection of stably β2-m-transfected cancer cells (with either intermediate or high expression), these cell clones consistently had activated Stat3, Snail, LIV-1 and RANKL with all of the transfected cells expressing markers indicative of EMT and a morphologic transition to fibroblastic (data not shown). We further conducted studies to show a direct link between Snail and RANKL by overexpressing a Flag-tagged Snail and observed increased expression of RANKL only in Snail stably-transfected cells, but not in neo control clones (Fig. 5). These data further supported a direct link between Snail and RANKL expression.

To test if there is a link between LIV-1 and EMT in the ARCaP model, we overexpressed LIV-1 transiently in $ARCaP_E$ cells, which contain low levels of LIV-1, and found that $ARCaP_E$ cells underwent EMT by the expression of mesenchymal markers, increased Snail, vimentin, and RANKL but decreased E-cad expression (Fig. 6). This observation linking LIV-1 and EMT is further supported by a follow up experiment whereby the knockdown of LIV-1, which is expressed abundantly in $ARCaP_M$ cells, with LIV-1 siRNA resulted in the expression of epithelial markers (increased expression of E-cad, and decreased expression of N-cad, vimentin and RANKL, Fig. 6). These studies led

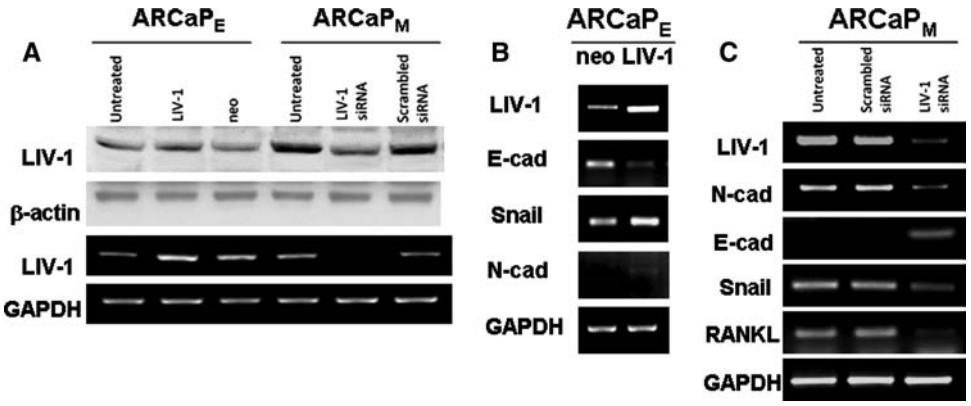

Fig. 6 LIV-1 plays an important role in ARCaP EMT. (**a**) LIV-1 antibody recognized a single band at 85 kDa and was expressed at higher levels in $ARCaP_M$ than in $ARCaP_E$ cells and is sensitive to siRNA targeting LIV-1 at both RNA and protein levels. Since this was a transient knockdown study, we observed only a slight change of LIV-1 protein level possibly due to the longer t1/2 of this protein in comparison to LIV-1 mRNA. (**b**) LIV-1 transfected $ARCaP_E$ cell clones expressed increased Snail and decreased E-cad, an indication of mesenchymal-like transition. (**c**) LIV-1 siRNA treated $ARCaP_M$ cells expressed decreased levels of LIV-1, Snail, N-cad, vimentin and RANKL, but increased E-cad, indicative of epithelial differentiation in comparison to untreated or scrambled LIV-1 siRNA-treated $ARCaP_M$ cells

to the conclusion that LIV-1, a zinc transporter protein known to promote EMT in Zebrafish gastrula organizer [34] and associated with human breast cancer [13], plays a central role in $ARCaP_E$ transition to $ARCaP_M$ and is possibly correlated with the progression of human prostate cancer. We have confirmed this concept in localized and bone metastatic human prostate cancer tissue arrays where LIV-1 protein expression level had statistically significant association with prostate cancer progression from normal, benign, PIN, primary cancer to bone metastasis [35].

EMT, MET, MErT and MMT: dynamics of the ARCaP model

EMT is a dynamic process which may occur at primary as well as metastatic sites where reversion of EMT toward an epithelial phenotype via MET takes place [16, 36, 37]. The plasticity of ARCaP cells was supported by the experimental observation that parental epithelial-like $ARCaP_E$ cells, exposed to bone or cultured in vitro in the presence of TGFβ1 plus EGF, underwent mesenchymal transition. Because the importance of the bone microenvironment, which is rich in growth factors that can drive ARCaP EMT, we suggest that although the homing of prostate cancer cells to bone is important, it is even more critical that soluble factors released during bone turnover play a key role in the promotion of EMT and subsequent prostate cancer cell growth, survival and bone colonization. This idea is also supported by clinical observations, where patients with serum prostate-specific antigen (PSA) < 0.1 ng/ml were found to harbor prostate cancer cells in bone marrow. Since only a fraction of these patients will develop bone metastasis in their lifetime, this supports the idea that while the presence of prostate cancer cells in bone is common, they are mostly "dormant" and only if they are responsive to soluble factors eliciting the expression of bone-like properties, such as the expression of OC, BSP and RANKL, they gain the ability to undergo EMT, with increased expression of RANKL which promotes bone turnover, cancer cell survival and subsequent colonization in bone.

Mesenchymal to epithelial reversing transition or MErT occurred when a human prostate cancer cell line, DU-145, was co-cultured with human hepatocytes under three-dimensional (3-D) conditions [16]. In analogous conditions, $ARCaP_M$ cells cultured by 3-D Rotary Wall Vessel (RWV) underwent MET (data not included). Such rapid transition of $ARCaP_M$ to $ARCaP_E$ under 3-D conditions showed how $ARCaP_M$ cells could "settle" comfortably in the skeleton as a part of the metastastic cascade, since re-expressing E-cad provides $ARCaP_M$ cells with strong intercellular adhesion and facilitates their colonization in bone. This, however, did not seem to be the case with $ARCaP_M$ cells isolated from the bone environment, which retained mesenchymal features despite establishing stable bone metastatic potential and exhibiting osteolytic response when residing in bone. The derivation of a mesenchymal subline from he bone marrow environment is consistent with the findings of vimentin positivity in 15 of 15 breast cancer cell lines developed by Pantel and co-workers from micrometastases in this environment [38].

MMT, mesenchymal to mesenchymal transition, occurs in situ and during embryonic development, such as with the induction of "reactive" stroma [39]. The plasticity of cancer cells and their surrounding fibromuscular stromal cells involves a highly dynamic *reverting* program (or

trans-differentiation) of cells toward certain phenotypes through selective activation of cell signaling pathways [14, 40, 41]. The underlying biologic basis of these transitions is found in embryonic development and apparently persists in adult cells and contributes to neoplastic progression. Further analysis of the ARCaP model system may reveal the molecular mechanisms underlying such dynamic transitions.

Conclusions

We demonstrated that the host bone microenvironment and soluble growth factors are crucial in facilitating EMT and RANKL expression, which subsequently promote prostate cancer cell migration, invasion and metastasis to the skeleton and soft tissues. Our data demonstrated a close link between the ARCaP EMT model and human prostate cancer bone metastasis. This model, therefore, is well suited to investigate the biology and targeting of the lethal progression of human prostate cancer to bone.

We confirmed the plasticity of prostate cancer cells in the ARCaP EMT model and their ability to express the embryonic EMT-associated LIV-1 gene. Our results suggest that through proper cell signaling switches mimicking embryonic development, invasive ARCaP cells armed with mesenchymal gene expression profiles gained invasive and migratory phenotypes and can then re-acquire epithelial and embryonic phenotypes and grow and flourish in the metastatic niche. We suggest that tumor cell-host microenvironment interaction is critical in determining the temporal and spatial transition of epithelial and mesenchymal cells. The ARCaP model provides an excellent tool to dissect the molecular links in heterogeneous cancer cells between EMT, RANKL and bone turnover, fundamental to understanding why many solid tumors, including prostate cancer, metastasize to bone.

Acknowledgements We thank Gary Mawyer for editing. The helpful discussion and support from Guodong Zhu, Weiping Qian, Daqing Wu and Clayton Yates are greatly appreciated. The authors are particularly indebted to the helpful suggestions made by the editors, Drs. Rik Thompson and Elizabeth Williams, during the revision of this manuscript. This study was supported in part by CA082739 (HYEZ), U54 CA119338, CA098912 and CA766201 (LWKC). We are grateful to the generous gift from Frances and Clarence Wilkins in support of this study.

References

1. Robinson VL, Kauffman EC, Sokoloff MH et al (2004) The basic biology of metastasis. Cancer Treat Res 118:1–21
2. Tu SM, Lin SH (2004) Clinical aspects of bone metastases in prostate cancer. Cancer Treat Res 118:23–46
3. Wu TT, Sikes RA, Cui Q et al (1998) Establishing human prostate cancer cell xenografts in bone: induction of osteoblastic reaction by prostate-specific antigen-producing tumors in athymic and SCID/bg mice using LNCaP and lineage-derived metastatic sublines. Int J Cancer 77(6):887–894. doi:10.1002/(SICI) 1097-0215(19980911) 77:6<887::AID-IJC15>3.0.CO;2-Z
4. Xu J, Wang R, Xie ZH et al (2006) Prostate cancer metastasis: role of the host microenvironment in promoting epithelial to mesenchymal transition and increased bone and adrenal gland metastasis. Prostate 66(15):1664–1673. doi:10.1002/pros.20488
5. Zhau HY, Chang SM, Chen BQ et al (1996) Androgen-repressed phenotype in human prostate cancer. Proc Natl Acad Sci USA 93(26):15152–15157. doi:10.1073/pnas.93.26.15152
6. Odero-Marah V, Shi C, Zhau HE et al (2007) Dual role of Snail transcription factor in epithelial to mesenchymal transition and neuroendocrine differentiation in human prostate cancer cells. AACR Proc 48:247
7. Chung LW, Baseman A, Assikis V et al (2005) Molecular insights into prostate cancer progression: the missing link of tumor microenvironment. J Urol 173(1):10–20
8. Chung LW, Huang WC, Sung SY et al (2006) Stromal–epithelial interaction in prostate cancer progression. Clin Genitourin Cancer 5(2):162–170
9. Huang WC, Xie Z, Konaka H et al (2005) Human osteocalcin and bone sialoprotein mediating osteomimicry of prostate cancer cells: role of cAMP-dependent protein kinase A signaling pathway. Cancer Res 65(6):2303–2313. doi:10.1158/0008-5472.CAN-04-3448
10. Gotzmann J, Mikula M, Eger A et al (2004) Molecular aspects of epithelial cell plasticity: implications for local tumor invasion and metastasis. Mutat Res 566(1):9–20. doi:10.1016/S1383-5742(03) 00033-4
11. Huber MA, Kraut N, Beug H (2005) Molecular requirements for epithelial–mesenchymal transition during tumor progression. Curr Opin Cell Biol 17(5):548–558. doi:10.1016/j.ceb.2005.08.001
12. Brabletz T, Hlubek F, Spaderna S et al (2005) Invasion and metastasis in colorectal cancer: epithelial–mesenchymal transition, mesenchymal–epithelial transition, stem cells and beta-catenin. Cells Tissues Organs 179(1–2):56–65. doi:10.1159/000084509
13. Taylor KM, Hiscox S, Nicholson RI (2004) Zinc transporter LIV-1: a link between cellular development and cancer progression. Trends Endocrinol Metab 15(10):461–463. doi:10.1016/j.tem.2004.10.003
14. Larue L, Bellacosa A (2005) Epithelial–mesenchymal transition in development and cancer: role of phosphatidylinositol 3′ kinase/AKT pathways. Oncogene 24(50):7443–7454. doi:10.1038/sj.onc.1209091
15. Thiery JP (2003) Epithelial–mesenchymal transitions in development and pathologies. Curr Opin Cell Biol 15(6):740–746. doi:10.1016/j.ceb.2003.10.006
16. Yates C, Shepard CR, Papworth G et al (2007) Novel three-dimensional organotypic liver bioreactor to directly visualize early events in metastatic progression. Adv Cancer Res 97:225–246. doi:10.1016/S0065-230X(06) 97010-9
17. Albalate M, de la Piedra C, Fernandez C et al (2006) Association between phosphate removal and markers of bone turnover in haemodialysis patients. Nephrology Dialysis Transplantation 21(6):1626–1632. doi:10.1093/ndt/gfl034
18. Graham T R ZHE, Odero-Marah VA, Osunkoya AO, Kimbro KS, Tighiouart M, Liu T, Simons JW, O'Regan RM (2008) IGF-1-dependent upregulation of ZEB1 expression drives EMT in human prostate cancer cells in vitro. Cancer Res 68(7): 2479–2488

19. Gleave M, Hsieh JT, Gao CA et al (1991) Acceleration of human prostate cancer growth in vivo by factors produced by prostate and bone fibroblasts. Cancer Res 51(14):3753–3761
20. Thalmann GN, Sikes RA, Wu TT et al (2000) LNCaP progression model of human prostate cancer: androgen-independence and osseous metastasis. Prostate 44(2):91–103
21. Huang WC, Wu D, Xie Z et al (2006) beta2-microglobulin is a signaling and growth-promoting factor for human prostate cancer bone metastasis. Cancer Res 66(18):9108–9116. doi:10.1158/0008-5472.CAN-06-1996
22. Zhou BP, Deng J, Xia W et al (2004) Dual regulation of Snail by GSK-3beta-mediated phosphorylation in control of epithelial–mesenchymal transition. Nat Cell Biol 6(10):931–940. doi:10.1038/ncb1173
23. Takahashi N, Akatsu T, Udagawa N et al (1988) Osteoblastic cells are involved in osteoclast formation. Endocrinology 123(5):2600–2602
24. Fichtner-Feigl S, Strober W, Kawakami K et al (2006) IL-13 signaling through the IL-13alpha2 receptor is involved in induction of TGF-beta1 production and fibrosis. Nat Med 12(1):99–106. doi:10.1038/nm1332
25. Kawakami K (2005) Cancer gene therapy utilizing interleukin-13 receptor alpha2 chain. Curr Gene Ther 5(2):213–223. doi:10.2174/1566523053544227
26. Mori K, Le Goff B, Charrier C et al (2007) DU145 human prostate cancer cells express functional receptor activator of NFkappaB: new insights in the prostate cancer bone metastasis process. Bone 40(4):981–990. doi:10.1016/j.bone.2006.11.006
27. Vessella RL, Corey E (2006) Targeting factors involved in bone remodeling as treatment strategies in prostate cancer bone metastasis. Clin Cancer Res 12(20 Pt 2):6285s–6290s. doi:10.1158/1078-0432.CCR-06-0813
28. Armstrong AP, Miller RE, Jones JC et al (2008) RANKL acts directly on RANK-expressing prostate tumor cells and mediates migration and expression of tumor metastasis genes. Prostate 68(1):92–104. doi:10.1002/pros.20678
29. Mundy GR (2002) Metastasis to bone: causes, consequences and therapeutic opportunities. Nat Rev Cancer 2(8):584–593. doi:10.1038/nrc867
30. Roodman GD (2004) Mechanisms of bone metastasis. N Engl J Med 350(16):1655–1664. doi:10.1056/NEJMra030831
31. Chamulitrat W, Schmidt R, Chunglok W et al (2003) Epithelium and fibroblast-like phenotypes derived from HPV16 E6/E7-immortalized human gingival keratinocytes following chronic ethanol treatment. Eur J Cell Biol 82(6):313–322. doi:10.1078/0171-9335-00317
32. Thomas RJ, Guise TA, Yin JJ et al (1999) Breast cancer cells interact with osteoblasts to support osteoclast formation. Endocrinology 140(10):4451–4458. doi:10.1210/en.140.10.4451
33. Schwaninger R, Rentsch CA, Wetterwald A et al (2007) Lack of noggin expression by cancer cells is a determinant of the osteoblast response in bone metastases. Am J Pathol 170(1):160–175. doi:10.2353/ajpath.2007.051276
34. Yamashita S, Miyagi C, Fukada T et al (2004) Zinc transporter LIVI controls epithelial–mesenchymal transition in zebrafish gastrula organizer. Nature 429(6989):298–302. doi:10.1038/nature02545
35. Arnold RCL, Farah-Carson MC et al (2008) Prostate cancer bone metastasis: reactive oxygen species, growth factors and heparan sulfate proteoglycans provide a signaling triad that supports progression. J Urol 179(Suppl 4):192
36. Chaffer CL, Brennan JP, Slavin JL et al (2006) Mesenchymal-to-epithelial transition facilitates bladder cancer metastasis: role of fibroblast growth factor receptor-2. Cancer Res 66(23):11271–11278. doi:10.1158/0008-5472.CAN-06-2044
37. Vincan E, Brabletz T, Faux MC et al (2007) A human three-dimensional cell line model allows the study of dynamic and reversible epithelial–mesenchymal and mesenchymal–epithelial transition that underpins colorectal carcinogenesis. Cells Tissues Organs 185(1–3):20–28. doi:10.1159/000101299
38. Willipinski-Stapelfeldt B, Riethdorf S, Assmann V et al (2005) Changes in cytoskeletal protein composition indicative of an epithelial–mesenchymal transition in human micrometastatic and primary breast carcinoma cells. Clin Cancer Res 11(22):8006–8014. doi:10.1158/1078-0432.CCR-05-0632
39. Cat B, Stuhlmann D, Steinbrenner H et al (2006) Enhancement of tumor invasion depends on transdifferentiation of skin fibroblasts mediated by reactive oxygen species. J Cell Sci 119(Pt 13):2727–2738. doi:10.1242/jcs.03011
40. Lee JM, Dedhar S, Kalluri R et al (2006) The epithelial–mesenchymal transition: new insights in signaling, development, and disease. J Cell Biol 172(7):973–981. doi:10.1083/jcb.200601018
41. Thiery JP, Sleeman JP (2006) Complex networks orchestrate epithelial–mesenchymal transitions. Nat Rev Mol Cell Biol 7(2):131–142. doi:10.1038/nrm1835

Cell Research (2008) 18:858-870.

www.nature.com/cr

ORIGINAL ARTICLE

Receptor activator of NF-κB Ligand (RANKL) expression is associated with epithelial to mesenchymal transition in human prostate cancer cells

Valerie A Odero-Marah[1], Ruoxiang Wang[1], Gina Chu[1], Majd Zayzafoon[2], Jianchun Xu[1], Chunmeng Shi[1], Fray F Marshall[1], Haiyen E Zhau[1], Leland WK Chung[1]

[1]Molecular Urology and Therapeutics Program, Department of Urology and Winship Cancer Institute, Emory University School of Medicine, 1365B Clifton Road, NE, Atlanta, GA 30322, USA; [2]Department of Pathology, University of Alabamn, Birmingham, AL 35294, USA

Epithelial-mesenchymal transition (EMT) in cancer describes the phenotypic and behavioral changes of cancer cells from indolent to virulent forms with increased migratory, invasive and metastatic potential. EMT can be induced by soluble proteins like transforming growth factor β1 (TGFβ1) and transcription factors including Snail and Slug. We utilized the $ARCaP_E$/$ARCaP_M$ prostate cancer progression model and LNCaP clones stably overexpressing Snail to identify novel markers associated with EMT. Compared to $ARCaP_E$ cells, the highly tumorigenic mesenchymal $ARCaP_M$ and $ARCaP_{M1}$ variant cells displayed a higher incidence of bone metastasis after intracardiac administration in SCID mice. $ARCaP_M$ and $ARCaP_{M1}$ expressed mesenchymal stromal markers of vimentin and N-cadherin in addition to elevated levels of Receptor Activator of NF-κB Ligand (RANKL). We observed that both epidermal growth factor (EGF) plus TGFβ1 treatment and Snail overexpression induced EMT in $ARCaP_E$ and LNCaP cells, and EMT was associated with increased expression of RANKL protein. Finally, we determined that the RANKL protein was functionally active, promoting osteoclastogenesis *in vitro*. Our results indicate that RANKL is a novel marker for EMT during prostate cancer progression. RANKL may function as a link between EMT, bone turnover, and prostate cancer skeletal metastasis.

Keywords: EMT, bone microenvironment, RANKL, prostate cancer, bone metastasis, EGF, TGFβ1, Snail

Cell Research (2008) **18**:858-870. doi: 10.1038/cr.2008.84; published online 22 July 2008

Introduction

EMT in cancer cells is an event reminiscent of the invasion front of migrating cells during embryonic development [1]. A switch from a tightly clustered cobblestone-like appearance to loosely associated spindle-shaped mesenchymal stromal morphology characterizes EMT. This morphologic switch is accompanied by markedly elevated expression of mesenchymal-associated genes, such as vimentin, N-cadherin, and fibronectin, and decreased production of epithelial-specific markers, including E-cadherin and cytokeratins. It has been widely reported that, by undergoing EMT, cancer cells gain increased growth and malignant potential [2-4]. Results obtained from various experimental models revealed that through EMT cancer cells became more migratory, invasive, and metastatic [5-7]. Although EMT is well studied *in vitro*, data on EMT occurrence in specific solid tumors *in vivo* and its relevance to the process of cancer progression have been scarce.

Soluble factors such as epidermal growth factor (EGF), scatter factor/hepatocyte growth factor (SF/HGF), and members of the transforming growth factor, TGFβ1, and basic fibroblast growth factor (bFGF) families have been shown to promote EMT in several model systems [1, 8, 9]. The EpH4 mouse mammary epithelial cell line, for example, was promoted to undergo EMT by cooperation of active Ras and TGFβ via signaling through the MAPK, ERK, and phosphoinositide 3 kinase (PI3K) pathways [10]. Insulin-like growth factor II (IGF-II) stimulated EMT in

Correspondence: Haiyen E Zhau[a], Leland WK Chung[b]
Tel: +1-404-778-4319; Fax: +1-404-778-3675
E-mail: [a]hzhau@emory.edu; [b]lwchung@emory.edu
Abbreviations: EMT (epithelial-mesenchymal transition); RANKL (receptor activator of NF-κB ligand); TGFβ1 (transforming growth factor β1); EGF (epidermal growth factor); OPG (osteoprotegerin)
Received 11 April 2007; revised 3 March 2008; accepted 7 March 2008; published online 22 July 2008

NBT-II rat bladder carcinoma cells via nuclear translocation of β-catenin [11]. These soluble growth factors, known to be abundant in the bone microenvironment [12], are released upon increased bone turnover and could fuel cancer growth. The Snail transcription factor, a downstream target of TGFβ1, has been shown to induce EMT in several *in vitro* cell models for breast, ovarian, and bladder cancers [3, 13-15]. In a human squamous cell carcinoma (SCC) model, EMT was induced by overexpression of Snail and SIP1, or by TGFβ1 treatment [16]. A common theme seems to be a coordinated suppression of adhesion molecules E-cadherin and desmosomal proteins (desmoplakin, desmoglein), with a concomitant activation of vimentin, fibronectin, and collagens [1, 5, 9].

EMT is not as well studied in prostate cancer as in other cancers. Prostate cancer cells have been shown to overexpress TGFβ1, which stimulates angiogenesis and inhibits immune responses, and thus promotes cancer growth [17]. Zhau *et al.* observed increased invasion and growth of human prostate cancer PC-3 cells following transfection with c-erbB2/neu, coordinated by vimentin overexpression [18]. EMT was also induced in PC-3 cells through transfection with human kallikrein 4 gene [19].

Receptor Activator of NF-κB Ligand (RANKL), a member of the TNF family, is a protein normally expressed on the surface of stromal cells and osteoblasts, and mediates osteoclast differentiation and osteolytic bone resorption [20, 21]. Physiologically, RANKL binds RANK receptor on the surface of the osteoclast, and this interaction can be blocked by osteoprotegerin (OPG), a decoy receptor for RANKL [22]. Although prostate cancer bone metastases are mostly osteoblastic in nature, both osteoblastic and osteolytic lesions can be seen [23, 24]. Bone resorption can be shown by an increase in serum and urine markers, demonstrating increased bone turnover during prostate cancer bone metastasis [25]. The 'vicious cycle' theory proposes that increased bone resorption results in elevated TGFβ, which promotes cancer cells to synthesize parathyroid hormone-related peptide (PTHrP) that stimulates RANKL expression by osteoclasts, resulting in osteoclastogenesis [26]. Recently, increased RANKL expression has been detected in human prostate cancers [27, 28], indicating a direct effect of the prostate cancer cells on osteoclastogenesis [27, 29].

We recently reported the establishment of the first human prostate cancer EMT animal model [30]. ARCaP human prostate cancer cells were found to acquire mesenchymal stromal properties following xenograft growth in the host bone. We report here that soluble factors EGF and TGFβ1, or Snail transcription factor, can also induce EMT in ARCaP cells, and EMT in LNCaP cells can be induced by Snail overexpression. Upon inducing EMT, elevated expression of functional RANKL was found in both the ARCaP and LNCaP models. Our data suggest a possible link between EMT and elevated RANKL expression and provide supportive rationales for targeting RANKL-mediated signaling in prostate cancer bone metastasis.

Results

The bone microenvironment promoted EMT and increased prostate cancer invasion in mice

We previously reported that, based on morphologic and behavioral features, ARCaP human prostate cancer cells could be separated into epithelial-like $ARCaP_E$ and mesenchymal stromal-like $ARCaP_M$ subclones, while $ARCaP_E$ underwent EMT after interaction with both bone and adrenal gland in immune-compromised mice [30]. In the current study, to investigate the mechanism for the transition, $ARCaP_E$ and $ARCaP_M$ cells were injected by the intracardiac route into SCID mice for spontaneous bone metastasis.

This series of experiments revealed that $ARCaP_M$ cells displayed more aggressive bone metastatic capability, with

Table 1 Metastatic potential of ARCaP sublines in the progression model[a]

Cell	Incidence (%)	Bone metastatic sites	Latency (range in days)
$ARCaP_E$	1/8 (12.5)	Femur, tibia	71
$ARCaP_M$	7/18 (38.9)	Mandible, femur, tibia, spine	119.4±42.9 (70-165)
$ARCaP_{M1}$[b]	11/14 (78.6)	Mandible, femur, tibia, pelvis, rib, sternum, spine	77.9±26.4 (51-130)[c]

ARCaP progression model: incidence, sites, and latency of bone metastasis. $ARCaP_E$ or $ARCaP_M$ cells injected intracardiacally in SCID mice metastasized to various bone sites with increased incidence rates and shorter latency periods. $ARCaP_{M1}$ was derived from $ARCaP_M$.

[a]The SCID mice were used in the study. Tumor metastases were evaluated following intracardiac inoculation in SCID mice.

[b]$ARCaP_{M1}$ is a derivative subline of the $ARCaP_M$.

[c]$p<0.003$ (refers to the statistically significant difference in latency between $ARCaP_{M1}$ and $ARCaP_M$ experimental groups. Student's *t*-test compared to $ARCaP_M$).

an incidence of 38.9% compared to $ARCaP_E$, which had a 12.5% incidence of tumor formation in the bone (Table 1). We then isolated cancer cells from the $ARCaP_M$ bone tumors and denoted the isolate as $ARCaP_{M1}$. Cells from $ARCaP_{M1}$, upon another round of intracardiac administration, showed a markedly increased 78.6% incidence of bone metastasis. Moreover, a significantly shortened latency period was observed for $ARCaP_{M1}$ as compared to $ARCaP_M$ (Table 1).

We have previously observed a similar effect from the bone microenvironment on $ARCaP_E$ cells [30]. Cancer cells derived from $ARCaP_E$ bone tumor exhibited markedly increased tumorigenicity upon a second intracardiac implant. In addition, the cancer cells from $ARCaP_E$ bone tumor displayed morphologic changes, from the original cobblestone to a spindle-shaped scattered shape in culture, suggestive of the occurrence of EMT. To further investigate the process, we performed a series of histopathological

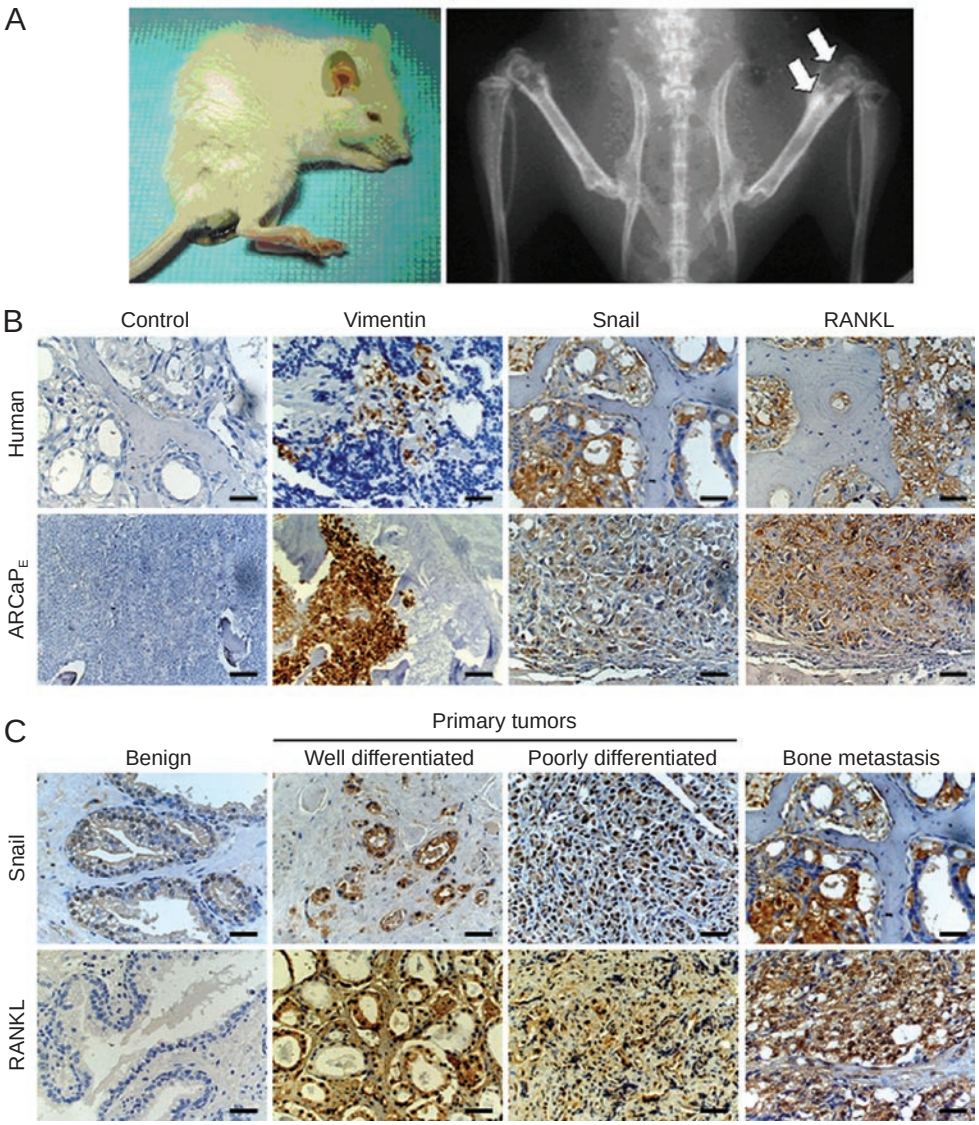

Figure 1 ARCaP subclones exhibited bony metastases. $ARCaP_E$ and $ARCaP_M$ cells were injected intracardiacally into SCID mice for spontaneous bone tumor formation. **(A)** A representative mouse developed cachexia and paraplegia during the late stages of $ARCaP_E$ bone metastasis (left panel). A representative X-ray depicts osteoblastic and osteolytic lesions (arrows) in the mouse femur (right panel). **(B)** EMT is a general feature in prostate cancer bone metastasis. A human specimen of prostate cancer bone metastasis (upper row, human) and an $ARCaP_E$ xenograft bone tumor (lower row, $ARCaP_E$) were examined to identify the occurrence of EMT in a parallel immunohistochemical analysis. Bar = 120 μm. **(C)** Progressive expression of Snail and RANKL in human prostate cancer specimens. Representative tumor tissue histopathologies are shown. Bar = 120 μm.

analyses of $ARCaP_E$ bone tumor.

Mice bearing the $ARCaP_E$ bone tumor developed cachexia as shown in the representative picture (Figure 1A, left panel). Under X-ray radiography, regions of bone metastases were seen with mixed osteoblastic/osteolytic lesions (Figure 1A, right panel), and these results were confirmed by H&E staining of the tumor specimens harvested from mouse bone (data not shown). To confirm that the $ARCaP_E$ cells in the bone tumor have undergone EMT, we examined the expression of vimentin, which was considered a mesenchymal-specific protein and a typical EMT marker. A collection of human specimens of clinical prostate cancer bone metastasis was stained in parallel with the $ARCaP_E$ bone tumors. We found increased vimentin staining in both the human specimens and the $ARCaP_E$ bone tumors, and the stains appeared to be specifically located in the tumor cells (Figure 1B). Using the same strategy, we examined the expression of a panel of genes that were considered to be mesenchymal-specific, and observed that tumor cells transitioning to express mesenchymal markers emerged as a general trend (data not shown).

Interestingly, this series of analysis revealed a coordinated expression of Snail and RANKL upon the occurrence of EMT (Figure 1B). In another examination of these two genes in a series of clinical prostate cancer specimens, both Snail and RANKL were found to be differentially expressed during prostate cancer progression and metastasis (Figure 1C). Snail, as a transcription factor, is known to promote EMT both in developmental processes and in cancer metastasis [31-33]. RANKL is a potent paracrine factor for osteoclastogenesis and bone resorption [34, 35]. Because of the pathophysiological importance of these genes, we performed further investigations to illuminate the regulatory relationship between these genes.

RANKL is a novel EMT marker in the ARCaP human prostate cancer progression model

Since RANKL is known to be an important protein in the colonization of prostate cancer cells in bone [27, 29], we examined whether RANKL is a specific biomarker associated with EMT in the ARCaP progression model. We compared the expression of the conventional EMT markers and RANKL in $ARCaP_E$, $ARCaP_M$, and $ARCaP_{M1}$ cells. Morphologically, $ARCaP_E$ formed tight cobblestone clusters while $ARCaP_M$ and its variant, $ARCaP_{M1}$, were more spindle-shaped and scattered in culture (Figure 2A). Western blot analysis showed decreased E-cadherin but increased N-cadherin, vimentin, and RANKL expression in $ARCaP_M$ and $ARCaP_{M1}$, when compared to $ARCaP_E$ (Figure 2B). With the exception of vimentin, RT-PCR results corresponded with the Western blot results. Vimentin expression only differed at the protein level, indicative of a post-transcriptional regulation of this protein. Our results show that the differential expression of RANKL is associated with EMT in the ARCaP prostate cancer progression model.

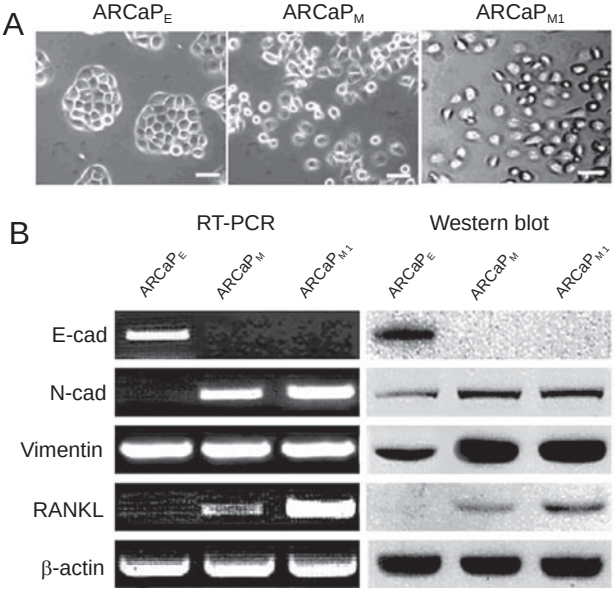

Figure 2 RANKL is a novel EMT marker in the ARCaP EMT model. **(A)** Phase contrast microscopy revealed cobblestone epithelial clusters for $ARCaP_E$, while $ARCaP_M$ and $ARCaP_{M1}$ were more fibroblastic. Bar = 120 μm. **(B)** RT-PCR (left panel) and Western blot (right panel) analyses showed decreased E-cadherin (E-cad), and increased N-cadherin (N-cad), vimentin, and RANKL in the EMT model, from $ARCaP_E$ to $ARCaP_M$ and $ARCaP_{M1}$. Levels of the β-actin were used as loading controls. Note that vimentin expression differences could only be detected at the protein level. Results shown are representative of three independent experiments.

Both EGF and TGFβ1 were required to induce and maintain EMT in $ARCaP_E$ cells

TGFβ1 and EGF have been shown to induce EMT in many cancer cells [36-38]. Since these soluble factors are known to be available in bone and at primary sites of prostate cancer growth, we tested whether these growth factors could stimulate EMT in the $ARCaP_E$ cells. We found that treatment with either EGF (50 ng/ml) or TGFβ1 (4 ng/ml) for 72 h was unable to induce morphologic changes in $ARCaP_E$ cells. A combination of EGF with TGFβ1, however, led to cell morphologic changes from predominantly cobblestone epithelial shape to spindle fibroblast-like shape (Figure 3A).

We performed immunocytochemical staining to further confirm the occurrence of EMT in the treated $ARCaP_E$ cells. Following combinatory treatment with EMT and TGFβ1, N-cadherin expression increased at 48 h, followed by de-

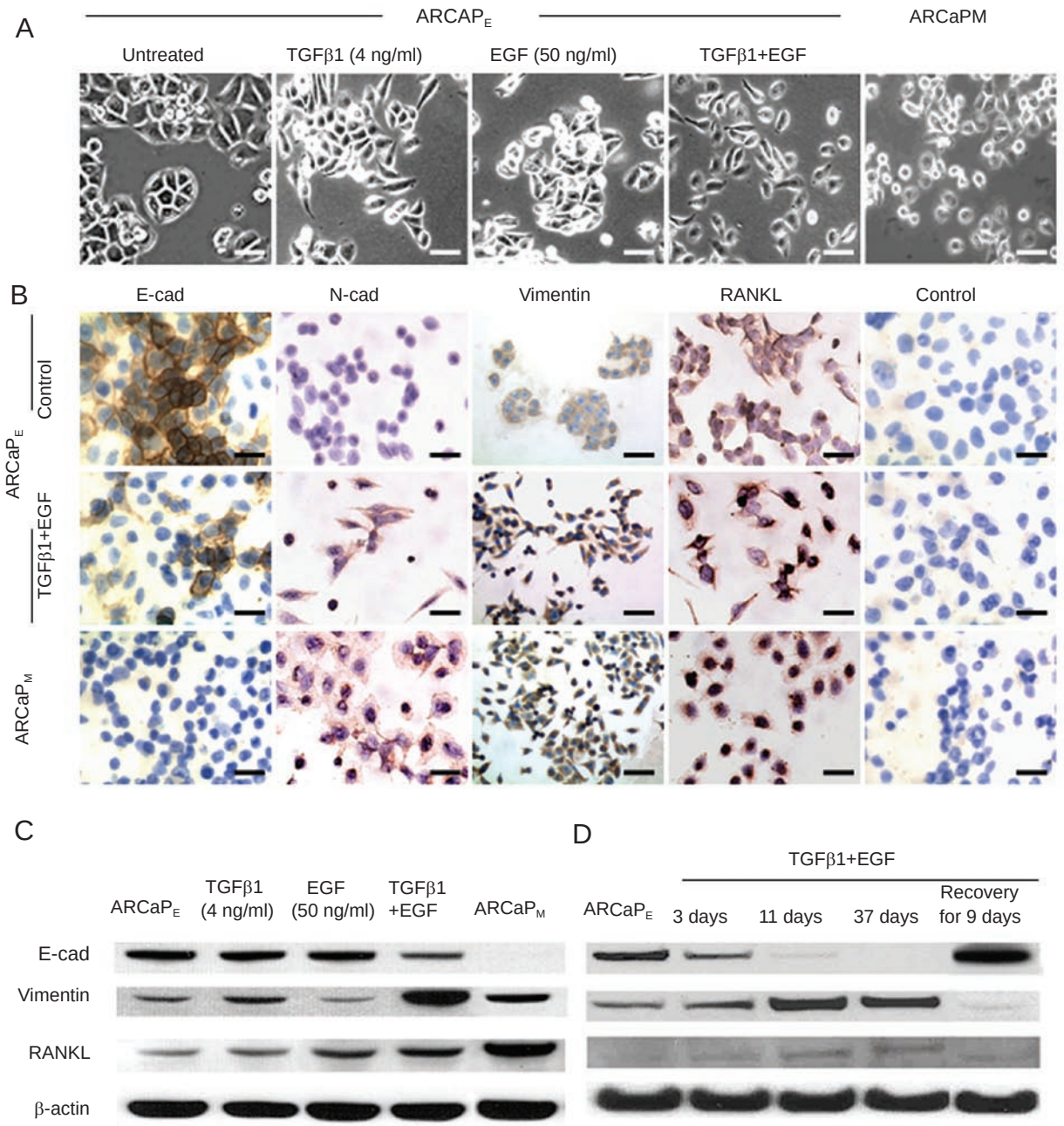

Figure 3 TGFβ1 plus EGF, but not individual growth factor alone, induced ARCaP$_E$ to undergo EMT associated with increased RANKL expression. **(A)** Treatment with both growth factors was required to induce changes in cell morphology from epithelial to spindle shaped. Bar = 120 μm. **(B)** EMT marker gene expression was detected by immunocytochemistry. Bar = 120 μm. **(C)** EMT-associated protein profiles were confirmed by Western blot analysis, showing decreased E-cad, increased vimentin and RANKL. **(D)** Western blot analysis of ARCaP$_E$ cells treated with TGFβ1 plus EGF (T + E) for 3, 11, 37, or 37 days, followed by withdrawal of growth factors for 9 days. The absence of (T + E) reversed EMT. All blots were stripped and subsequently re-probed for β-actin as a loading control.

creased E-cadherin and increased vimentin and RANKL expression at 72 h (Figure 3B). Western blot analysis showed that, while separate treatment with TGFβ1 or EGF for 72 h only slightly decreased E-cadherin and increased vimentin and RANKL levels, the combination treatment significantly and additively decreased the expression of E-cadherin and increased the expression of vimentin and RANKL (Figure 3C).

Long-term treatment with 4 ng/ml TGFβ1 plus 50 ng/ml EGF (T + E) for up to 37 days supported the EMT transition of $ARCaP_E$ cells, as illustrated by decreased E-cadherin and increased vimentin protein expression (Figure 3D). This growth factor-mediated EMT was associated with increased RANKL protein expression. Upon growth factor withdrawal for 9 days following the 37-day treatment [37d(T + E), 9d(–)], the EMT was reversed, as shown by a switch of gene expression profiles toward that of the original $ARCaP_E$ cells (Figure 3D). In a separate study addressing the effect of Snail on $ARCaP_E$ cells [39], we also observed increased expression of Snail, a transcription factor that can induce EMT, in $ARCaP_E$ cells treated with TGFβ1 and EGF, most significantly after 11 and 37 days. These results support the hypothesis that the growth factor milieu is required to maintain the EMT phenotype, possibly through up-regulation of Snail transcription factor. In addition, co-treatment of $ARCaP_E$ cells with the RANK decoy receptor, OPG (50 ng/ml), did not block expression of EMT markers induced by TGFβ1 and EGF, nor did it inhibit RANKL expression, suggesting that the inhibition of RANK binding to RANKL does not affect EMT (data not shown). Similarly, treatment of $ARCaP_M$ with 50 ng/ml OPG did not abolish EMT; vimentin and RANKL expression and levels of E-cadherin expression were not changed in these studies (data not shown). Therefore, both TGFβ1 and EGF are required to induce and maintain EMT in the human prostate cancer ARCaP cell model, while blocking RANKL-RANK interaction using OPG does not abolish EMT.

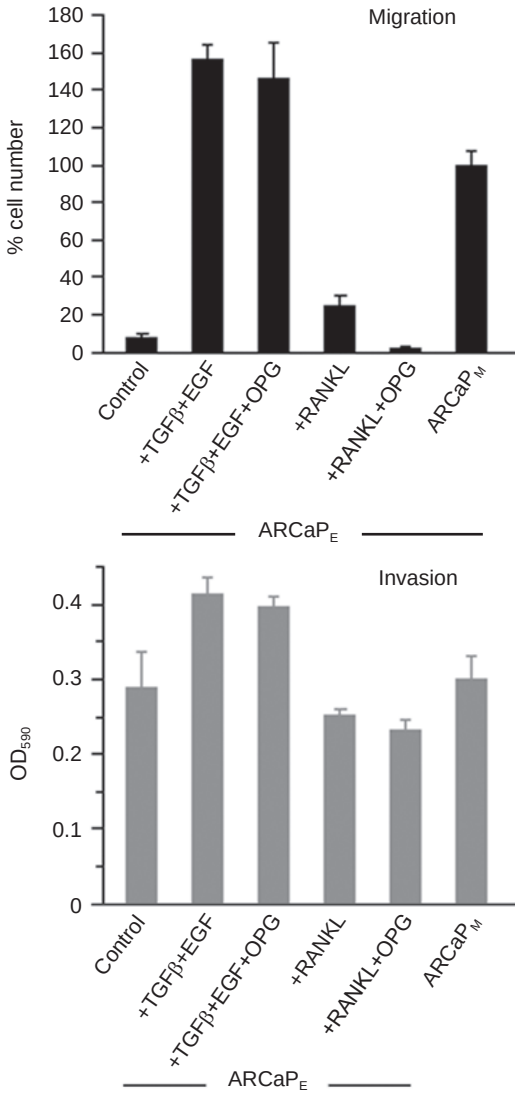

Figure 4 Increased migration and invasion are associated with EMT promoted by growth factor treatment of $ARCaP_E$ cells. Growth factor-treated cells that had migrated across collagen matrix were counted to determine the percentage cell migration relative to $ARCaP_M$ as a positive control (top panel). Cells that invaded through matrigel matrix were fixed, stained, solubilized, and OD590 nm read to obtain relative invasion (bottom panel). Data represent the average ± standard deviation from four separate experiments with 2-3 replicates per experiment.

EMT induced by TGFβ1 plus EGF is accompanied by increased migration and invasion of ARCaP cells

We assessed ARCaP cell behavioral changes after growth factor-induced EMT. Cell migration in the Boyden chambers increased approximately 15-fold after treatment of $ARCaP_E$ with both TGFβ1 and EGF for 48 h (Figure 4). Since RANKL protein expression was induced by the exposure of $ARCaP_E$ cells to the growth factor milieu, we tested whether RANKL could mediate the growth factor-induced increase in cell migratory behaviors in an autocrine manner through interaction with RANK receptor on the cell surface. Co-treatment of $ARCaP_E$ cells with growth factors and a RANK decoy receptor, OPG (50 ng/ml), failed to show any suppressive effects on the migration of $ARCaP_E$ cells (Figure 4). In addition, OPG did not affect the migratory rate of $ARCaP_M$ (data not shown). Conversely, the three-fold increase of $ARCaP_E$ migration stimulated by recombinant RANKL (200 ng/ml) was completely abolished by co-treatment of these cells with both recombinant RANKL and OPG (Figure 4). Together, these results suggest that RANKL was not directly responsible for the increase in cell migration induced by EGF and TGFβ1, but instead EGF and TGFβ1 may induce cell migration via a RANKL-independent pathway. Although EGF and TGFβ1 did increase invasion slightly in $ARCaP_E$ cells, the difference was not statistically significant. In addition, neither RANKL nor its inhibitor OPG was able to affect cell invasion (Figure 4). These results are consistent with the interpretation that EGF and TGFβ1 utilize distinct signaling pathways, independent

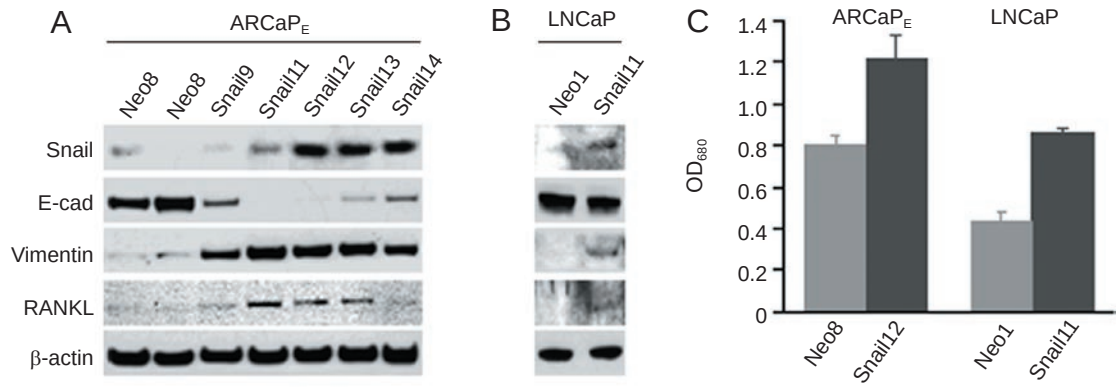

Figure 5 Ectopic expression of Snail-induced EMT and increased RANKL expression in ARCaP$_E$ and LNCaP cells. An expression vector containing a constitutively active Snail cDNA was stably transfected into **(A)** ARCaP$_E$ cells or **(B)** LNCaP cells, and EMT markers were analyzed by Western blot. Panels **(A)** and **(B)** are the representative blots of gene expression in selected Snail- and neo-transfected clones. **(C)** Cell migration was analyzed using a Boyden chamber coated on the underside with collagen. OD590 nm represents relative migration. Panel **(C)** represents the average ± standard deviation from four separate experiments with 2-3 replicates per experiment.

of RANKL and its interaction with RANK, in the induction of cell migration and invasion of ARCaP$_E$ cells.

Snail is a common mediator of EMT in human LNCaP and ARCaP prostate cancer cell models: evidence of increased RANKL expression and cell migration

Because of the possible roles of Snail in EMT, we transfected ARCaP$_E$ and LNCaP cells with either Snail cDNA or empty Neo control vector. Stable clones were generated by neomycin selection and characterized. The Snail-transfected ARCaP$_E$ clones expressed higher levels of Snail than those in the Neo control on Western blot analysis (Figure 5A). In addition, the Snail-transfected clones had decreased E-cadherin and increased vimentin and RANKL expressions, consistent with EMT. The Snail-transfected LNCaP cells also underwent EMT with concomitant gene expression changes, with the exception that E-cadherin expression was not changed at the cellular level (Figure 5B). Instead, immunocytochemical analysis of the transfected clones suggested a re-organization of the E-cadherin proteins, shifted from cell junctions to a predominantly cytoplasmic localization (Supplementary information, Figure S1). Importantly, the Snail-induced EMT was accompanied by increased cell migration in both ARCaP$_E$ (30%) and LNCaP (50%) when representative Snail transfectants were compared to control Neo clones (Figure 5C).

Increased in vitro osteoclastogenesis in ARCaP$_M$ and ARCaP$_E$-Snail cells

We next examined whether elevated RANKL expression by the ARCaP$_M$ or Snail-transfected ARCaP$_E$ cells was functional. An *in vitro* osteoclastogenesis assay was performed to quantify osteoclast maturation. Cancer cells co-cultured with mouse splenocytes for 14 days induced the pre-osteoclast progenitor cells to form mature multinucleated osteoclasts, which showed positive TRAP stain (Figure 6A and 6B). A two-fold increase in mature osteoclast numbers was noted in ARCaP$_M$ co-cultures, compared to ARCaP$_E$ co-cultures. Treatment of ARCaP$_M$ co-cultures with OPG abrogated the osteoclastogenesis and reduced the number of mature osteoclasts (Figure 6A and 6B). Similarly, ARCaP$_E$ cells overexpressing Snail (ARCaP-Snail12) led to increased TRAP staining with a drastic 40-fold increase in multi-nucleated osteoclasts, and this increase could be partially inhibited by OPG (Figure 6C). These results suggest that the RANKL produced by ARCaP$_M$ and ARCaP$_E$-Snail cells is biologically functional, inducing osteoclastogenesis *in vitro*. Finally, to assess the regulation of RANKL expression by the Snail transcription factor, clones of the Snail-transfected ARCaP$_E$ cells were intracardiacally injected to SCID mice. The spontaneous bone tumors were dissected for TRAP staining for osteoclasts. There was an elevated number of TRAP-positive osteoclasts lining the bone surface (Figure 6D), indicative of increased RANKL activity in the Snail-transfected ARCaP$_E$ clones.

Discussion

The prevalence of prostate cancer and its propensity to skeletal metastases are well recognized [40]. Most men who die of prostate cancer have metastatic bone disease [41]. The present communication focused on determining the causal relationship between human prostate cancer

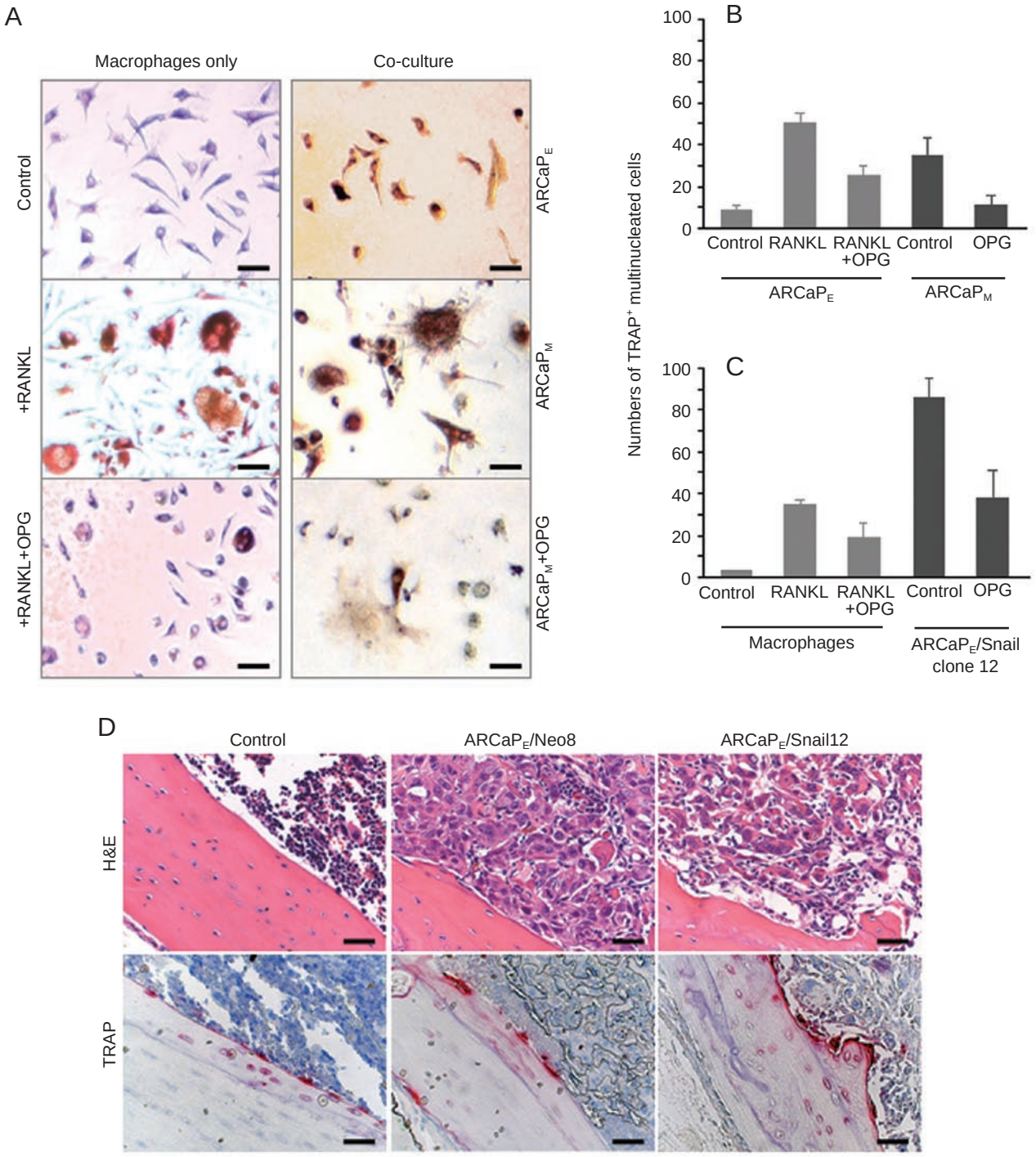

Figure 6 Increased osteoclastogenesis *in vitro* upon co-culturing mouse macrophage cells with ARCaP$_M$ or ARCaP-Snail transfectants. **(A)** ARCaP$_M$ cells that overexpress RANKL when co-cultured with mouse macrophage cells induced more TRAP staining as seen under light microscopy, as compared to ARCaP$_E$ co-cultures, which was effectively antagonized by OPG, suggesting that the RANKL overexpressed by ARCaP$_M$ cells is functional. Bar = 120 μm. **(B)** Multinucleated TRAP positive cells from ARCaP$_E$ or ARCaP$_M$ co-cultures were counted under a light microscope. **(C)** Co-culture of ARCaP-Snail12 performed similarly revealed increased multinucleated TRAP-positive cells compared to the Neo control. The results represent triplicate results obtained from two independent experiments. **(C)** One of the Snail-transfected ARCaP$_E$ cell clones was intracardiacally injected to SCID mice and the spontaneous bone metastatic tumors were dissected for TRAP staining of osteoclasts. An elevated number of TRAP-positive osteoclasts lining the bone surface was observed, indicative of an increased RANKL activity in the Snail-transfected ARCaP$_E$ clones. Bar = 240 μm.

bone metastasis and EMT using a newly established human prostate cancer ARCaP EMT model. Results of our study demonstrated that the host bone microenvironment, selected soluble growth factors, and the Snail transcription factor could provoke EMT in ARCaP human prostate cancer cells. Specifically, we identified the expression of functional RANKL as a novel EMT marker which may be responsible, in part, for increased bone turnover and subsequent prostate cancer cell growth and bone colonization.

EMT occurs during embryonic development, where the invasion front of migrating primordial epithelial cells undergoes morphologic and behavioral transition, starting to express mesenchymal phenotypes and biomarkers [1]. It has been widely reported that cancer cells similarly undergo EMT, leading to increased migratory, invasive, and metastatic potential [5-7]. Despite reports claiming that vimentin may be co-expressed in localized and disseminated prostate cancers with increased oncogenic signals [30, 42], there was little documentation of biologic and molecular associations between vimentin expression and the behaviors of human prostate cancer cells. In this study, we showed that vimentin expression was intimately associated with EMT in both the ARCaP and LNCaP prostate cancer cell lines, and we have identified classical as well as novel biomarkers associated with this transition.

We noted consistent morphologic and behavioral changes associated with EMT in the ARCaP model and this transition could predict the metastatic potential of prostate cancer cells to bone. We identified RANKL as a novel EMT-associated biomarker in both ARCaP and Snail-transfected LNCaP cells. Under physiologic conditions, RANKL, expressed by osteoblasts, stimulates osteoclast maturation and bone resorption through the surface RANK receptor-expressing osteoclasts [43, 44]. Our data indicated that $ARCaP_M$ cells expressing mesenchymal phenotype and Snail-transfected LNCaP cells could mimic osteoblasts by expressing higher levels of RANKL, and the expression led to increased osteoclast maturation. These results suggest that EMT may be associated with bone-homing or increased bone turnover elicited by the invading prostate cancer cells.

The soluble factors TGFβ1 and EGF were also able to induce EMT in ARCaP cells by down-regulating E-cadherin, and up-regulating vimentin, Snail, and RANKL. TGFβ1 has been shown previously to increase Snail expression and osteoclastogenesis through regulation of RANKL protein, while EGF has so far only been shown to regulate Snail [45-48]. We propose that the regulation of bone turnover by TGFβ may be mediated, in part, through Snail-regulated RANKL expression, and we are currently testing this hypothesis. Recent findings indicated that RANKL is important for the migration and homing of melanoma cancer cells to bone [49]. It is possible that EMT may couple with prostate cancer bone homing through RANKL expression, its ability to increase bone turnover, and subsequent bone colonization.

It appears that up-regulation of RANKL is a common feature of EMT, whether it is induced by cellular interaction with the bone microenvironment, treatment with TGFβ1 and EGF, or by transfecting with the Snail transcription factor. To our knowledge this is the first report showing that the additive effects of TGFβ1 and EGF, and Snail transfection can increase RANKL expression. TGFβ1 has previously been shown to induce RANKL expression and subsequently stimulate osteoclast differentiation [45, 48]. There are no reports of RANKL regulation by EGF alone or co-regulation by TGFβ1 plus EGF. Our results indicated that combined EGF and TGFβ1, but not these growth factors alone, elicited increased cell migration and that these effects could not be abrogated by OPG. In control experiments, however, pharmacologic doses of recombinant RANKL did lead to increased cell migration, and the effect could be blocked by OPG. These results are in agreement with a previous report that RANKL induced migration in breast and prostate cancer cells [49]. Because very high concentrations of RANKL were needed to promote prostate cancer cell migration, the RANKL level observed in ARCaP cells may be too low to elicit a cell migration effect. Instead, the level of RANKL in ARCaP may be sufficient for osteoclastogenesis, bone resorption, and turnover, and for supporting prostate cancer bone colonization.

The Snail transcription factor has been shown to induce EMT in breast, ovarian, and bladder cancers [13-16]. Its direct effect on prostate cancer cells, however, has not been extensively investigated. Down-regulation of prostasin gene in hormone-refractory prostate cancer has been shown to be mediated by the Snail homolog, Slug, through the repression of prostasin promoter [28]. In the TRAMP/FVB mouse prostate cancer progression model, genistein was shown to inhibit cancer growth and progression *in vivo* by down-regulating Snail [50]. We demonstrated that overexpression of Snail in $ARCaP_E$ and LNCaP cells was able to drive EMT characterized by decreased E-cadherin expression, or relocalization of E-cadherin in LNCaP from the cytoplasmic membrane junction to the cytosol. This was accompanied by increased vimentin and RANKL protein expression, as well as increased cell migration. Furthermore, the Snail-induced RANKL in $ARCaP_E$ cells was functional and could increase osteoclastogenesis *in vitro*. This is the first documented report of Snail regulation of RANKL protein and osteoclast maturation and provides a crucial link between EMT and possible bone turnover. Snail has been reported to be important for chondrocyte differentiation and was highly expressed in hypertrophic

chondrocytes of developing mouse limb [51]. There is no documentation of the role of Snail in bone, and further studies are going on to investigate the link between Snail regulation of RANKL, bone turnover, and prostate cancer bone metastasis.

Our results revealed that the factors that drive EMT can also regulate RANKL expression in human prostate cancer, and RANKL is a common mediator downstream from growth factors (TGFβ1 and EGF), bone microenvironment, and Snail activation. Several studies have shown the efficacy of targeting RANKL in myeloma and prostate cancer bone lesions. Recombinant OPG linked to an Fc portion of immunoglobulins (OPG-Fc), decoy RANK-Fc receptor, or humanized RANKL antibodies has been developed [52-54]. On the other hand, our studies suggest that inhibitors of TGFβ1, EGF, or Snail signaling may not only prevent EMT, but also retard the RANK-RANKL signaling. These inhibitors should be evaluated for their efficacy to prevent EMT, metastasis, and subsequent colonization of prostate cancer cells in bone.

In summary, we showed that EMT in human prostate cancer could be induced and maintained through interaction with the bone microenvironment, by treatment with growth factors EGF and TGFβ1, and following Snail overexpression. The morphologic and behavioral switch for $ARCaP_E$ cells to undergo EMT was accompanied by decreased E-cadherin, and increased N-cadherin, vimentin, and RANKL expression. The functional RANKL could enhance bone resorption and bone turnover, which could facilitate subsequent prostate cancer bone metastasis. Since increased RANKL expression was detected in both LNCaP and ARCaP human prostate cancer EMT models, targeting RANKL-RANK plus specific growth factor signaling interrupting EMT may offer advantages for the treatment of human prostate cancer bone metastasis.

Materials and Methods

Reagents and antibodies

T-medium was purchased from Invitrogen (Carlsbad, CA). Penicillin-streptomycin was from BioWhittaker (Walkersville, MD). RPMI 1640 medium was from Life Technologies, Inc. (Rockville, MD). The protease inhibitor cocktail was from Roche Molecular Biochemicals (Indianapolis, IN). Mouse monoclonal anti-human E-cadherin and N-cadherin antibodies were from BD Transduction Laboratories (Lexington, KY). Goat polyclonal anti-human RANKL and mouse monoclonal anti-human vimentin antibodies were from Santa Cruz Biotechnology (Santa Cruz, CA). Recombinant human TGFβ1, recombinant mouse RANKL, recombinant mouse M-CSF, and recombinant human OPG were from R&D Systems, Inc. (Minneapolis, MN). Fetal bovine serum (FBS), recombinant human EGF, G418, anti-flag M2 monoclonal antibody, and mouse monoclonal anti-human β-actin antibody were from Sigma-Aldrich, Inc. (St Louis, MO). Rat monoclonal anti-human Snail antibody and HRP-conjugated goat anti-rat antibody were from Cell Signaling Technology, Inc. (Danvers, MA). HRP-conjugated sheep anti-mouse antibody and the Enhanced chemiluminescence (ECL) detection reagent were purchased from Amersham Biosciences (Buckingham, England). HRP-conjugated rabbit anti-goat antibody was from Zymed Laboratories Inc. (San Francisco, CA). Matrigel and rat tail type-1 collagen were from BD Biosciences. Charcoal/dextran-treated FBS (DCC-FBS) was from Hyclone (South Logan, UT). The Snail cDNA construct was kindly provided by Dr Mien-Chie Hung, University of Texas (Houston, TX).

Cells and culture conditions

The human prostate cancer LNCaP cell line was obtained from ATCC (Manassas, VA). ARCaP cells were established from the ascites fluid of a patient with prostate cancer bone metastasis [55]. $ARCaP_E$ and $ARCaP_M$ are sublines of the ARCaP, generated in our laboratory by limited dilution cloning [30]. All the cells were grown in T-medium supplemented with 5% fetal bovine serum (10% for ARCaP sublines) and 1× penicillin-streptomycin, at 37 °C with 5% CO_2 in a humidified incubator.

Transfection assay

Stable transfection of Snail cDNA was performed in $ARCaP_E$ and LNCaP cells utilizing Lipofectamine 2000 (Invitrogen). A constitutively active Snail construct (6SA) was previously utilized to induce EMT in MCF7 breast cancer cells [33]. Briefly, 1.6 μg Snail cDNA or empty vector (Neo) was transfected into cells cultured in 12-well dishes at 90% confluence as per the manufacturer's instructions. Stable clones were selected using 800 μg/ml G418, isolated, and maintained in 400 μg/ml G418. Snail expression was verified in the clones by Western blot analysis.

Animal experiments

All animal procedures were approved and performed in accordance with institutional guidelines, and all mice were purchased from National Cancer Institute (Frederick, MD). $ARCaP_E$ cells were injected by intracardiac route (5×10^5 cells/50 μl PBS) into five- to seven-week-old male SCID mice (n = 8) using a 28G1/2 needle. Prior to injection, mice were anesthetized and placed in a supine position and the needle inserted 5 mm above the middle of the left side of sternum. The appearance of fresh arterial blood in the syringe signaled successful penetration into the left ventricle, and cells were subsequently infused slowly and directly into the left ventricle of the mouse for systemic circulation. Tumor formation in bone was monitored closely by biweekly X-ray radiography. The time taken for the tumor to be visualized by X-ray was termed the latency period, and metastasis was confirmed by radiography and histomorphology of the tumor specimens.

Bone metastasis tumor was dissected to clone cancer cells from the tumor. Cells were derived from bone metastatic tumor tissue by culturing tumor dices *in vitro*. Cloned cells represented the bone metastatic variant of the original cancer cell line. The variant cells were used in another round of bone tumor formation following intracardiac injection into SCID mice.

Reverse transcription-polymerase chain reaction (RT-PCR)

Total RNA was isolated from cells using RNA-Bee as per the manufacturer's instructions (Tel-Test, Inc., Friendswood, TX). The RNA (2 μg) was reverse transcribed with oligo-dT using MMLV-

reverse transcriptase (Invitrogen, Carlsbad, CA), to generate cDNA. PCR analyses were subsequently performed with 2 μl of the cDNA reaction utilizing the primers and conditions as follows. E-cadherin primers used were: 5′-TCC ATT TCT TGG TCT ACG CC-3′ and 5′-CAC CTT CAG CCA ACC TGT TT-3′; N-cadherin, 5′-GTG CCA TTA GCC AAG GGA ATT CAG C-3′ and 5′-GCG TTC CTG TTC CAC TCA TAG GAG G-3′. The PCR conditions for E-cadherin and N-cadherin were 95 °C, 5 min, 35 cycles of 95 °C, 30 s; 60 °C, 30 s; 72 °C, 60 s, and 72 °C, 8 min final extension. Vimentin primers used were: 5′-TGG CAC GTC TTG ACC TTG AA-3′ and 5′-GGT CAT CGT GAT GCT GAG AA-3′; RANKL: 5′-GCT TGA AGC TCA GCC TTT TGC TCA T-3′ and 5′-GGG GTT GGA GAC CTC GAT GCT GAT T-3′. The PCR conditions for vimentin were 94 °C, 2 min, 29 cycles of 94 °C, 30 s; 55 °C, 30 s; 72 °C, 2 min, and 72 C, 7 min final extension, while those for RANKL were 94 °C, 2 min, 36 cycles of 94 °C, 15 s; 55 °C, 30 s; 72 °C, 60 s, and 72 °C, 5 min final extension.

Western blot analysis

Confluent cells were lysed in a modified RIPA buffer (50 mM Tris, pH 8.0, 150 mM NaCl, 0.02% NaN_3, 0.1% SDS, 1% NP-40, 0.5% sodium deoxycholate) containing 1.5× protease inhibitor cocktail, 1 mM phenylmethylsulfonyl fluoride, and 1 mM sodium orthovanadate. The cell lysates were centrifuged, and supernatants collected and quantified using a micro BCA assay. In all, 25–30 μg of cell lysate was resolved on a 4–12% SDS-PAGE, followed by transblotting onto nitrocellulose membrane (Schleicher & Schuell, Keene, NH). The membranes were blocked in TBSTB (TBS with 0.05% Tween-20, 0.05% BSA) containing 5% fat-free milk, and subsequently incubated with diluted antibody in blocking buffer. After washing, the membranes were incubated in peroxidase-conjugated secondary antibodies, washed, and visualized using ECL reagent. The membranes were stripped using stripping buffer (Pierce Biotechnology, Inc., Rockford, IL) prior to re-probing with a different antibody. For growth factor treatments, 70% confluent cells were serum-starved in phenol-free serum-free RPMI containing penicillin/streptomycin for 24 h prior to treatment with 4 ng/ml TGFβ1, or 50 ng/ml EGF, or a combination of both for various time periods in the RPMI1640 supplemented with 5% DCC-FBS. Cell lysates were subsequently prepared.

Invasion and migration assays

Cells treated with 4 ng/ml TGFβ1 plus 50 ng/ml EGF, 200 ng/ml RANKL, or 50 ng/ml OPG for 3 days were harvested and 5×10^4 cells plated in the upper chamber of a 24-well costar transwell Boyden chamber (Becton Dickinson, Franklin Lakes, NJ) that had been previously coated on the inside of the well with matrigel:media (1:4) for invasion, or on the underside of each well with 2.5 μg/cm^2 collagen I for migration assays. The haptotactic invasion and migration assays were performed in RPMI 1640 media supplemented with 5% DCC in the case of ARCaP cells, while for the less migratory LNCaP cells a chemotactic migration assay was performed by adding 0.1% FBS to the bottom wells. The cells that had invaded/migrated to the underside of the membrane and the bottom chamber were fixed with formaldehyde after 48 h (for migration) or 72 h (for invasion), and stained with 0.5% crystal violet. For invasion assays, cells stained on the underside of the membrane and in the bottom chamber were solubilized with extraction buffer (Chemicon International, Inc., Temecula, CA), and OD590 nm was subsequently read to get the relative invasion. For migration assays cells on the underside of the membrane were scraped, and stained cells that had migrated to the bottom chamber were manually counted or solubilized and OD590 nm was read to obtain the relative migration.

Immunohistochemical analysis

2×10^4 cells were plated onto chamber slides in T-media containing 10% FBS. After overnight culture, the cells were placed in phenol-free serum-free RPMI 1640 medium containing penicillin/streptomycin for 24 h prior to treatment with 4 ng/ml TGFβ1 and 50 ng/ml EGF for various time periods up to 72 h in RPMI media supplemented with 5% DCC-FBS. The cells were fixed with ice-cold methanol/acetone (1:1), followed by immunoperoxidase staining utilizing the DAKO Autostainer Plus System (DAKO, Capinteria, CA). All common reagents for staining were from DAKO. Briefly, the slides were blocked with dual endogenous enzyme block (DEEB) for 10 min, incubated for 1 h with primary antibody, E-cadherin (1:1 000), vimentin (1:50), N-cadherin (1:500), RANKL (1:500), or control UNC antibodies (DAKO). A thorough rinse in Tris-buffered saline with 0.05% Tween (TBST) was followed by 30 min incubation with Envision + Labelled Polymer-HRP or 15 min incubation with Biotinylated Link Universal and 15 min Streptavidin-HRP. The staining signal was detected by incubating with peroxidase substrate buffer with chromogen, diaminobenzidine (DAB), followed by hematoxylin counterstain. Following cover-slipping, images were acquired using a laser-scan confocal microscope 410 (Carl Zeiss, Minneapolis, MN).

In vitro osteoclastogenesis assay

Osteoclastogenesis assay was performed as described previously with minor modifications [56]. Briefly, 1×10^3 cancer cells were seeded together with 2×10^5 pre-osteoclastic macrophage cells harvested from adult mouse spleen by disaggregation through a wire sieve. The co-cultures were performed in a 48-well plate containing 500 μl of α-MEM media supplemented with 10% FBS, and 1 ng/ml mouse recombinant M-CSF. As a positive control, 100 ng/ml mouse recombinant RANKL was added to 2×10^5 pre-osteoclastic cells. 50 ng/ml recombinant OPG was added to certain wells to block RANKL-mediated osteoclastogenesis. The cells were fed twice a week by replacement of half the media with fresh media containing M-CSF (and RANKL for the positive control). After 14 days, the cells were fixed and analyzed by TRAP staining (Sigma-Aldrich, Inc., St Louis), and the TRAP$^+$ multinucleated cells in the entire well were counted as mature osteoclasts. Note that TRAP stain is associated solely with macrophage cells; ARCaP cells when cultured individually or in co-culture with macrophage cells had a distinct morphology and individually were devoid of TRAP stain (data not shown).

Acknowledgments

We thank Dr Neale Weitzmann (Department of Medicine, Emory University School of Medicine) for helpful discussion and support, and Mr Gary Mawyer (Department of Urology, the University of Virginia) for editing. We acknowledge the following grant supports: CA 082739 (HEZ); CA 119338, CA 098912, CA 132388, CA 108468 and PC060866 (LWKC).

References

1 Hay ED. An overview of epithelio-mesenchymal transformation. *Acta Anat (Basel)* 1995; **154**:8-20.

2 Bellovin DI, Bates RC, Muzikansky A, Rimm DL, Mercurio AM. Altered localization of p120 catenin during epithelial to mesenchymal transition of colon carcinoma is prognostic for aggressive disease. *Cancer Res* 2005; **65**:10938-10945.

3 Rosano L, Spinella F, Di Castro V, *et al*. Endothelin-1 promotes epithelial-to-mesenchymal transition in human ovarian cancer cells. *Cancer Res* 2005; **65**:11649-11657.

4 Yang AD, Camp ER, Fan F, *et al.* Vascular endothelial growth factor receptor-1 activation mediates epithelial to mesenchymal transition in human pancreatic carcinoma cells. *Cancer Res* 2006; **66**:46-51.

5 Boyer B, Valles AM, Edme N. Induction and regulation of epithelial-mesenchymal transitions. *Biochem Pharmacol* 2000; **60**:1091-1099.

6 Petersen OW, Nielsen HL, Gudjonsson T, *et al*. Epithelial to mesenchymal transition in human breast cancer can provide a nonmalignant stroma. *Am J Pathol* 2003; **162**:391-402.

7 Thiery JP. Epithelial-mesenchymal transitions in tumour progression. *Nat Rev Cancer* 2002; **2**:442-454.

8 Savagner P. Leaving the neighborhood: molecular mechanisms involved during epithelial-mesenchymal transition. *Bioessays* 2001; **23**:912-923.

9 Savagner P, Boyer B, Valles AM, Jouanneau J, Thiery JP. Modulations of the epithelial phenotype during embryogenesis and cancer progression. *Cancer Treat Res* 1994; **71**:229-249.

10 Janda E, Lehmann K, Killisch I, Jechlinger M, Herzig M, Downward J, *et al.* Ras and TGF[beta] cooperatively regulate epithelial cell plasticity and metastasis: dissection of Ras signaling pathways. *J Cell Biol* 2002; **156**:299-313.

11 Morali OG, Delmas V, Moore R, Jeanney C, Thiery JP, Larue L. IGF-II induces rapid beta-catenin relocation to the nucleus during epithelium to mesenchyme transition. *Oncogene* 2001; **20**:4942-4950.

12 Hauschka PV, Mavrakos AE, Iafrati MD, Doleman SE, Klagsbrun M. Growth factors in bone matrix. Isolation of multiple types by affinity chromatography on heparin-Sepharose. *J Biol Chem* 1986; **261**:12665-12674.

13 Kurrey NK,Amit K, Bapat SA. Snail and Slug are major determinants of ovarian cancer invasiveness at the transcription level. *Gynecol Oncol* 2005; **97**:155-165.

14 Moody SE, Perez D, Pan TC, *et al.* The transcriptional repressor Snail promotes mammary tumor recurrence. *Cancer Cell* 2005; **8**:197-209.

15 Yokoyama K, Kamata N, Fujimoto R, *et al.* Increased invasion and matrix metalloproteinase-2 expression by Snail-induced mesenchymal transition in squamous cell carcinomas. *Int J Oncol* 2003; **22**:891-898.

16 Taki M, Verschueren K, Yokoyama K, Nagayama M, Kamata N. Involvement of Ets-1 transcription factor in inducing matrix metalloproteinase-2 expression by epithelial-mesenchymal transition in human squamous carcinoma cells. *Int J Oncol* 2006; **28**:487-496.

17 Untergasser G, Gander R, Rumpold H, Heinrich E, Plas E, Berger P. TGF-beta cytokines increase senescence-associated beta-galactosidase activity in human prostate basal cells by supporting differentiation processes, but not cellular senescence. *Exp Gerontol* 2003; **38**:1179-1188.

18 Zhau HY, Zhou J, Symmans WF, *et al.* Transfected neu oncogene induces human prostate cancer metastasis. *Prostate* 1996; **28**:73-83.

19 Veveris-Lowe TL, Lawrence MG, Collard RL, *et al*. Kallikrein 4 (hK4) and prostate-specific antigen (PSA) are associated with the loss of E-cadherin and an epithelial-mesenchymal transition (EMT)-like effect in prostate cancer cells. *Endocr Relat Cancer* 2005; **12**:631-643.

20 Kong YY, Yoshida H, Sarosi I, *et al.* OPGL is a key regulator of osteoclastogenesis, lymphocyte development and lymph-node organogenesis. *Nature* 1999; **397**:315-323.

21 Yasuda H, Shima N, Nakagawa N, *et al.* Osteoclast differentiation factor is a ligand for osteoprotegerin/osteoclastogenesis-inhibitory factor and is identical to TRANCE/RANKL. *Proc Natl Acad Sci USA* 1998; **95**:3597-3602.

22 Standal T, Seidel C, Hjertner O, *et al.* Osteoprotegerin is bound, internalized, and degraded by multiple myeloma cells. *Blood* 2002; **100**:3002-3007.

23 Mundy GR. Metastasis to bone: causes, consequences and therapeutic opportunities. *Nat Rev Cancer* 2002; **2**:584-593.

24 Roudier MP, Corey E, True LD, Hiagno CS, Ott SM, Vessell RL. Histological, immunophenotypic and histomorphometric characterization of prostate cancer bone metastases. *Cancer Treat Res* 2004; **118**:311-339.

25 Seibel MJ. Clinical use of markers of bone turnover in metastatic bone disease. *Nat Clin Pract Oncol* 2005; **2**:504-517.

26 Mundy GR. Mechanisms of bone metastasis. *Cancer* 1997; **80**(8 Suppl):1546-1556.

27 Brown JM, Corey E, Lee ZD, *et al.* Osteoprotegerin and rank ligand expression in prostate cancer. *Urology* 2001; **57**:611-616.

28 Chen G, Sircar K, Aprikian A, Potti A, Goltzman D, Rabbani SA. Expression of RANKL/RANK/OPG in primary and metastatic human prostate cancer as markers of disease stage and functional regulation. *Cancer* 2006; **107**:289-298.

29 Brown JM, Zhang J, Keller ET. Opg, RANKl, and RANK in cancer metastasis: expression and regulation. *Cancer Treat Res* 2004; **118**:149-172.

30 Xu J, Wang RX, Xie ZH, *et al.* Prostate cancer metastasis: role of the host microenvironment in promoting epithelial to mesenchymal transition and increased bone and adrenal gland metastasis. *Prostate* 2006; **66**:1664-1673.

31 Barrallo-Gimeno A, Nieto MA. The Snail genes as inducers of cell movement and survival: implications in development and cancer. *Development* 2005; **132**:3151-3161.

32 Hemavathy K, Ashraf SI, Ip YT. Snail/slug family of repressors: slowly going into the fast lane of development and cancer. *Gene* 2000; **257**:1-12.

33 Zhou BP, Deng J, Xia W, *et al.* Dual regulation of Snail by GSK-3beta-mediated phosphorylation in control of epithelial-mesenchymal transition. *Nat Cell Biol* 2004; **6**:931-940.

34 Martin TJ. Paracrine regulation of osteoclast formation and activity: milestones in discovery. *J Musculoskelet Neuronal Interact* 2004; **4**:243-253.

35 Schoppet M, Preissner KT, Hofbauer LC. RANK ligand and osteoprotegerin: paracrine regulators of bone metabolism and vascular function. *Arterioscler Thromb Vasc Biol* 2002; **22**:549-553.

36 Bhowmick NA, Ghiassi M, Bakin A, *et al.* Transforming growth factor-beta1 mediates epithelial to mesenchymal transdifferentiation through a RhoA-dependent mechanism. *Mol Biol Cell* 2001; **12**:27-36.
37 Cui W, Fowlis DJ, Bryson S, *et al.* TGFbeta1 inhibits the formation of benign skin tumors, but enhances progression to invasive spindle carcinomas in transgenic mice. *Cell* 1996; **86**:531-542.
38 Oft M, Peli J, Rudaz C, Schwarz H, Beug H, Reichmann E. TGF-beta1 and Ha-Ras collaborate in modulating the phenotypic plasticity and invasiveness of epithelial tumor cells. *Genes Dev* 1996; **10**:2462-2477.
39 Zhau HE, Odero-Marah V, Lue HW, *et al*. Epithelial to mesenchymal transition (EMT) in human prostate cancer: lessons learned from ARCaP model. *Clin Exp Metastasis* 2008 Jun 6. doi: 10.1007/s10585-008-9183-1
40 Boring CC, Squires TS, Tong T, Montgomery S. Cancer statistics, 1994. *CA Cancer J Clin* 1994; **44**:7-26.
41 Tu SM, Lin SH. Clinical aspects of bone metastases in prostate cancer. *Cancer Treat Res* 2004; **118**:23-46.
42 Lang SH, Hyde C, Reid IN, *et al.* Enhanced expression of vimentin in motile prostate cell lines and in poorly differentiated and metastatic prostate carcinoma. *Prostate* 2002; **52**:253-263.
43 Aubin JE, Bonnelye E. Osteoprotegerin and its ligand: a new paradigm for regulation of osteoclastogenesis and bone resorption. *Osteoporos Int* 2000; **11**:905-913.
44 Wong BR, Josien R, Lee SY, *et al.* TRANCE (tumor necrosis factor [TNF]-related activation-induced cytokine), a new TNF family member predominantly expressed in T cells, is a dendritic cell-specific survival factor. *J Exp Med* 1997; **186**:2075-2080.
45 Ishida A, Fujita N, Kitazawa R, Tsuruo T. Transforming growth factor-beta induces expression of receptor activator of NF-kappa B ligand in vascular endothelial cells derived from bone. *J Biol Chem* 2002; **277**:26217-26224.
46 Peinado H, Olmeda D, Cano A. Snail, Zeb and bHLH factors in tumour progression: an alliance against the epithelial phenotype? *Nat Rev Cancer* 2007; **7**:415-428.
47 Peinado H, Quintanilla M, Cano A. Transforming growth factor beta-1 induces snail transcription factor in epithelial cell lines: mechanisms for epithelial mesenchymal transitions. *J Biol Chem* 2003; **278**:21113-21123.
48 Zhang J, Lu Y, Dai J, *et al. In vivo* real-time imaging of TGF-beta-induced transcriptional activation of the RANK ligand gene promoter in intraosseous prostate cancer. *Prostate* 2004; **59**:360-369.
49 Jones DH, Nakashima T, Sanchez OH, *et al.* Regulation of cancer cell migration and bone metastasis by RANKL. *Nature* 2006; **440**:692-696.
50 El Touny LH, Banerjee PP. Akt GSK-3 pathway as a target in genistein-induced inhibition of TRAMP prostate cancer progression toward a poorly differentiated phenotype. *Carcinogenesis* 2007; **28**:1710-1717.
51 Seki K, Fujimori T, Savagner P, *et al.* Mouse Snail family transcription repressors regulate chondrocyte, extracellular matrix, type II collagen, and aggrecan. *J Biol Chem* 2003; **278**:41862-41870.
52 Body JJ, Facon T, Coleman RE, *et al.* A study of the biological receptor activator of nuclear factor-kappaB ligand inhibitor, denosumab, in patients with multiple myeloma or bone metastases from breast cancer. *Clin Cancer Res* 2006; **12**:1221-1228.
53 Croucher PI, Shipman CM, Van Camp B, Vanderkerken K. Bisphosphonates and osteoprotegerin as inhibitors of myeloma bone disease. *Cancer* 2003; **97**(Suppl):818-824.
54 Zhang J, Dai J, Yao Z, Lu Y, Dougall W, Keller ET. Soluble receptor activator of nuclear factor kappaB Fc diminishes prostate cancer progression in bone. *Cancer Res* 2003; **63**:7883-7890.
55 Zhau HY, Chang SM, Chen BQ, *et al.* Androgen-repressed phenotype in human prostate cancer. *Proc Natl Acad Sci USA* 1996; **93**:15152-15157.
56 Takahashi N, Yamana H, Yoshiki S, *et al.* Osteoclast-like cell formation and its regulation by osteotropic hormones in mouse bone marrow cultures. *Endocrinology* 1988; **122**:1373-1382.

(Supplementary Information is linked to the online version of the paper on the Cell Research website)